University of South Bohemia

Faculty of Science

Phylogeny and genetic diversity of two solitary African mole-rat genera *Heliophobius* and *Georychus*

Master thesis

Bc. Michaela Uhrová

Supervisor: doc. Mgr. Radim Šumbera, Ph.D.

Consultant: Mgr. Ondřej Mikula, Ph.D.

České Budějovice 2020

Uhrová, M., 2020: Phylogeny and genetic diversity of two solitary African mole-rat genera *Heliophobius* and *Georychus*. Mgr. Thesis, in English. – 94 p., Faculty of Science, University of South Bohemia, České Budějovice, Czech Republic.

Abstract:

Two solitary genera of African mole-rats, *Heliophobius* and *Georychus*, had been for a long time considered as monotypic, yet some of the recent studies proposed species complexes. This thesis evaluates intrageneric relationships of both genera by using extended dataset of six nuclear markers and a large number of loci acquired during ddRADseq. Both datasets confirmed highly genetically structured populations within both genera. Nevertheless, while multilocus coalescent based on nuclear markers defined nine gene pools within *Heliophobius* and five within *Georychus*, processing of ddRADseq data revealed both, significantly finer (fineRADstructure) or broader (Infomap) structure. Based on the genetic evidence, we are inclined towards using two species within genus *Heliophobius*, comprised of northern and southern lineages separated by Eastern Arc Mountains, and one species for all evolutionary lineages of *Georychus*. The final taxonomic revision should await further morphological, ecological, or behavioural studies.

Prohlašuji, že svoji diplomovou práci jsem vypracovala samostatně pouze s použitím pramenů a literatury uvedených v seznamu citované literatury.

Prohlašuji, že v souladu s § 47b zákona č. 111/1998 Sb. v platném znění souhlasím se zveřejněním své diplomové práce, a to v nezkrácené podobě elektronickou cestou ve veřejně přístupné části databáze STAG provozované Jihočeskou univerzitou v Českých Budějovicích na jejích internetových stránkách, a to se zachováním mého autorského práva k odevzdanému textu této kvalifikační práce. Souhlasím dále s tím, aby toutéž elektronickou cestou byly v souladu s uvedeným ustanovením zákona č. 111/1998 Sb. zveřejněny posudky školitele a oponentů práce i záznam o průběhu a výsledku obhajoby kvalifikační práce. Rovněž souhlasím s porovnáním textu mé kvalifikační práce s databází kvalifikačních prací Theses.cz provozovanou Národním registrem vysokoškolských kvalifikačních prací a systémem na odhalování plagiátů.

V Českých Budějovicích, 22. 5. 2020

Acknowledgments

First, I would like to express my gratitude to my supervisor Radim Šumbera for not only patience, help, and sharing the knowledge, but also for his immense enthusiasm and emotional support during work. Equal sincere thanks also go to Ondřej Mikula, my consultant, who led me through the abstract and imaginery world of phylogenetic analyses. My next gratitude belongs mainly to Lubomír Piálek, without him ddRAD sequencing would not be such a pleasant work, but also to all other people who shared with me their knowledge and experience, namely Radka Piálková, Jarmila Krásová, Anna Bryjová, and Josef Bryja. I must not forget on Bettine Van Vuuren for providing me with samples of *Georychus* and many other collectors who had done the field works in many African countries.

Last but not least, my sincere thanks go to my whole family and friends, who supported me during my studies not only financially, but mostly emmotionally. I think its no exaggeration to say that without them, I would not be right here.

Content:

1 Introduction

1.1 Biology of subterranean mammals

Subterranean environment provides to its inhabitants mainly safety and microclimatic stability. Animals take advantages of life in burrows, where they are protected from high predation or extreme climatic fluctuations (Nevo 1999). On the other hand, strict subterranean life brings serious restrictions as well. Burrow inhabitants have to overcome specific environment conditions such as hypercapnic and hypoxic atmosphere (but concentrations of oxide and carbon dioxide in burrow systems evidently do not always differ from aboveground concentrations, e.g. Roper et al. 2001; Šumbera et al. 2004), highly water saturated air, or complete darkness. In addition, there are extremely high energetic demands of burrowing, poor productivity and low carrying capacity connected with restricted food availability, and compared to the aboveground environment differently driven senses of orientation and navigation (Nevo 1979; Nevo 2007). Yet despite hostile conditions of such environment, many mammalian lineages independently colonised this ecotope and specialize to a strictly subterranean life, such as moles, marsupial moles, golden moles, and many rodent groups like pocket gophers, octodonts, tuco-tucos, voles, African mole-rats, or blind mole rats (Nevo 1979).

In spite of colonizing this environment in different times and places, all subterranean mammals are exposed to strong pressure from very similar conditions, which results in convergent evolution of morphological, behavioural, molecular, and physiological traits (Nevo 1979, 1995, 1999, 2007; Lessa 1990; Lacey et al 2000; Begall et al. 2007). They all possess cylindrical body shape with significant reductions of body extremities, like limbs, tail, or auricles. Yet, some morphological structures have undergone remarkable developments. The most evident is the adaptation of burrowing apparatus: from specialized muscled and clawed forelimbs (Talpidae, Notoryctidae, Myospalacinae), ever-growing curved incisors (Rhizomyidae, Bathyergidae, Spalacidae, *Ellobius*), or their combination (Geomyidae, Ctenomyidae). Sensory organs have also specialized to the subterranean environment according to degree of fossoriality. While vision and hearing undertook more or less functional and structural reductions, tactile and olfactory senses have rapidly developed (Nevo 1979, 1999; Lacey et al. 2000). Except for odours and sounds, some of them use magnetic compass for a more precise spatial orientation (Moritz et al. 2007). Regarding energetics, most of them

have low basal metabolic rates and low body temperatures (Buffenstein 2000). They share K-strategy of life, meaning high longevity, low mortality rates, low reproduction rates, and relatively slow development (Nevo 1979, 1999).

The subterranean mammals also tend to form spatially highly structured populations. Due to the low productivity and carrying capacity of subterranean environment, feeding strategies are generalized to use limited resources, which imposes strong selective pressure on both, intra and interspecific level. As a result of intraspecific competition, local populations are relatively small and gene flow between them limited. The interspecific competition limits co-existence of the species and makes their distribution mainly parapatric. Taken together with their low dispersal abilities and low degree of emigration, the subterranean mammals are very prone to speciation, but thanks to the same selective pressure also incline to develop into cryptic species (Nevo 1979).

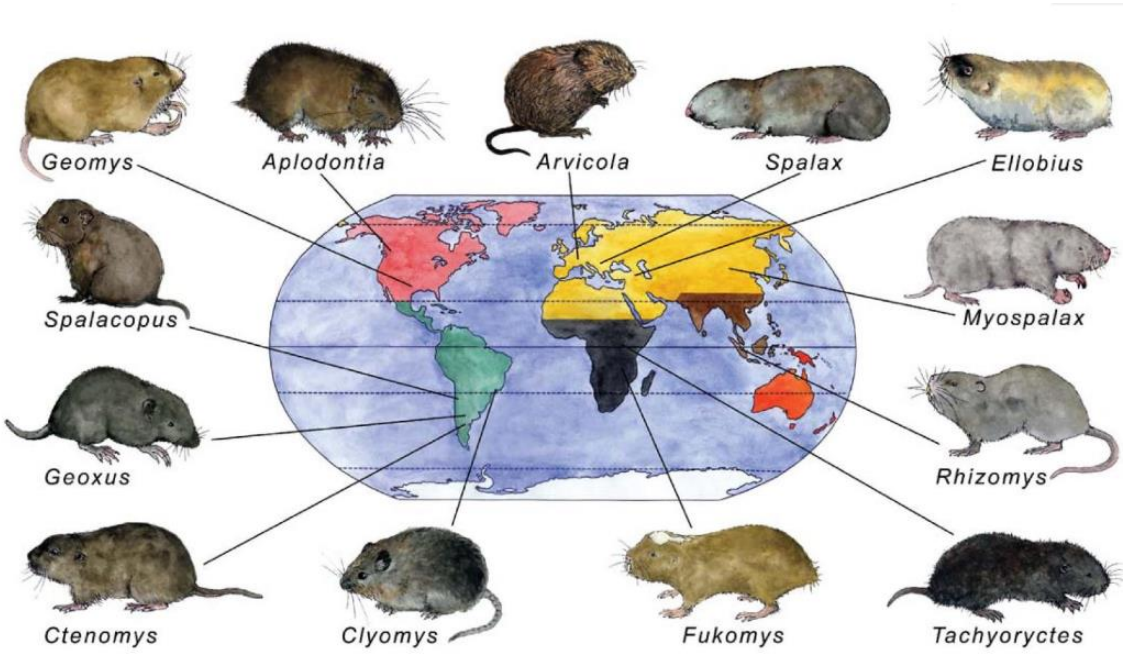

Fig. 1: Morphological convergence of representatives of different subterranean rodent lineages across the world (taken from Begall et al. 2007).

1.2 African mole-rats (Bathyergidae)

One of the most studied groups of strictly subterranean mammals are African mole-rats (Bathyergidae); hystricognathous rodents distributed in sub-Saharan Africa. They have attracted scientists mainly because of diversity of their social systems, ranging from strictly solitary species to highly social including (by some authors) so-called eusocial species

(reviewed in Faulkes and Bennett 2007). Due to intensive research and strictly subterranean style of life, many peculiar traits were revealed, such as magnetic orientation (Burda et al. 1990), longevity (Dammann et al. 2007), poikilothermy (Bennet 2009), or anti-cancer mechanisms (Buffenstein 2008; Seluanov et al. 2009). African mole-rats have become model group for many morphological, physiological, behavioural, and biomedical fields (Jarvis, Bennett and Spinks 1998; Buffenstein 2005; Gomes Rodrigues et al. 2011; Šklíba et al. 2016; Kott et al. 2016; Junker et al. 2017; Sahm et al. 2018; Kelley et al. 2019; Zhao et al. preprint).

1.3 The current view of bathyergid phylogeny

The African mole-rats were found to be sister to a pair of families: the rock rats (Petromuridae) and the cane rats (Thryonomyidae), and together with Old World porcupines (Hystricidae) form an "Old World" hystricomorph group Phiomorpha distributed throughout Africa, southern Europe and southern and south-eastern Asia (Nedbal et al. 1994; Huchon and Douzery 2001).

Regarding internal bathyergid classification, the widely accepted consensus is, that the family consists of six genera (Fig. 2). The most basal branch belongs to a highly social genus *Heterocephalus,* followed by a solitary genus *Heliophobius*. Afterwards, the ancestor of two social genera *Fukomys* and *Cryptomys* ((*Fukomys* was emancipated from *Cryptomys* by Kock et al. (2006)), split from ancestor of two solitary genera *Georychus* and *Bathyergus*. This division is well supported by many studies (Allard and Honeycutt 1992; Faulkes et al. 1997, 2004; Walton et al. 2000; Ingram et al. 2004; Kock et al. 2006; Davies et al. 2015; Patterson and Upham 2014; Bryja et al. 2018b; Visser et al. 2019b). Some studies suggested an exclusion of genus *Heterocephalus* either to a subfamily Heterocephalinae, with Bathyerginae comprising of the remaining genera (Visser et al. 2019b), or to a monotypic family Heterocephalidae (Patterson and Upham 2014). Nevertheless, there is also a discordance in a tree topology; *Bathyergus*, *Georychus*, and *Cryptomys* karyotypically resemble each other (Deuve et al. 2008), which contradicts to a generally accepted monophyly of two groups *Bathyergus – Georychus* and *Cryptomys – Fukomys*.

Nowadays, bathyergids are morphologically well characterized by a unique combination of ancestral and derived traits. With respect to Ctenohystrica (comprising of Ctenodactylidae (gundis), Diatomyidae (kha-ynou) and Hystricognathi; López-Antoñanzas 2016), their ancestral traits are, for instance, hystricognathous mandible (the angular process does not

originate in the same plane as the alveolus of the incisors; Hautier at al. 2011), shape of the skull and the positions of jaw muscles (Wood 1985), multiserial incisor enamel, pterygoid fossa communicating with the orbit, fusion of malleus with incus (Patterson 2016), or several characteristics of their reproductive system, such as their ovarian cycle length, long gestational periods, and the modified ovary structure called accessory corpora lutea (Faulkes et al. 1990). Traits supporting the phylogenetic placement into the Phiomorpha group comprise of at least three dental characteristics (Barbiére and Marivaux 2015). The situation with derived traits is more complicated, due to the morphological convergence with other subterranean rodents. Yet, there are some distinctive features, for example, enlarged angular process of mandible, incisors without pigment and rooted posteriorly to molars, which are simplified (Patterson 2016), and different morphology of upper and lower molars (Mein and Pickford 2008).

Individual extant genera possess unique characteristics as well. At first sight, they vary in size (from *Heterocephalus* with up to 80 g to *Bathyergus* reaching 2 kg) and pelage colour (from generally unicoloured of various tinges of brown to strikingly black-white-russet marking in *Georychus*). The internal recognition features are based mainly on the number of cheek teeth (3/3 in *Heterocephalus*, up to 4/4 in *Bathyergus*, *Georychus*, *Fukomys*, *Cryptomys*, and up to 6/6 in *Heliophobius*) and their infolding of enamel (De Graaf 1968; Jarvis 2013; Monadjem et al. 2015).

1.4 History of bathyergid taxonomy

As it is common for all subterranean mammals, selective pressure of an underground environment decreases the diversity of morphological traits between taxa. Thus, providing a clear taxonomy based on morphology represented a challenging task for scientists. Firstly, morphological systematics placed the African mole-rats mainly among mouse-like rodents (Muridae: Waterhouse 1841; Myomorpha: Alston 1876; Thomas 1896; Trouessart 1899). Although in most taxonomic studies bathyergid representatives were considered as monophyletic, there were also other opinions. For instance, Alston (1876) placed bathyergids into two subfamilies of family Spalacidae; genus *Heterocephalus* into Spalacinae together with *Rhizomys* and *Spalax*, and the remaining genera (*Georychus*, *Heliophobius*, and *Bathyergus*) into Bathyerginae.

At that time, the position of African mole-rats among rodents was extensively debated. While some morphologists excluded this family from mouse-like rodents, considering

bathyergids as an isolated rodent group (Miller and Gidley 1918 and Weber 1928 in Ellerman 1940; Wood 1955), others highlighted their affinities to hystricomorphs (Tullberg 1899 and Winge 1924 in Ellerman 1940; De Graaff 1979). In addition, Romer (Romer 1958 in De Graaff 1979) included African mole-rats among sciuromorphs according to two fossils. Finally, Wood (1985) reviewed known and used morphometric traits including mainly shape of the skull and the positions of jaw muscles and strongly supported the affinities of bathyergids to hystricomorphs, which was confirmed by molecular characters (Nedbal et al. 1994). Later, several characteristics of mole-rat were found to be more similar to members of this sub-order, supporting their affinity (in the chapter 1.3).

1.5 Species diversity of bathyergids

In contrast to the highly supported generic classification of bathyergids, the species (intrageneric) diversity is still not well resolved. This is, among others, caused by inconsistent application of species delimitation criteria. New species have been described on the ground of morphological and karyotypic data, or using one (or possibly a few) genetic markers (e.g. Faulkes et al. 2004, 2010, 2011, 2017; Van Daele et al. 2004; 2007b, 2013; Gippoliti and Amori 2011; Visser et al. 2014).

1.5.1 Problems of used approaches determining the species diversity

Species concepts and the criteria for species delimitation were extensively discussed for a long time (Cotterill et al. 2017; Gippoliti 2019; Taylor et al. 2019; Zachos et al. 2019). In subterranean rodents, exclusively morphological approach is limited by the lack of diagnostic characters, as it is described above. Thus, many cryptic species can remain unrevealed unless genetic methods are applied.

Yet, molecular approaches have also their own limits and ambiguities and the existing experience suggest their results should be considered critically. Most importantly, physically unlinked loci in DNA evolve independently, as the genealogies of particular loci (gene trees) may differ each other as well as from the population-level phylogeny (species tree). Thus, single locus analyses are not reliable. Especially the mitochondrial (mtDNA) and nuclear DNA, are prone to this phylogenetic discordance due to different mode of inheritance (Toews and Brelsford 2012). Complete or partial mitochondrial introgression was evidenced in several taxa (e.g. Runck et al. 2009; Zinner et al. 2009; Furman et al. 2014; Good et al. 2015; Ait

Belkacem et al. 2016; Cannicci et al. 2017; Schmidt et al. 2017; Bryja et al. 2018a), and in bathyergids it can explain the observed discordance between mtDNA and karyotypic differences (Van Daele et al. 2007b). Mitochondrial DNA also has generally higher mutation rate and lower effective population size and thus it shows finer population structure than typical nuclear markers (Galtier et al. 2009), as it was observed among vertebrates (Weibel and Moore 2002; Steppan et al. 2005; Eytan et al. 2010). This can explain, why the division into up to six mitochondrial lineages observed in bathyergid genus *Georychus* (Visser et al. 2018) were not exactly confirmed by analysis of three nuclear markers (Visser et al. 2019a).

Modelling phylogenetic discordance at different loci allows more robust inference of species limits and species phylogeny although its success is dependent on the number of markers (Felsenstein 2006, Faircloth et al. 2012). In contrast the interpretation of single-locus analyses is always questionable, especially when mtDNA is involved (Zachos et al. 2013).

1.6 Factors affecting diversification of mammals in the Eastern Africa

It is well known that diversification of many mammalian taxa in the Eastern Africa was affected by the formation and later by the presence of EARS. Its rich geomorphological structures either prevent gene flow across natural barriers, such as mountain ranges, depressions, and lakes. Alternatively, the geomorphological complexity of the landscape has provided inhabitants with plentiful habitats, changing over time with fluctuations of climate. These factors together with dramatic climatic changes during the Plio- Pleistocene created from the EARS a speciation cradle for many mammals in this part of continent. Even though the EARS impact has been significant for many mammals (Girman et al. 2001; Pitra et al. 2002; Dubach et al. 2005; Potts 2013), it seems that it impacted mainly evolution of the small ones, because of their limited ability for dispersal, dependence on specific habitat, and short generation times (e.g. Demos et al. 2014; Bryja et al. 2014; Rowan et al. 2016; Lavrenchenko et al. 2016; Petružela et al. 2018; Mazoch et al. 2018; Krásová et al. 2019).

1.7 Evolution of mammals in African savannas

At present, African ecosystems comprise of various types, such as forests, deserts, or islands of afro-alpine vegetation. Yet, savanna ecosystems, defined as mainly grassland with discontinuous woods or shrubs (Ratnam et al. 2011), are one of the most widely distributed ones, covering around half of the African land (Mayaux et al. 2004). Various types of

savannas, from mainly grasslands to savannas with trees and shrubs forming a light canopy, are characterized mainly by annual rainfall and density of woods (Sankaran et al. 2005). Extensive grasslands occurred around Late Miocene and a very complex network of savannas-like and forest-like habitats was formed. During following periods of climatic oscillations, a complex of periodically isolated and re-united savannas was generating, as forests dominated in wet periods, and grasslands spread during arid periods (deMenocal 2004). Not only climate was responsible for this dynamic. The natural barriers, such as mountain ranges, rifts, or lakes and rivers, could have a significant effect on spreading of ecosystems with its inhabitants or also directly restricted dispersions of particular mammalian species. For example, in the Southern Africa, the dynamic river system had a significant effect on genetic diversification of mammalian taxa (Cotterill 2003; Van Daele 2004, 2007a, b; Castiglia et al 2012; McDonough et al. 2015). Yet, because of the rich geomorphology of EARS, probably the most complex of savanna-woodland mosaic was and still is in the Eastern Africa. Therefore, various studies suggest that savannas of Eastern Africa played a crucial role in speciation of many mammalian lineages (Moodley and Bruford 2007; Van Daele et al. 2007b; Verheyen et al. 2011; Faulkes et al. 2011; Colangelo et al. 2013), including humans (Gibernau and Montuire 1996; Potts 1998).

1.8 Historical biogeography of bathyergids

Although bathyergids life expectancy is generally longer than in other small mammals, their very limited dispersal abilities and association with savanna habitats resulted in a sensitivity to vegetation changes. Taking their life history traits and current distribution of African mole-rats, the diversification is expected to be highly affected by the presence of EARS (Ingram et al. 2004; Van Daele et al. 2007a; Faulkes et al. 2011; Bryja et al. 2018b; Visser et al. 2019b).

To provide a credible/plausible scenario about the evolutionary history of bathyergid family and to identify factors responsible for their diversification, it is necessary to have well founded information about historical processes of the area. Under assumption the present day distribution ranges of bathyergids reflect where genera originally evolved, the colonisation scenario can be roughly reconstructed from their phylogeny and distribution. Two basal genera (*Heterocephalus* and *Heliophobius*) occur mainly in EARS or east of it, whereas the remaining genera (*Bathyergus, Georychus, Fukomys, Cryptomys*) occupying mostly in the south-west off the EARS. Later, three genera occur in the southern part of continent with *Fukomys* distributed from the Western up to the Central Africa. It is widely accepted, that the family originated in

the Eastern Africa and spread through the arid corridor to the South Africa, where two generic complexes separated. While *Bathyergus* and *Georychus* remained there, the ancestor of *Cryptomys* and *Fukomys* continued northward, with *Fukomys* reaching the Central Africa (Faulkes et al. 2004; Van Daele et al. 2007a; depicted in Fig. 2). Such scenario slightly differs among studies, for example, Visser et al. (2019b) assume that the separation of *Bathyergus* – *Georychus* and *Cryptomys* – *Fukomys* happen shortly after their ancestors left the East Africa (around 22 Mya) and separately dispersed through their own routes.

On the other hand, it should be mentioned that so far published temporal diversification scenarios of bathyergids vary significantly (Tab. 1) attributing the same phylogenetic splits with different historical events. While in some studies estimated *Heterocephalus* split from the rest prior to the formation of EARS (Faulkes et al. 2004; Van Daele et al. 2007a; Visser et al. 2019b), results of others indicate the opposite scenario (Faulkes et al. 2017), or they hypothesized these events being co-incident (Bryja et al. 2018b). Similarly, the intrageneric evolution of *Heliophobius* was driven mainly either by the formation of EARS (diversification in 20-7 Mya; Faulkes et al. 2011), whereas Bryja et al. (2018b) demonstrated the Plio-Pleistocene climatic changes in the already formed EARS environment (start of the diversification in 4 Mya). Also, the subdivision of the ancestral populations of *Fukomys* might be mainly due to tectonic activity and climatic fluctuations (Faulkes et al. 2004, 2010, 2017) or changes of major river systems (Van Daele et al. 2004, 2007a, b).

Differences in dating of major bathyergid diversification events are caused mainly by employing of different calibration of molecular clock. Even though a relatively high number of extinct bathyergids was found, there is no reliable evidence about direct relationship of most of them with particular extant genera (c.f. Winkler et al. 2010). Including them as calibration points (Ingram et al. 2004; Faulkes et al. 2011; Visser et al. 2019a, b) could bring large distortion of divergence estimates, if they are assigned to wrong lineages. In addition, some authors (Faulkes et al. 2004, 2017; Van Daele et al. 2007b) used for the dating so-called secondary calibration points, i.e. applying already estimated divergence time from earlier studies. Recently, a relatively new approach estimates the diversification times by implementing suitable fossil data into a fossilized birth-death model without need of a prior node calibration solving the situation of high number of uncategorized fossil taxa (Heath et al. 2014). Applying this method to the phylogeny of bathyergids, Bryja et al. (2018b) obtained much younger divergence times, e.g. the root of the family tree was only as old as 22 million years (Ma), where the previous studies mentioned above showed it older than 30 or even 40

Ma (see Tab. 1). Interestingly, divergence dating studies of older mammal radiations based on multiple nuclear genes and fossil calibration points also placed the origin of bathyergids to the early Miocene, about 26 Ma (Sallam et al. 2009; Fang et al. 2014).

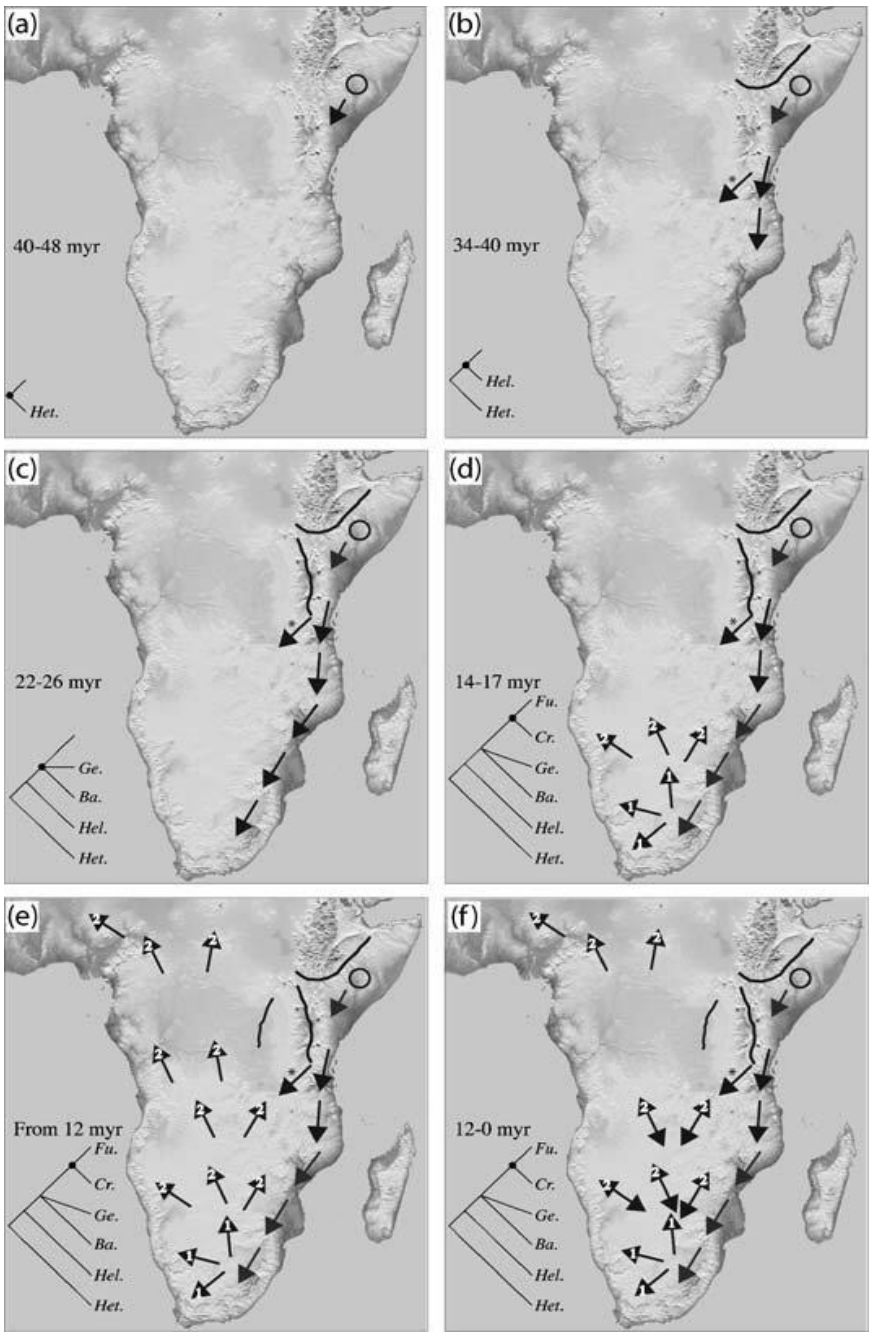

Fig. 2: Phylogeographic patterns of bathyergids published by Van Daele et al. (2007a). The individual maps show their divergence step by step from (a) the origin of *Heterocephalus* (Het.) lineage in East Africa, across (b) gradual distribution of *Heliophobius* led by formation of Rift Valley and (c) spreading *Bathyergus* (Ba.) and *Georychus* (Ge.) lineages into Southern Africa to the last radiation (d-f) of *Cryptomys* (Cr.) mainly in South Africa (1) and *Fukomys* spreading north into Southern, Central and West Africa (2). For critical consideration of the indicated timescale see Tab. 1.

Tab. 1: The different dating of the diversification of bathyergid genera (in million years ago) in hitherto studies.

	Diversification between …. (in Mya)				
A study	*Heterocephalus* × rest	*Heliophobius* × rest	*Cryptomys/ Fukomys* × *Georychus/ Bathyergus*	*Bathyergus* × *Georychus*	*Cryptomys* × *Fukomys*
Huchon and Douzery (2001)	48-40	15-12	11-9	-	-
Faulkes et al. (2004)	48-40	40-34	26-22	19-16	17-14
Ingram et al. (2004)	35-33	20-19	-	-	12-11
Sallam et al. (2009)	26	-	-	-	-
Faulkes et al. (2011)	32	20-19	-	-	-
Patterson and Upham (2014)	31	18	13	11	10
Fang et al. (2014)	26	-	-	-	-
Faulkes et al. (2017)	-	20-19	-	-	11
Bryja et al. (2018b)	22	11	9	8	6-7
Visser et al. (2019a)	-	-	16-15	15-12	-
Visser et al. (2019b)	35	35	29	22	25

1.9 The silvery mole-rat *Heliophobius argenteocinereus*

So far, the silvery mole-rat (*Heliophobius argenteocinereus*) is considered to be the only member of this genus (Bennett and Faulkes 2000; Happold et al. 2013; Wilson et al. 2016), but there are also different opinions such as three (Visser et al. 2019b) or six species (Faulkes et al. 2011; Monadjem et al. 2015). Bryja et al. (2018b), on the contrary, suggested only one species of silvery mole-rat.

The silvery mole-rat is a medium-sized mole-rat, with the mean weight of 190g for males and 162g for females (Šumbera et al. 2003). As the species name indicates, their silky and quite long pelage has silvery-grey colour (Fig. 3A), getting slightly paler on the ventral side. Some individuals have small white patches on their foreheads (Happold et al. 2013). Their body size and pelage colour slightly vary through the species distribution (Faulkes et al. 2011; Happold et al. 2013).

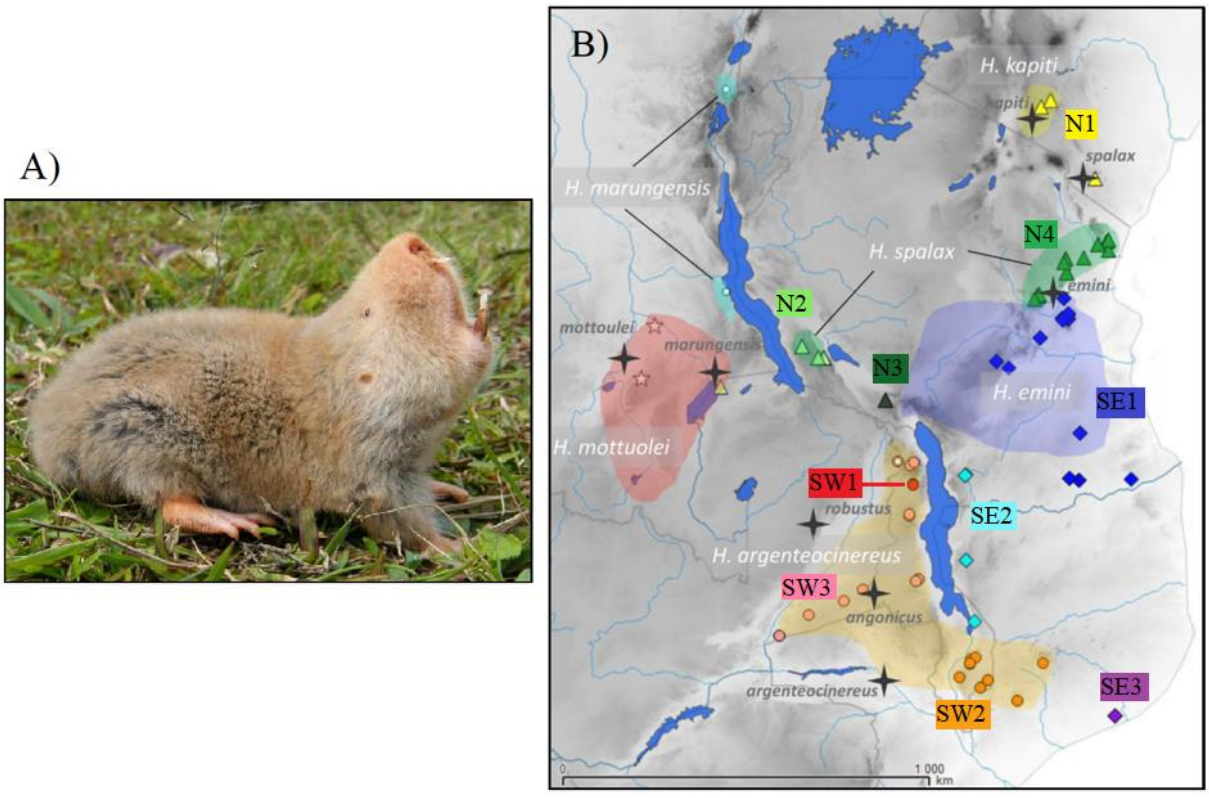

Fig. 3: A) A representative of *Heliophobius argenteocinereus* (photo by Radim Šumbera); B) Areas with different colours and white names show the distribution of species published by Monadjem et al. (2015), black crosses with grey names indicate the geographic position of type localities of *Heliophobius* species, and remaining symbols corresponds to cytb lineages found by study of Bryja et al. (2018b), from which the picture is taken and modified.

Heliophobius argenteocinereus is a strictly solitary species, aggressively defending its own burrow system against all conspecifics, except of short period of breeding season in which adults tolerate opposite sex and pups in case of female. The individuals may disperse aboveground and because of their limited ability to move on the surface, the distances are relatively short. As a result, even relatively close geographical populations tend to be genetically highly isolated (localities were 41 to 70 km apart; Patzenhauerová et al. 2010). *Heliophobius* is sexually monomorphic in size, it has relatively small testes and balanced sex-ratio (Šumbera et al. 2003) which generally suggests the monogamous mating system (Parker et al. 1997), but the cases of polygyny and multiple paternity were found based on paternity analysis (Patzenhauerová et al. 2010). This mole-rat is supposed to search for their mates also aboveground and such trips could be even 700m long (Patzenhauerová et al. 2010).

This species has the largest distribution of all African mole-rats inhabiting the areas of the southern Kenya, Tanzania, eastern Democratic republic of Congo, north-eastern Zambia, Malawi, and northern Mozambique (

Fig. *5*) (Happold et al. 2013). Most of its distribution lies in mesic area with >900 mm of rainfall annually and wide range of altitudes up to 2000 m above sea level where it occupies various savanna habitats from grassland to miombo woodland. In the northern most part of its distribution in Kenya, *Heliophobius* occurs in warmer and sandy areas with lower annual rainfall 250-600 mm (Jarvis and Sale 1971; Burda 2001; Šumbera et al. 2007). The range of soil types throughout its distribution is wide – from black cotton soil, which is extremely hard when dry and sticky and heavy when wet to soft cultivated farmland soils.

1.9.1 The taxonomy and genetic structure of *Heliophobius*

Across *Heliophobius* distribution, about nine forms were described in an early literature. Taxonomic simplification by Ellerman (1940) rearranged all nine taxa, except for *H. spalax*, to subspecies of *H. argenteocinereus*, namely *H. a. argenteocinereus, H. a. angonicus, H. a. robustus, H. a. marungensis, H. a. emini, H. a. kapiti, H. a. albifrons,* and *H. a. mottoulei*. Later, the re-examination of *H. spalax* detected used diagnostic features as age dependent and thus indistinguishable to species *H. argenteocinereus* (Honeycutt et al. 1991). Also, Happold (2013) synonymised all other species with *H. argenteocinereus*, although molecular approaches revealed apparent mitochondrial and small karyotype divergence between some populations. For instance, the 7.3% pairwise difference on 12S ribosomal RNA was found

between the silvery mole-rats from Kenya on the one side and from Zambia and Malawi on the other side (Ingram et al. 2004). Alternatively, a study of Faulkes et al. (2004) revealed significant divergence on cytochrome b (cytb). The karyotype of Zambian and Malawian (2n=62) populations slightly differ from the Kenyan (2n=60) population (Scharff et al. 2001, Šumbera et al. 2007).

With the increased sampling, Faulkes et al. (2011) revealed, on the grounds of the cytb marker, six clades with a clear geographic separation within a population of *Heliophobius*. Clades 2a, 2b and 3 were found to occupy eastwards to the EARS and the remaining clades 1, 4, and 5 are distributed mainly westwards to this geomorphological formation. The basal clade 1 consisted of sequences retrieved from the museum samples from Democratic republic of Congo. Following two monophyletic clades 2a and 2b are distributed northwards to and in the northern part of the Eastern Arc Mts (EAM) and are by this mountain range separated from clade 3 occupying the south. Yet, two localities (Nguru Forest, Msembe) suggest a distributional overlap between clades 2b and 3. Clade 4 contains samples from Zambia and Malawi, and all museum samples found in Democratic republic of Congo, Rwanda, and Zambia form the clade 5. All their performed analyses (maximum parsimony, maximum likelihood, Bayesian phylogeny) consistently resolved these main clades with similar topology and good supports. Also, the genetic differences (uncorrected p distances) were calculated to be relatively low within (2.4-7.2%) and relatively high between clades (6.3-17.7 %). Moreover, calculated diversification times of all clades were found to be very deep. The diversification process started around 20 Mya and ended around 7 Mya. These results led the authors to suggest change status of found clades into species. However, they also mentioned the need for wider sampling and further work with nuclear markers and microsatellites to test potential gene flow. This taxonomic arrangement (Fig. 3B) was adopted in recently published Rodents of Sub-Saharan Africa (Monadjem et al. 2015), but not in other compendia (Happold 2013; Wilson et al. 2016).

For studying the relationships within *Heliophobius* population, Bryja et al. (2018b) sampled new localities and except for cytochrom b, they use also three nuclear markers (NADSYN, TRPV, DHCR) and eight polymorphic microsatellites (DMR2, DMR7, CH1, CH2, Harg02, Harg03, Harg07, Harg08). With the extended sampling, they revealed even higher genetic structure then was revealed by Faulkes et al. (2011). According to Bryja et al. (2018b), this genus comprises of ten lineages with very similar geographical pattern: a separation by EARS and EAM. This result was proven by both, mitochondrial and nuclear

markers. Nevertheless, microsatellites suggest gene flow across delimited lineages, even across the geographical barriers mentioned above. Moreover, new method for estimation of divergence times suggest notably younger split of extant *Heliophobius* populations. The delimited lineages diversified in the Plio- Pleistocene (starting in 3.7 Mya).

On top of that, Bryja et al (2018b) found serious errors in study of Faulkes et al. (2011). First, the geographical overlap of two clades in the EAM suggesting their reproductive isolation was caused by wrongly positioned localities (Nguru Forest, Msembe). If these two localities are placed correctly, there is no evidence for sympatric distribution between the clades. Secondly, at least some sequences obtained from museum specimens represent chimeras originated probably during the PCR processing. As the museum DNA is of a low quality, a potential contamination during the PCR amplification can happen. In this case, successfully acquired sequences compose only of a short part of the whole cytb, in some cases of short parts connected together with unspecified nucleotides (N). Bryja and colleagues found out, that if fragments of one Faulkes at al. (2011) sequence are taken separately into a new phylogenetic analysis, each fragment independently cluster with other analysed individuals across the whole tree, in two cases even with a genus *Cryptomys*. This is probably the reason, why sequences from museum samples formed unique clades in a study of Faulkes et al. (2011). Consequently, these clades (1 and 5) are not trustworthy and can not be consider as valid. Based on all the findings, authors recommend using again a single species *H. argenteocinereus*, awaiting a more detailed study.

1.10 The Cape mole-rat *Georychus capensis*

Traditionally, a genus *Georychus* consists of a single member, the Cape mole-rat (*Georychus capensis*), but authors of recently published studies propose five Georychus species (Visser et al. 2019a, b).

Similarly to the silvery mole-rat, the Cape mole-rat is a strictly solitary and strongly territorial species, occupying and aggressively defending its own burrow system. This medium-sized bathyergid (on the average 181 g) possess a white facial and head mask, not found in any other mole-rat species. Its fur is grayish from the ventral side and brown with various tinges from the dorsal side, going to darker shades on its head (Fig. 4). Brown tinges of the body colour vary through the population; however, colours are not specific for any locality (Bennett et al. 2006).

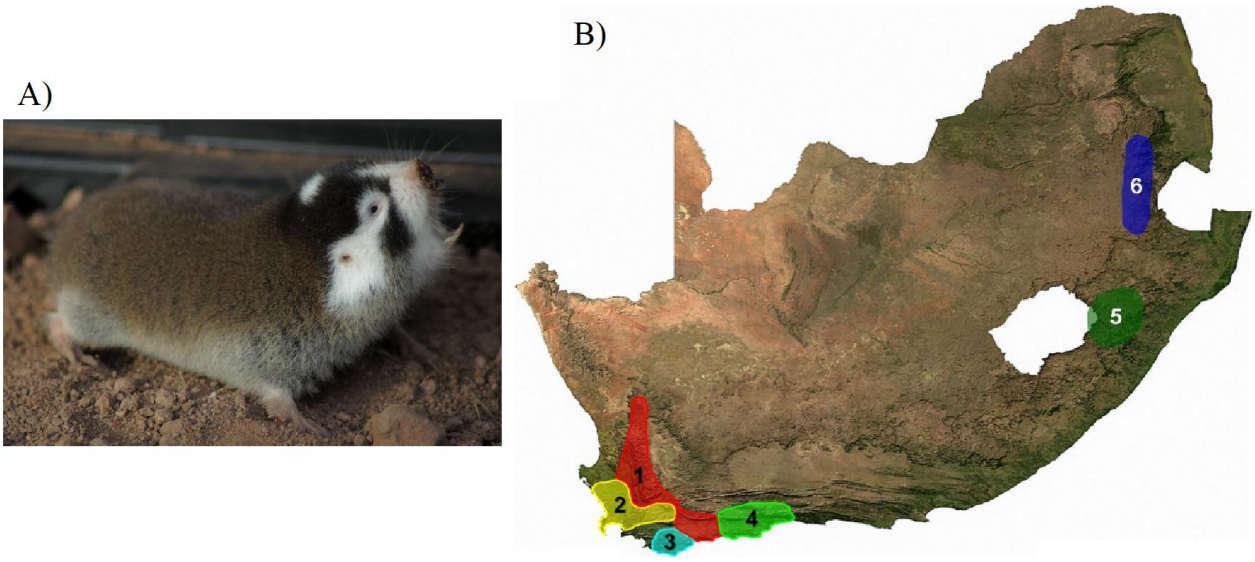

Fig. 4: A) A representative of *Georychus capensis* (photo by Jan Okrouhlík); B) Genetic clusters found in studies by Visser et al. (2018, 2019a, b).

The centre of the Cape mole-rat`s distribution lies in south-western coasts of South Africa, but there are two isolated populations in KwaZulu Natal and Mpumalanga regions (depicted in a map by numerals 5 and 6 respectively; Fig. *4*B) (Bronner 1990; Visser et al. 2018). Fossil evidence indicates wider distribution in the past. Some representatives of *G. capensis* were found in northern South Africa (Svartkrans Cave and Sterkfontein Valley) around 2.8-1 Mya (Avery 1998, 2001) and near the south-eastern coast of South Africa (Umhlatuzana) in late Holocene around 4000-1000 years ago (Avery 1991). A Plio-Pleistocene fossil is known also from northern Botswana (Ngamiland) (Pickford and Mein 1988 in Winkler et al. 2010).

Georychus capensis generally prefers areas with moderate temperature around 25 °C and annual rainfall ranging from 285 to 655 mm in the Western Cape and around 900 mm in KwaZulu Natal and Mpumalanga regions. They occur in different elevations from coasts in the western part of its distribution to the highlands with the altitude up to 2000 m in the eastern part of its distribution (Visser et al. 2017; Bennett et al. 2006). The most preferred types of substrates of this species are sandy loams, particularly coastal dunes, alluvium and clay soil along rivers and in montane areas (De Graaff 1981; Bennett et al. 2006). Although *Georychus* occurs in various vegetation types, such as fynbos, renosterveld, grassland and is commonly found in human modified areas, the main feature that shaped its distribution is believed to be areas with vleis or the vicinity of rivers (Visser et al. 2017). The mesic regions of south-

western Cape which is typical with extremely high geophyte diversity represent a typical locality for *Georychus*. On the other hand, similarly to other mole-rats, their non-random and effective search for food enables to inhabits habitats with low biomass productivity of geophytes, such as the montane fynbos (Du Toit et al. 1985).

1.10.1 The taxonomy and genetic structure of *Georychus*

According to an early scientific literature, *Georychus capensis* was divided to three subspecies: *G. c. capensis* distributed in the Western Cape Province, *G. c. canescens* occupying the southern Cape Province, *G. c. yatesi* from Mpumalanga region (Ellerman 1940; Ellerman et al. 1953). Several studies in last 30 years based on allozymes, restriction fragment length polymorphisms and mitochondrial sequences, suggested a deep separation of the disjunct populations from Western Cape, KwaZulu Natal and Mpumalanga warranting distinct species (Janecek et al. 1992; Honeycutt et al. 1987, 1991; Nevo et al. 1987; Faulkes et al. 2004; Ingram et al. 2004). Moreover, Janecek et al. (1992) found also considerable genetic differences of individuals in Nature`s Valley from other Cape populations.

The most recent studies confirmed findings about strong genetic structure across the genus distribution (Fig. 4B). The first study (Visser et al. 2018) covering whole geographic range revealed, on the grounds of cytb and control region of mtDNA, six genetic clusters. The highest and simultaneously comparable divergences were between Western Cape (lineages 1-4 in a map (Fig. *4*B)), KwaZulu Natal (lineage 5), and Mpumalanga populations (lineage 6). The genetic variability was partitioned from 47% among these three groups, from 44% among populations within each group, and only from 8% within each population. The following papers (Visser et al. 2019a, b) supported the previous division, with the exception of lineages 1 and 2 in the Western Cape (Fig. 4B), which in those studies formed one cluster. Visser et al (2019a) used a combination of mtDNA (namely cytb) and nuclear markers, namely GHR, TTR, and BFibr, while the later study (Visser et al. 2019b) based the delimitation mainly on sequence divergence from cytb marker. Both studies reached more or less the similar topology of trees, according to maximum likelihood and Bayesian analyses with cytb or combined datasets. Only a phylogeny based solely on nuclear markers merged a group containing lineages 1 and 2 also with a lineage 3 from Struisbaai (near the Cape Agulhas). Simultaneously, both studies revealed the significant sequence divergences between delimited clades on a cytb (up to 12.2 % in a former and up to 12.1 % in a later study) and three nuclear markers (ranging from 0.3 to 0.8 %) datasets. According to authors, diversification process of

all clades occurred already during Miocene. Yet, the estimated times considerably vary depending the used markers and calibration of clock: 6-4 or 10-5 Mya (nuclear or mitochondrial datasets respectively with a fossil *Proheliophobius* as a calibration point; Visser et al 2019a) or even 16-9 Mya (mitochondrial dataset with the same calibration point, but most probably set to a different node of a tree; Visser et al 2019b). Different types of soil, altitude, and annual rainfall between the main localities are in these studies considered as supporting facts for the uniqueness of revealed clusters. Taking all evidences together, the authors proposed the delimitation of all five genetic lineages into separate species.

2 Aims of the thesis

Main aim of this thesis is to reconstruct intrageneric relationships of two solitary African mole-rat genera (*Heliophobius* and *Georychus*) by using two molecular approaches:

1) Sanger sequencing of six nuclear markers (RAG1, FGB, DHCR, NADSYN, SMO, and TRPV)
2) High-throughput sequencing, specifically double digest Restriction-site Associated DNA sequencing (ddRADseq)

3 Materials and methods

3.1 Sampling and DNA isolation

In total, the material consists of 101 specimens of *Heliophobius argenteocinereus* and 43 of *Georychus capensis*. *Heliophobius* samples were collected during field expeditions to Kenya, Malawi, Mozambique, Tanzania and Zambia from 32 localities between years 2000 and 2016 (Fig. 5, Tab. S1 in the Supplement). Samples of the genus *Georychus* from 13 localities in the Republic of South Africa were provided by Bettine van Vuuren from the Centre for Ecological Genomics and Wildlife Conservation in the University of Johannesburg (for details about collection procedures see Visser et al. (2018)) (Fig. 6, Tab. S1 in the Supplement). The tissue from *Heliophobius* were taken after the dissection of wild caught individuals, while the samples of *Georychus* were obtained from frozen animals. Tissue samples (spleen, liver, muscle or toe) were taken and stored in 96% ethanol until DNA extraction.

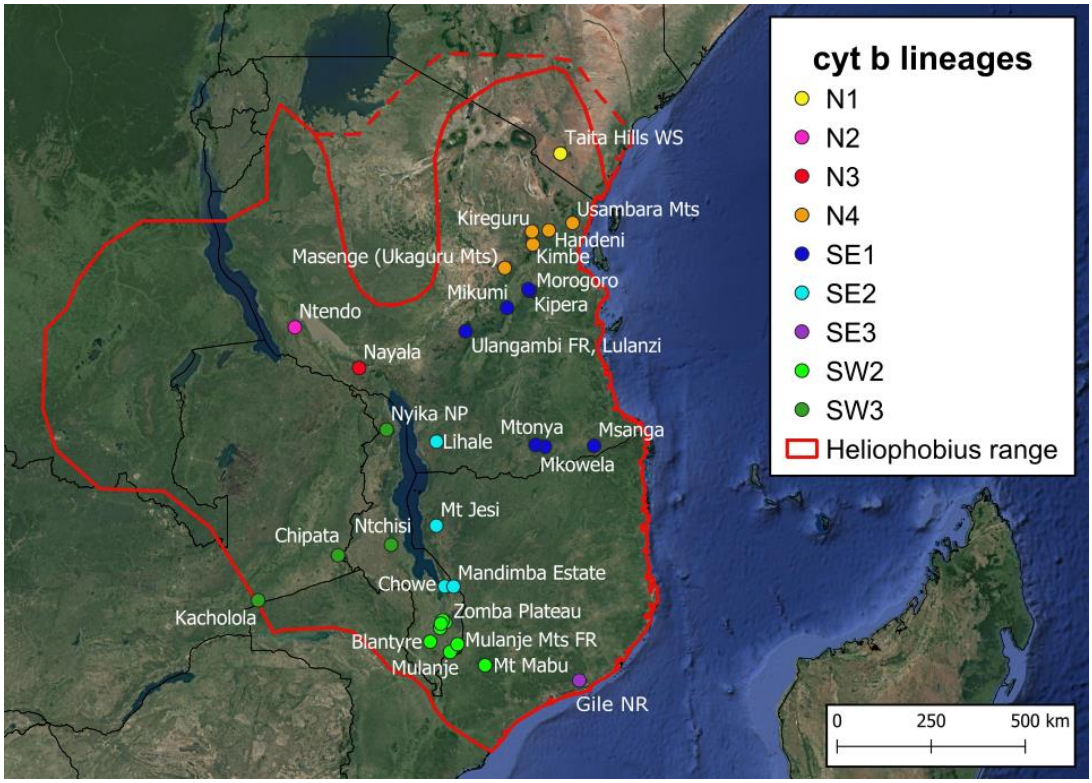

Fig. 5: The map of 32 localities of *Heliophobius* samples grouped according to mitochondrial lineages found in a previous study (Faulkes et al. 2011; Bryja et al. 2018b). Red line depicts the geographic distribution; the part of the distribution marked by a dashed link, is considered as probable (IUCN 2019). The name Zomba Plateau in fact represents four nearby sites (Zomba plateau, Domasi, Malosa, and Mpalanganga estate).

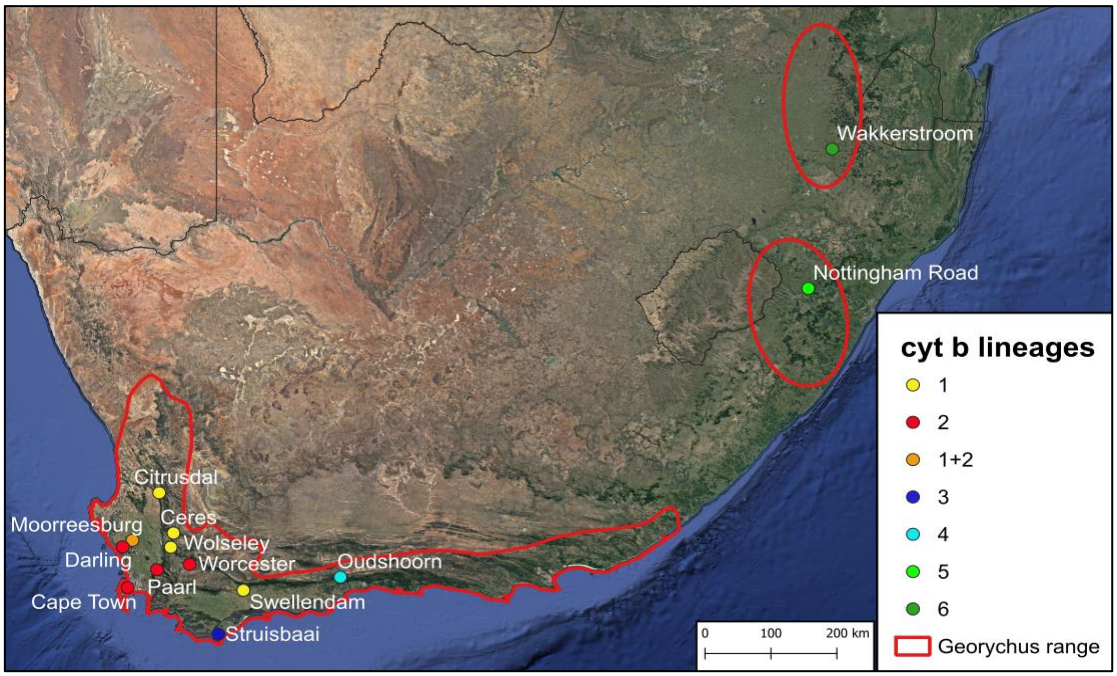

Fig. 6: The map showing 13 localities of *G. capensis* with mitochondrial lineages from a study of Visser et al. (2018) with the area of distribution (IUCN 2020).

DNA was isolated using a commercial kit DNeasy Blood & Tissue Kit (Qiagen) according to enclosed protocol. Since the DNA for the genomic use (ddRADseq) should not be fragmented, I verified the quality of extractions. Isolates were electrophoresed on an 1% agarose gel for the detection of product length and fluorometrically measured by The Qubit® 2.0 Fluorometer using dsDNA BR Assay Kit (Qubit) to analyse the DNA concentration.

3.2 Analysis of genetic structure with nuclear markers

23 individuals of *Heliophobius* from 19 localities and 13 of *Georychus* from 7 localities, representing all major mitochondrial lineages (*sensu* Bryja et al. 2018b; Visser et al. 2018) were selected for an analysis of nuclear markers (these specimens are marked in Tab. S1 in the Supplement).

3.2.1 PCR and sanger sequencing

A polymerase chain reaction (PCR) was used for targeting altogether six nuclear markers, one exon (RAG1) and five introns (DHCR, FGB, NAD SYN, SMO, TRPV) (Tab. 2), in all 36 isolated samples. Each 10 µl PCR reaction contained 5 µl of Qiagen Multiplex PCR Master Mix or Qiagen HotStarTaq Master Mix Kit, 0.3 µl of each forward and reverse primer

(10 μM), 0.5 μl of DNA, and 3.9 μl ddH_2O. The thermocycling conditions for RAG1, DHCR, NAD SYN, SMO, and TRPV consisted of initial denaturation step at 95°C for 15min, 10 cycles of 94°C for 30s, 65°C for 30s (decreasing by 1°C with each cycle), 72°C for 1min, then 25 cycles of 94°C for 30s, 55°C for 30s, and 72°C for 1min, with the final step of 72°C for 10min. Amplification for FGB gene started with initial denaturation at 95°C for 15min, following by 35 cycles of 94°C for 40s, 59°C for 45s, 72°C 1min 30s, and ending with final extension at 72°C for 10min. The quality and lengths of fragments were verified by an electrophoresis in an 1% agarose gel using Top-Bio DNA marker. The purification of all amplified PCR products was performed by two enzymes (Exonuclease I, *E.coli* (Exo I, 20,000 units/ml) and Alkaline Phosphatase, Calf Intestinal (CIP, 10,000 units/ml) from New England BioLabs)) according to the following protocol: 0.05 μl Exo I, 0.1 μl CIP, 1 μl ddH_2O and 5 μl of PCR product; 37°C for 30min, 85°C for 15min in thermocycler. All genes were commercially sequenced with forward primers and those with lower quality results, all specimens for NAD SYN and some for SMO introns, were sequenced from reverse side for the verification. The sequencing process was accomplished by GenSeq s.r.o. company.

Tab. 2: A list of nuclear markers with primers sequences and lengths of final sequences.

Gene	**Sequences of primers (5´-3´)**	**Lengths of alignments (bp)**	**Reference**
RAG1	L: GCTTTGATGGACATGGAAGAAGACAT H: GAGCCATCCCTCTCAATAATTTCAGG	1104	Teeling et al. 2000
DHCR	L: CAGGACATGCTGGTGCCCATGAA H: CCTGGCTGGCTGGGCAGGATGAA	351	Rodriǵuez-Prieto et al. 2014
FGB	L: GGGGAGAACAGAACCATGACCATCCAC H: ACCCCAGTAFTATCTGCCATTCGGATT	848	Wickliffe et al. 2003
NAD SYN	L: GTYCGYTACAAYTGCAGAGT H: TCCTKSHCCAKGGGGTRAACCA	568	Rodriǵuez-Prieto et al. 2014
SMO	L: GCCACCCTGCTCATCTGGAGGCG H: TTGGCRATCATCTTGCTYTTCTTGA	434	Rodriǵuez-Prieto et al. 2014
TRPV	L: TTACCRBACCACVGYGGACTACCT H: CTGGAAGGAGCCRTCGAYGAAGA	291	Rodriǵuez-Prieto et al. 2014

3.2.2 The processing of sequenced data

Obtained sequences were adjusted in software Geneious Prime. Firstly, I checked the quality of sequences and verified them by online nucleotide database of NCBI BLAST (Basic Local Alignment Search Tool, https://blast.ncbi.nlm.nih.gov/Blast.cgi). Individual forward and reverse sequences of NAD SYN and SMO genes were merged into so-called contigs. All low-quality ends and primers of sequences were cut off by function Trimm Ends and for finding heterozygote nucleotides I used function Find heterozygotes. All sequences of individual genes were aligned using Geneious Alignment and final alignments were manually adjusted.

For the following phylogenetic analyses, all sequences of specimens were phased to haplotypes, corresponding to a pair of chromosomes in every individual. This process was performed by PHASE v2.1.1 (Stephens et al. 2001, Stephens and Scheet 2005), which is a Bayesian method estimating posterior probability distribution over haplotypes compatible with the observed sequences. The model assumes haplotypes to be in Hardy-Weinberg equilibrium and no recombination within loci. Only the base pairs phased with posterior probability ≥ 0.90 were accepted, otherwise an ambiguous nucleotide was assigned to both haplotypes. For the following Bayesian analyses in program BEAST, a random representative of haplotype was chosen for each individual to guarantee a random choice of specimens from the population.

3.2.3 Species delimitation analysis

Mitochondrial lineages described in the previous studies (Bryja et al. 2018b, Visser et al. 2018) served as operational taxonomic units (OTUs). To reveal whether they correspond to distinct nuclear gene pools, I used a package STACEY (Jones 2017), running under BEAST v2.6.0 (Bouckaert et al. 2014), which performs a species delimitation analysis based on the multispecies coalescence model (Rannala and Yang 2003). It uses birth-death-collapse prior (Jones et al. 2015) for species tree shape to identify units, which are likely collapsed (or merged, i.e. conspecific). Because of a missing sequence of *Georychus* for DHCR gene from lineage 5, I created it artificially by replacing SNPs with IUPAC nucleotide code for any base (N). The alignment of gene RAG was split into separate partitions according to the codon positions (2 vs. 3). In the case of *Heliophobius*, I used HKY substitution model (Hasegawa et al. 1985) with a diffuse lognormal prior on the transition/transversion ratio (parameter Kappa). HKY model was selected as a simple, yet versatile model of sequence evolution. In *Georychus*, however, it caused low effective sample size of posterior sample and thus even simpler JC

model (Jukes and Cantor 1969) was used. Every locus was assumed to have its own genealogical history (gene tree) and every partition had its own substitution model and substitution rate, which was estimated as a multiple of an average strict clock rate (arbitrarily set to unity). The length of the Markov chain Monte Carlo (MCMC) was optimized to achieve sufficient effective size of the posterior sample. Finally, it was set to 50000000 generations in *Heliophobius* and 20000000 generations in *Georychus* (logging every 5000 generation in both cases). The convergence of MCMC was checked in a program Tracer v1.7.1 (Rambaut et al. 2018) and posterior probabilities of species delimitations in program R v 3.5.2 (R Core Team 2019) after removing of 10% of trees as a burn-in.

3.2.4 Reconstruction of gene and species trees

In the subsequent phylogenetic inference, gene pools identified in STACEY are treated as species, whether or not they are to be given this taxonomic rank. The species tree of each genus was estimated under multispecies coalescence model as implemented in StarBEAST2 v0.15.5 (Ogilvie et al. 2017), which is also a package of BEAST 2. Here, the species are kept fixed and just their phylogeny is estimated. The data partitions, substitution and clock models were set as in STACEY, but as a species tree prior Yule Model was used, which is birth-death model assuming no extinction. The MCMC parameters were the same as in STACEY. I conducted two independent runs and checked in Tracer whether they converge to the same posterior distribution of parameter values.

3.2.5 Visualisation of haplotype diversity

An alternative view of genetic differentiation of mitochondrial lineages was provided by haplotype networks. The networks were created for each locus separately using TCS algorithm (Clement et al. 2002) in a program PopART v1.7 (Leigh and Bryant 2015). Because of the complexity of the whole dataset of the genus *Heliophobius*, I split the data to the northern (N1, N2, N3, and N4) and the southern group (SE1, SE2, SE3, SW2, and SW3) for a better presentation of relationships of their internal lineages.

3.2.6 Dating of divergence

Although relatively rich, the fossil record of bathyergids does not include many species showing clear affinity to extant genera and species and thus it does not allow node calibration

of molecular clock within reconstructed species trees. Therefore, to estimate divergence times among bathyergid lineages, I used a fossilised birth-death model (Heath et al. 2014) as implemented in Sampled Ancestors add-on package (Gavryushkina et al. 2014) of BEAST v 2.4.6. It estimates divergence times of recent species by modelling of speciation, extinction and fossilisation rates, which is informed by molecular data of extant species and by distribution of fossils in time.

In the analysis, I included all bathyergid genera and their sister lineage Phiomorpha (represented by *Petromus* and *Thryonomys*). Each genus was represented by its major mitochondrial lineages. Information about known fossils of bathyergids and phiomorphs were obtained from the paleontological literature (for more details see Tab. S2 in Supplement). Since markers sampled in this study are not available for all included genera, I used, instead, sequences of one mitochondrial (cytb) and three nuclear (GHR, IRBP, VWF) markers, acquired from Genbank database (https://www.ncbi.nlm.nih.gov). The alignment of cytb was split into two separate partitions (1+2) and 3, according to codon positioning. HKY substitution model with relaxed lognormal molecular clock was specified for all partitions. Every partition was set to have its own substitution model and substitution rate but share equal clock rate and phylogenetic tree. The removal probability parameter of the fossilised birth-death model was fixed to 1, which does not allow the fossils to be treated as direct ancestors of extant lineages. The parameters of MCMC were set to the overall length 30000000 generations with logging every 5000s. The progress of MCMC was checked in Tracer v1.7.1 and the maximum clade credibility tree was calculated in TreeAnnotator v2.6 (Bouckaert et al., 2014).

3.3 Analysis of genetic structure with ddRADseq loci

3.3.1 Library preparation

The complete DNA material comprising of 101 specimens of *Heliophobius* and 43 specimens of *Georychus* was processed into one final ddRAD library according to slightly altered protocol of Peterson et al. (2012). This final ddRAD library was prepared from three sub-libraries, each containing 48 samples ordered according to DNA concentrations as follows: LIB1 comprising of samples with ≥ 32.9 ng/µl, LIB2 14.4-32.6 ng/µl, and LIB3 ≤ 14.3 ng/µl. Because of such ordering, samples were randomly spread between libraries. In the first step, genomic DNA from each individual in the quantity of 300 ng or 200 ng, for samples with low

amount of DNA (LIB3), was digested by restriction enzymes. Overall volume and contents volume of restriction reactions varied according to sub-library. Total reaction volume was 30 µl in samples of LIB1 and LIB2 and 50 µl for samples of LIB3. Each reaction (LIB2 and LIB3) contained 0.25 µl of SphI-HF (5 U), 2 µl of MluCI (20 U), 3 µl of CutSmart buffer, and adequate amount of water. To ensure proper digestion of DNA in samples from LIB1, the volume of enzymes was increased (0.5 µl of SphI-HF, 2.5 µl of MluCI). After incubation in 37°C for 3 hours and purification of reaction products on magnetic beads, adapters (P1 and P2; Peterson et al. 2012) were ligated in a 40 ul reaction with 100 ng (LIB1, LIB2) or 80 ng (LIB3) of each restriction product. After this step, all 48 ligation products per sub-library differed in adapter barcode, so they could be pooled. Following precise size selection of 276-324 bp fragments from all three sub-libraries were performed on Pippin Prep preparative DNA platform. To amplify fragments, connect multiplex indexes and flowcell annealing sequences, several 50 ul PCR reactions were done for each sub-library. PCR amplified sub-libraries were purified on AMPure XP beads, quantitated and equimolary pooled into a final library. The sequencing process was realized on an Illumina HiSeq 2000/2500 in the EMBL Genomics Core Facility (Heidelberg, Germany).

3.3.2 The processing of raw data

Raw reads were filtered out from low quality sequences, sorted into individuals according to barcodes, and trimmed off from adapters in a component of a software Stacks v2.2 (Catchen et al. 2011) – process_radtags. Processed RAD sequences were aligned onto the reference genome (a bathyergid species *Fukomys damarensis* (GCA_000743615.1; https://www.ncbi.nlm.nih.gov)) using Bowtie v2.2.4. (Langmead and Salzberg 2012) with "very sensitive" set, and subsequently processed in the ref_map pipeline implemented in Stacks to assembly loci. Extracting of SNPs for the following phylogenetic analyses was processed in a population component of Stacks v2.3 for both genera separately. This step also filtered the datasets according to set parameters (minimum number of populations with present locus or minimum percentage of individuals in a population to process a locus for such population). From Stacks output, only loci with at least 90% sequencing success across individuals were selected. This step, done in a program R (R Core Team 2019), reduced the data sets from 105814 to a final 26594 loci from 101 individuals of *Heliophobius* and from 162295 to a final 40549 loci from 43 individuals of *Georychus*.

3.3.3 Cluster analyses

The similarities among individuals were visualised in the co-ancestry matrix estimated in RADpainter (Malinsky et al. 2018). It uses a modified algorithm of Lawson et al. (2012) for multiple discrete loci obtained by Restriction-Site Associated DNA sequencing (RADseq). The algorithm calculates, separately for each locus and each individual, the number of sequence differences (different alleles) between particular individual and all other individuals. Its nearest neighbour, showing the least number of differences, is considered as its closest relative at the locus. If multiple nearest neighbours are found, the co-ancestry is equally distributed within those neighbours, and in case of a missing allele, the average similarity of such allele to alleles of other individuals is assumed. At the end, all calculated co-ancestry values from all loci are summed to get the co-ancestry matrix for the whole data set.

To find and define cluster structures within the built co-ancestry matrix, two clustering methods were used: fineRADstructure and Infomap. The fineRADstructure clustering (Malinsky et al. 2018) estimates very fine population structure and uses a modified MCMC clustering algorithm of fineSTRUCTURE (Lawson et al. 2012) for RADseq data. It clusters rows of the matrix, which represent individual co-ancestry profiles as they mark similarity of one individual to all others. Since such co-ancestry profiles consist of counts (numbers of loci with detected co-ancestry), they can be modelled as coming from a multinomial distribution. fineRADstructure clusters only those profiles (i.e. individuals) that come from the same multinomial distribution. This method is Bayesian with built-in priors on the shape of multinomial distributions and the number of clusters. The posterior probabilities of clusters are estimated by MCMC (20000 generations with 50% burn-in and samples taken every 1000 generation in this case). The clustering with the maximum posterior probability was retained and the hierarchy of clusters was subsequently built by successively merging clusters in order of the minimum loss of likelihood.

The software Infomap detects broad structure among populations, and thus estimated clusters correspond more to phylogeographic lineages or species rather than families or local populations like in the case of fineRADstructure. This software uses the minimum description length (MDL) clustering (Rosvall and Bergstrom 2008) that works with the co-ancestry matrix as if it was a network. Nodes in such network stand for individuals and are connected by weighted directed links carrying information about counts of loci in the matrix. Each node in the description of the co-ancestry matrix is represented by a unique binary code, and the description length is expressed as the average code length calculated by the map equation

(Rosvall and Bergstrom 2008). The clustering algorithm (Blondel et al. 2008, Rosvall et al. 2009) seeks after tightly clustered nodes to assign them and their constituent nodes shorter codes, which makes the average code length shorter. The clustering minimizing description length is retained. Presented figures of maps and trees were created in R, using packages ape (Paradis & Schliep, 2018), rgdal (Bivand et al. 2019) and raster (Hijmans 2019).

4 Results

From all tissue samples, the DNA was successfully isolated in a sufficient concentration and volume for all laboratory procedures. PCR failed in one sample of *G. capensis* from Nottingham Road (lineage 5; Nrd3) for DHCR locus and two samples of *H. argenteocinereus* of the locus NADSYN from Mpalanganga estate (lineage SW2; M8x3085) and Chowe (lineage SE2; M8x3142).

4.1 The genetic diversity of *Heliophobius*

All OTUs were delimited as different species in STACEY analysis Tab. *3*: Posterior probabilities of lineage conspecificity in the genus Heliophobius estimated as proportions of species trees sampled by STACEY, where the lineages were collapsed.with the high posterior probability (PP = 0.83-1.00) (Tab. 3). These PP values are equal to the proportions of posterior samples where OTUs were not collapsed with any other OTU and hence supported as distinct "species".

In the maximum clade credibility species tree (Fig. 7) from StarBEAST analysis the lineages distributed southward to Eastern Arc Mountains (=EAM) (all SW and SE lineages) cluster together with PP=1.00, and the inner relationships are well supported for monophyletic groups SE1 (mainly south-eastern Tanzania) + SE2 (eastern side of Lake Malawi) with PP=0.91 and SW2 (southward from Lake Malawi) + SW3 (to the west from Lake Malawi) with PP=1.00. The monophyly of lineages distributed eastward to Lake Malawi (SE1, SE2, SE3) had lower PP (0.85). The northern group (northern part of EAM) cluster with a support PP=0.91, and within the group the support is strong only for monophyly of the group containing N3 (Nayala in south-western Tanzania) and N4 (northern part of EAM) lineages (PP=0.92). The support for N1+N2 (Taita Hills in southern Kenya and Ntendo south-eastward to Lake Tanganika respectively) was low (PP=0.48). All individual gene trees are available in the Supplement (Fig. S1), enabling better comparison with the following haplotype networks.

Haplotype networks of particular genes of northern lineages (Fig. 8) confirms, with some exceptions, the results of StarBEAST analysis, and show the genetic affinities of two most northern lineages of my data set (N1, N2) and lineages in Nayala and northern EAM (N3, N4). This trend is well visible in RAG and TRPV markers, on the other hand, the NAD SYN gene do not show any pattern among these lineages. The haplotype networks of the southern group (Fig. 9) do not correspond to the species tree. Haplotype network of FGB

marker mostly corresponds to the maximum clade credibility tree created in StarBEAST (Fig. *7*). Two separate clusters distributed eastward (SE lineages) and westward to Lake Malawi (SW lineages) are clearly visible, and the same, but weaker, pattern can be found in markers NADSYN and SMO. Nevertheless, the rest of the markers indicate no specific pattern.

The number of clusters in the ddRAD-based co-ancestry matrix differs between the clustering methods, as expected. While fineRADstructure method found 51 populations of very recent origin, Infomap clustering shows only two and evidently much older populations, i.e. the northern (N lineages) and the southern group (SE and SW lineages) (Fig. 10). The dendrogram made by fineRADstructure shows the identical topology and follows the delimitation of multilocus analyses of nuclear markers made in BEAST with two exceptions. Firstly, populations southeastward to Lake Malawi (SE lineages) are mixed up and do not correspond to the results of STACEY and StarBEAST analyses. Secondly, an individual from Taita Hills (lineage N1) integrated into a lineage SE1 from southeast of Tanzania (the second black branch from the top of the dendrogram). However, this outcome represents probably an error made during the library preparation. A map in a Fig. *11* demonstrates the geographic distribution of all 51 populations defined in fineRADstructure among sampled localities. For a greater clarity, neighbour localities closer than 10 km are merged and represented only by one site. On such space scale, genetic populations are more or less equally distributed with up to 6 populations per site. To get an idea of the space distribution of two multi-population sites (Masenge and Zomba Plateau), go to the Supplement (Fig. S3, S4).

Tab. 3: Posterior probabilities of lineage conspecificity in the genus *Heliophobius* estimated as proportions of species trees sampled by STACEY, where the lineages were collapsed.

	N1	N2	N3	N4	SE1	SE2	SE3	SW2	SW3
N1	0.99	0.01	0	0	0	0	0	0	0
N2	0.01	0.99	0	0	0	0	0	0	0
N3	0	0	1	0	0	0	0	0	0
N4	0	0	0	1	0	0	0	0	0
SE1	0	0	0	0	0.83	0.17	0	0	0
SE2	0	0	0	0	0.17	0.83	0	0	0
SE3	0	0	0	0	0	0	1	0	0
SW2	0	0	0	0	0	0	0	0.99	0.01
SW3	0	0	0	0	0	0	0	0.01	0.99

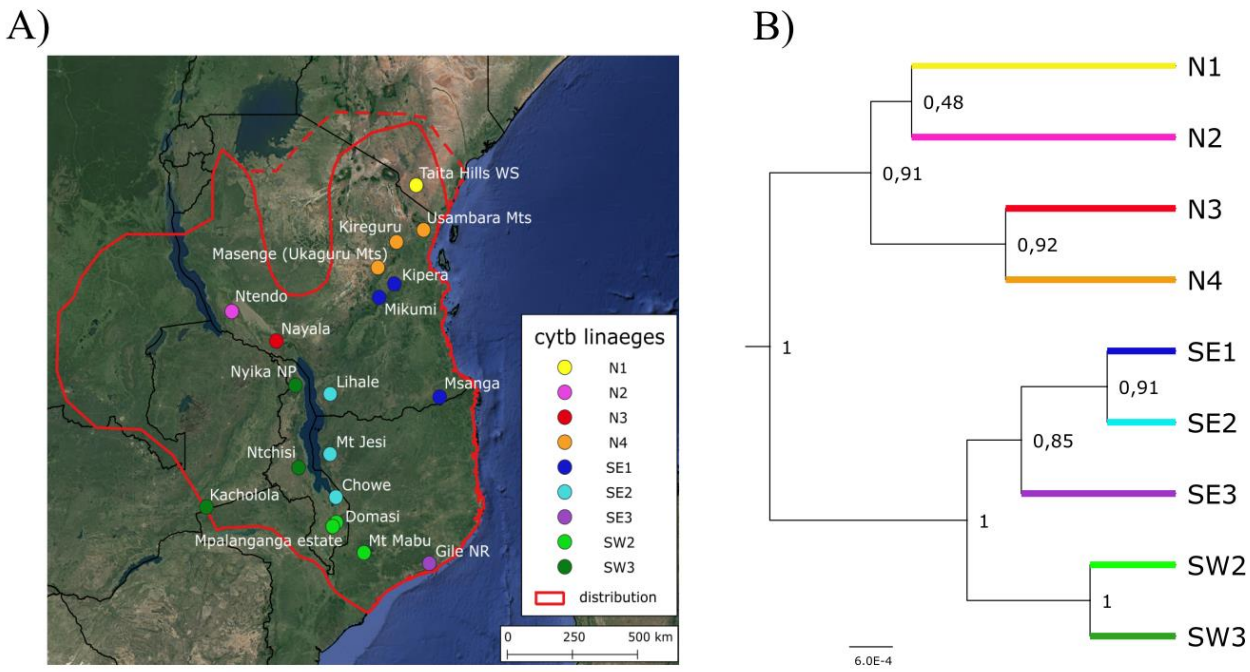

Fig. 7: A) The map with sampled localities for six nuclear markers of a silvery mole-rat coloured according to OTUs. B) The maximum clade credibility tree from StarBEAST analysis based on six nuclear markers for the genus *Heliophobius*. The numbers next to nodes show the posterior probabilities for the specific nodes and terminal nodes are named and branches coloured according to OTUs in the map.

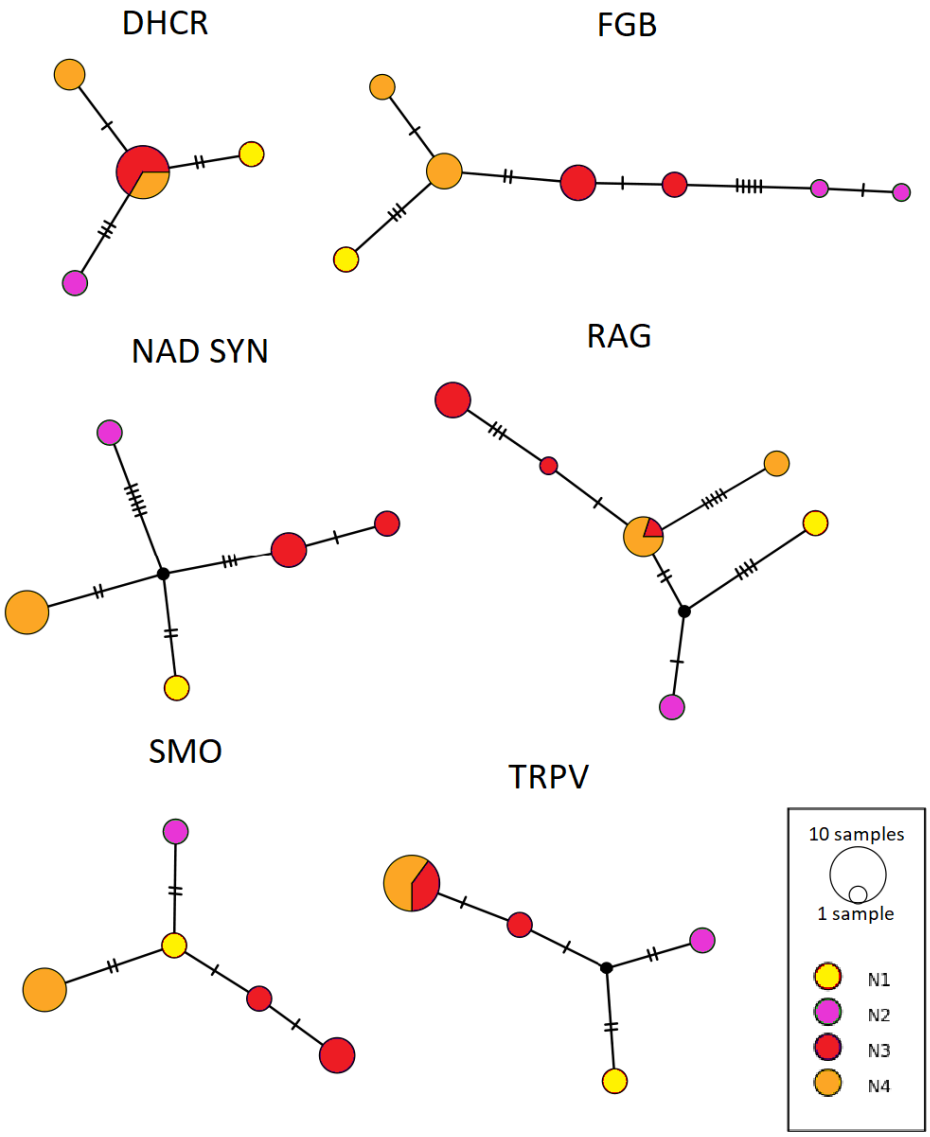

Fig. 8: Haplotype networks for the northern cytb lineages of the genus *Heliophobius* for all genes separately. Circles depict individual haplotypes, the size of circles corresponds to number of sequences, lines between circles represents mutual genetic connection, and number of transverse lines indicate the number of mutations between certain haplotypes.

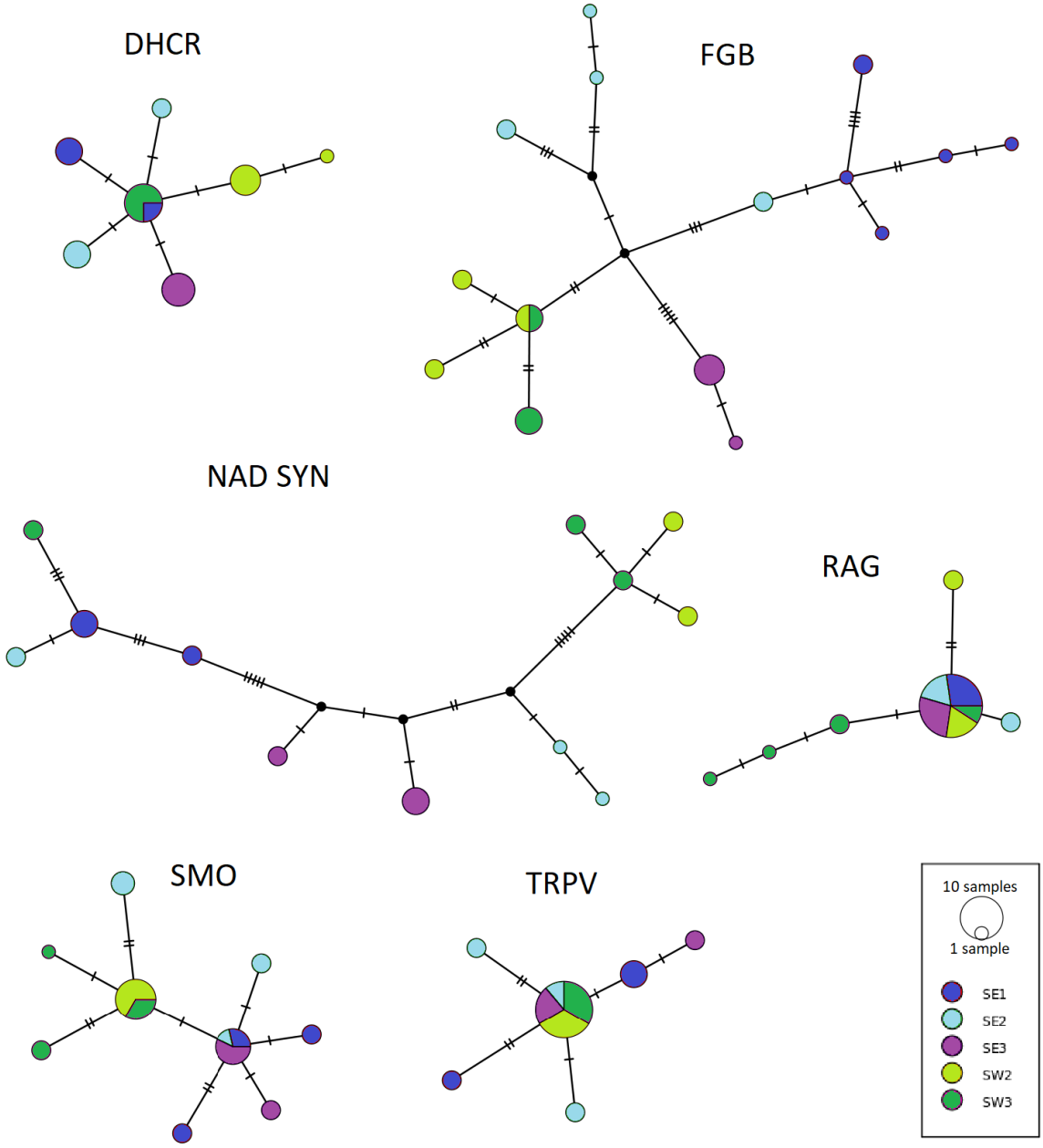

Fig. 9: Haplotype networks for the southern cytb lineages of the genus *Heliophobius* for all genes separately. Circles depict individual haplotypes, the size of circles corresponds to number of sequences, lines between circles represents mutual genetic connection, and number of transverse lines indicates the number of mutations between certain haplotypes.

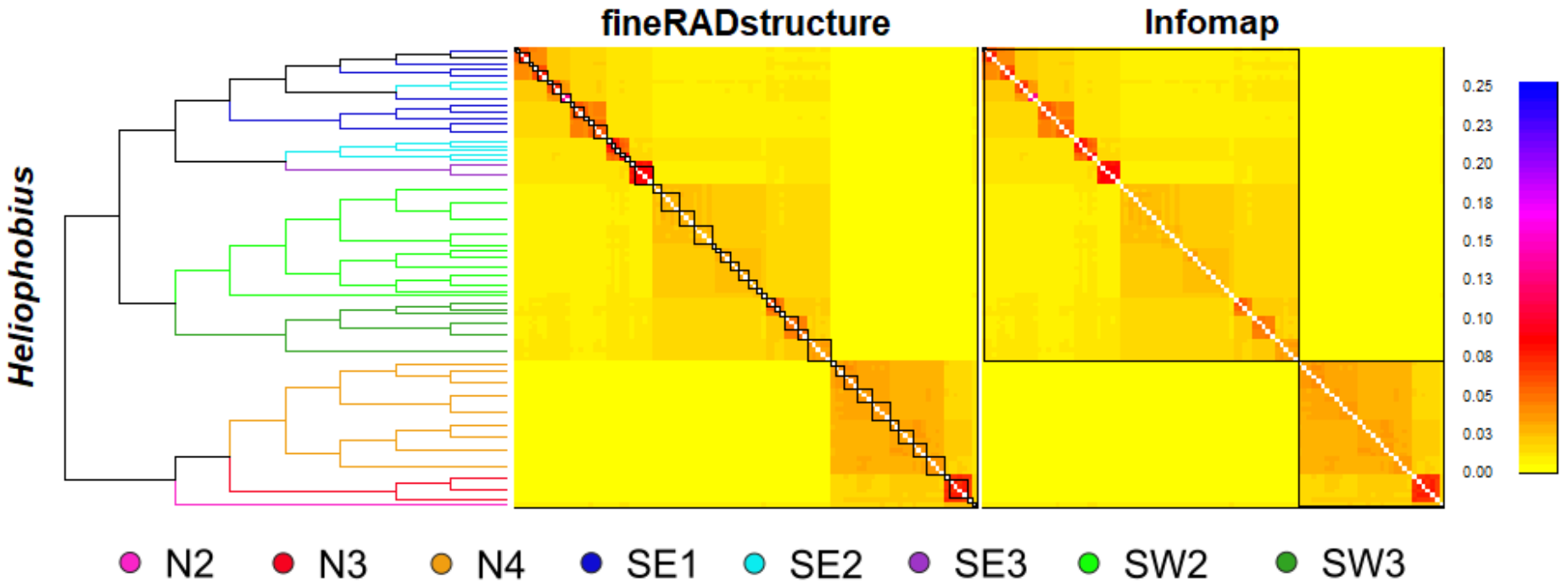

Fig. 10: Heatmaps of co-ancestry matrix with fineRADstructure and Infomap populations of *Heliophobius* specimens (each population is marked by black border). The colour scale is normalized and expresses co-ancestries as proportions rather than counts (higher proportion of similarities among specimens is marker by “darker” colour). The dendrogram next to the heatmaps was estimated by fineRADstructure and shows higher-order similarities of its populations. The colours of branches in the dendrogram indicate an affiliation to specific OTUs.

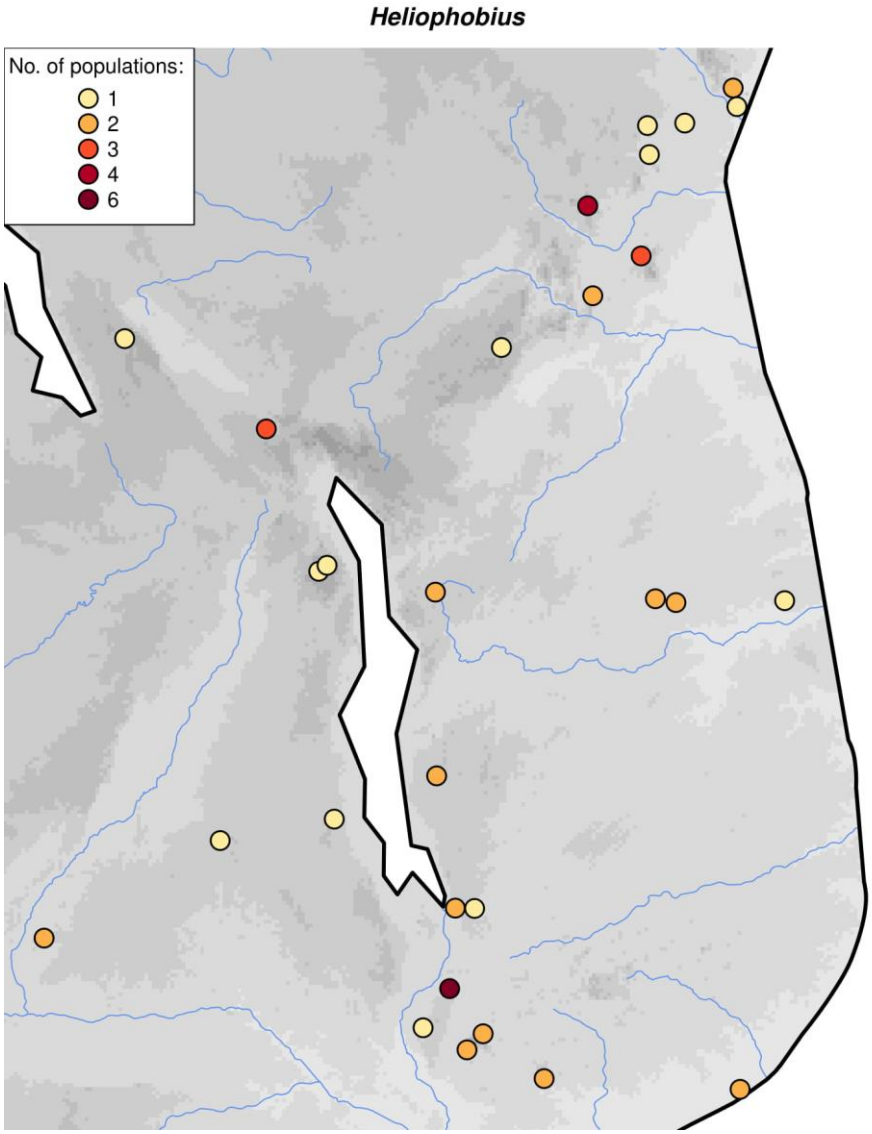

Fig. 11: The geographic distribution of genetic populations of *Heliophobius* revealed by fineRADstructure. Each dot represents a locality. In case that locality was less than 10km to another, they were merged. The colour of a dot stands for a number of populations in the locality.

4.2 The genetic diversity of *Georychus*

The species delimitation analysis STACEY indicates five well supported "species" (Tab. 4). Two lineages from the most western part of the Western Cape Province (L1, L2) clustered together with PP=0.59. The rest of OTUs are supported as distinct entities with PP=0.90-1.00.

According to the maximum clade credibility species tree from StarBEAST (Fig. 12), cytb lineages forming the densest populations in the Western Cape Province (L1+2, L3, L4) cluster together with PP=0.89, while a monophyly of geographically remote populations in KwaZulu Natal (Nottingham Road; L5) and Mpumalanga regions (Wakkerstroom; L6) is

supported with PP=0.9. For easier comparison of these results with haplotype networks, see the separate gene trees estimated along with the species tree (Fig. S2 in Supplement).

Well-supported delimitation of most lineages into species and high PP for clusters in a species tree is notable in the visualization of the data using haplotype networks (Fig. 13) for separate nuclear markers. Most haplotype networks display clear separation of haplotypes from two small and distinct populations (L5, L6) located northeast to the other haplotypes. More detailed trend apparent from networks of all markers is grouping of three lineages in the Western Cape (L1, L2, L3).

In the ddRAD dataset, fineRADstructure method estimated 24 populations while Infomap only one population (Fig. 14). All OTUs defined as species in a multilocus analysis of six nuclear markers cluster together also in a dendrogram made by fineRADstructure and also the topology of dendrogram follows a result of StarBEAST. The individuals from the Western Cape (lineages L1 and L2) united into a monophyletic group and also the rest representatives are gathered in the dendrogram according to OTUs. The distribution of 24 populations defined by fineRADstructure is displayed in a map (Fig. 15). The identical space scale of 10 km as in the case of *Heliophobius* is applied for merging nearby localities, but all of them remained without a change. Among sampled sites, populations are equally distributed with up to 4 populations per site. The space distribution of populations in two multi-population sites (Wakkestroom and Oudshoorn) is available in the Supplement (Fig. S5, S6).

Tab. 4: Posterior probabilities of lineage conspecificity in the genus *Georychus* estimated as proportions of species trees sampled by STACEY, where the lineages were collapsed.

	L1	L2	L3	L4	L5	L6
L1	0,40	0,59	0.08	0	0	0
L2	0,59	0,39	0.09	0	0	0
L3	0.08	0.09	0.9	0	0	0
L4	0	0	0	1	0	0
L5	0	0	0	0	1	0
L6	0	0	0	0	0	1

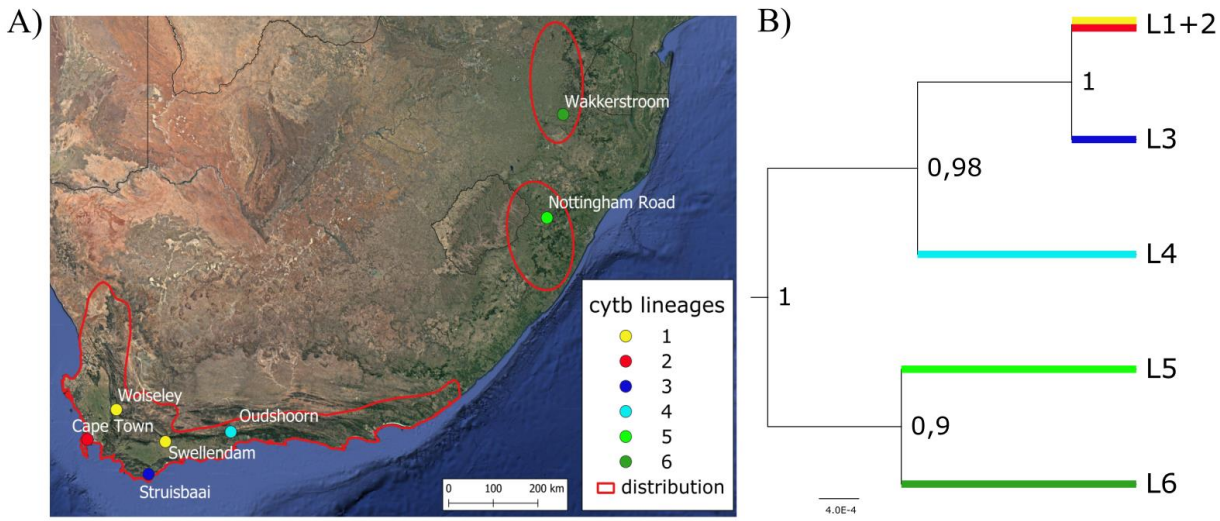

Fig. 12: A) The map with sampled localities with six nuclear markers coloured according to OTUs. B) The maximum clade credibility tree from StarBEAST analysis based on six nuclear markers for the genus *Georychus*. The numbers next to nodes show the posterior probabilities and terminal nodes are named and branches coloured according to OTUs in the map.

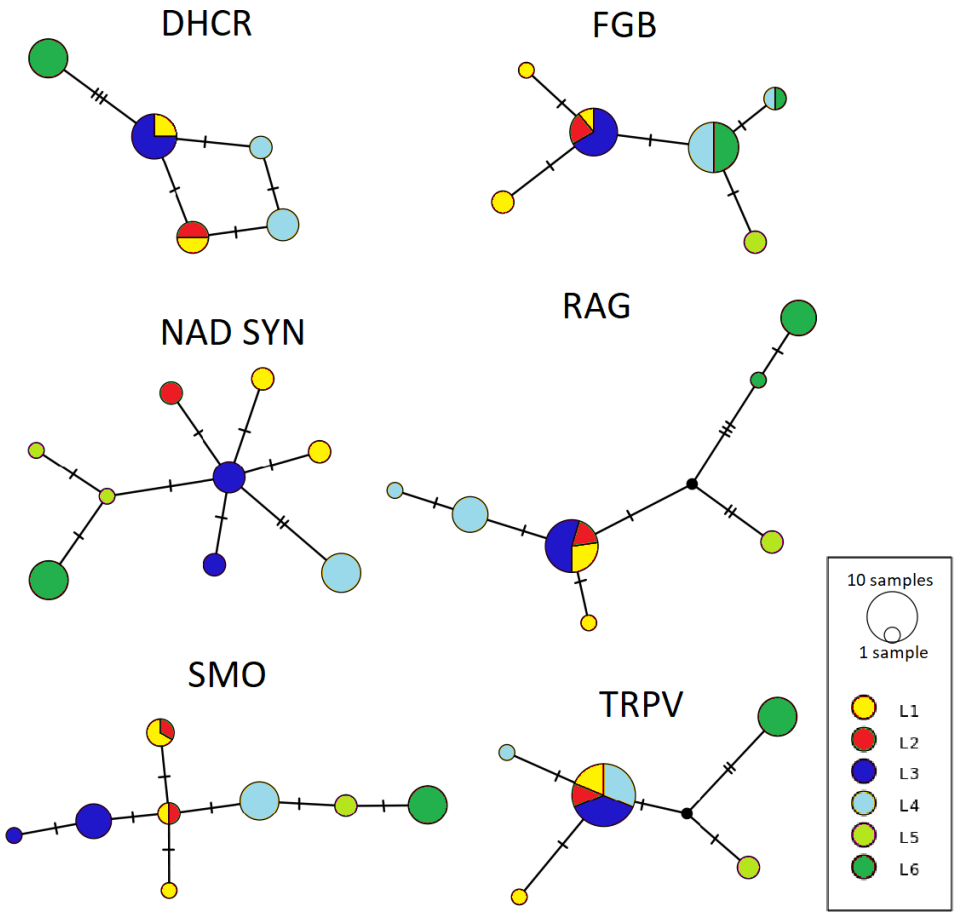

Fig. 13: Haplotype networks for the genus *Georychus* for all genes separately. Circles depict individual haplotypes, the size of circles corresponds to number of sequences, lines between circles represents mutual genetic connection, and number of transverse lines indicate the number of mutations between certain haplotypes.

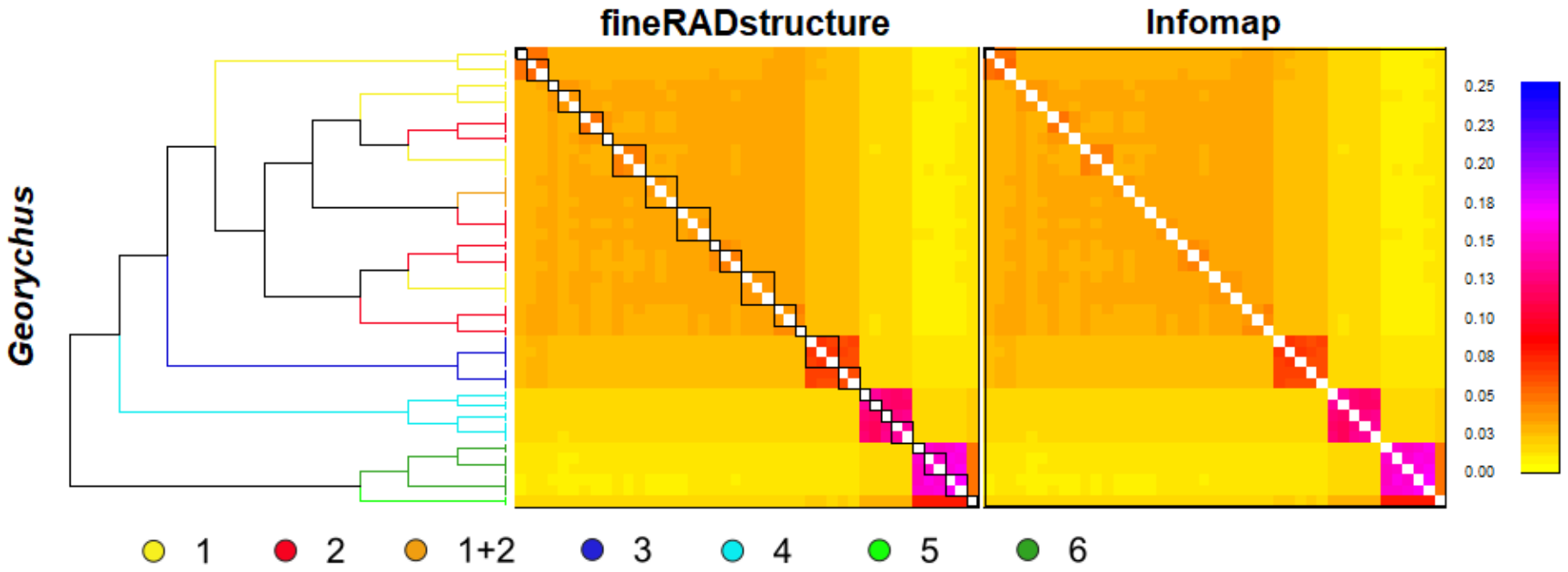

Fig. 14: Heatmaps of co-ancestry matrix with fineRADstructure and Infomap populations of *Georychus* specimens (each population is marked by black border). The colour scale is normalized and expresses co-ancestries as proportions rather than counts (higher proportion of similarities among specimens is marker by "darker" colour). The dendrogram next to the heatmaps was estimated by fineRADstructure and shows higher-order similarities of its populations. The colours of branches in the dendrogram indicate an affiliation to specific OTUs from Visser et al. (2018)**Chyba! Nenalezen zdroj odkazů.**.

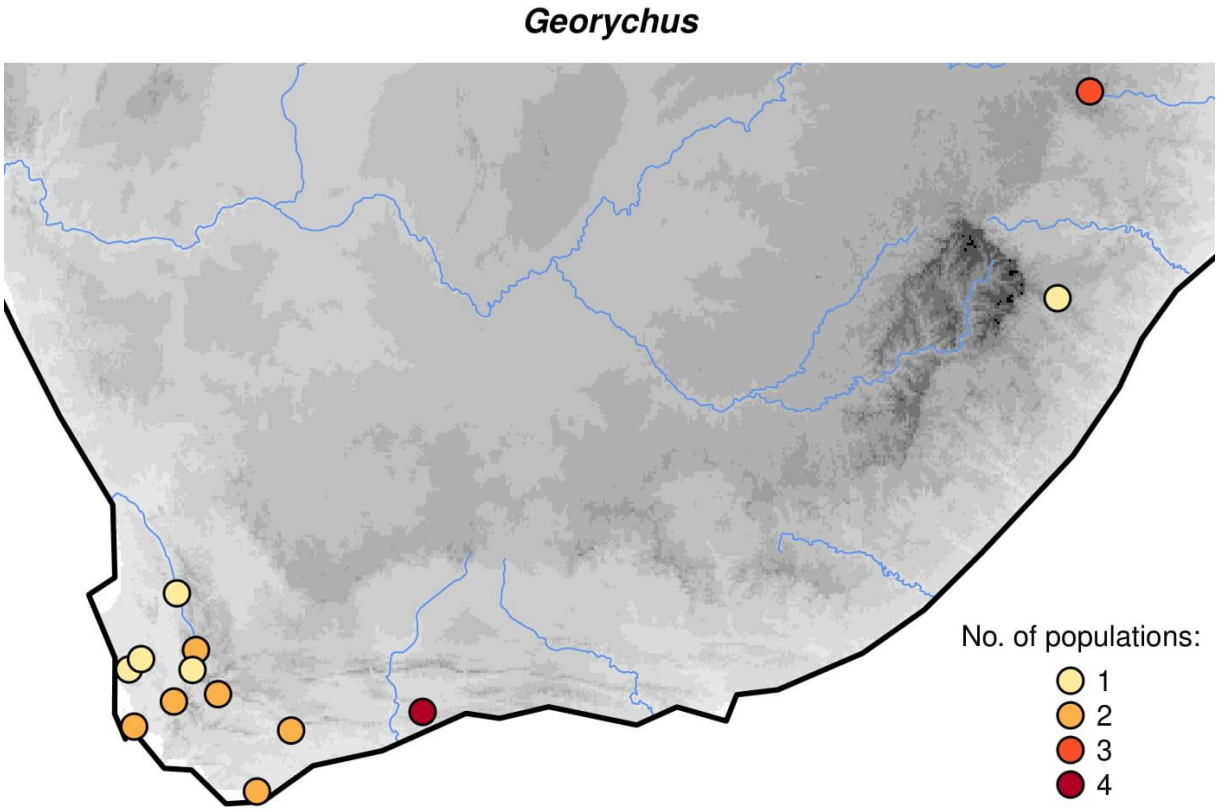

Fig. 15: The geographic distribution of genetic populations of *Georychus* delimited by fineRADstructure. Each dot represents a locality. The colour of a dot stands for a number of populations in that locality.

4.3 Dating of divergence

An estimation of bathyergids divergence dates (Fig. 16) using a fossilized birth-death model is based on four genetic markers and wide range of fossil taxa. According to the results, the diversification of bathyergid lineages began in the late Oligocene when *Heterocephalus* split from other genera (25.8 Mya). In the middle Miocene, the *Heliophobius* clade separated in 13.03 Mya, and clades *Bathyergus* + *Georychus* and *Cryptomys* + *Fukomys* divided in 10.53 Mya. Splits between a pair of *Georychus* + *Bathyergus* happened in 8.69 Mya and in 7.76 Mya between a pair of *Cryptomys* + *Fukomys*. The intrageneric diversifications of recent lineages of genera studied in this thesis occurred during Plio- Pleistocene and started in 4.14 Mya within *Heliophobius* and in 4.01 Mya within *Georychus*.

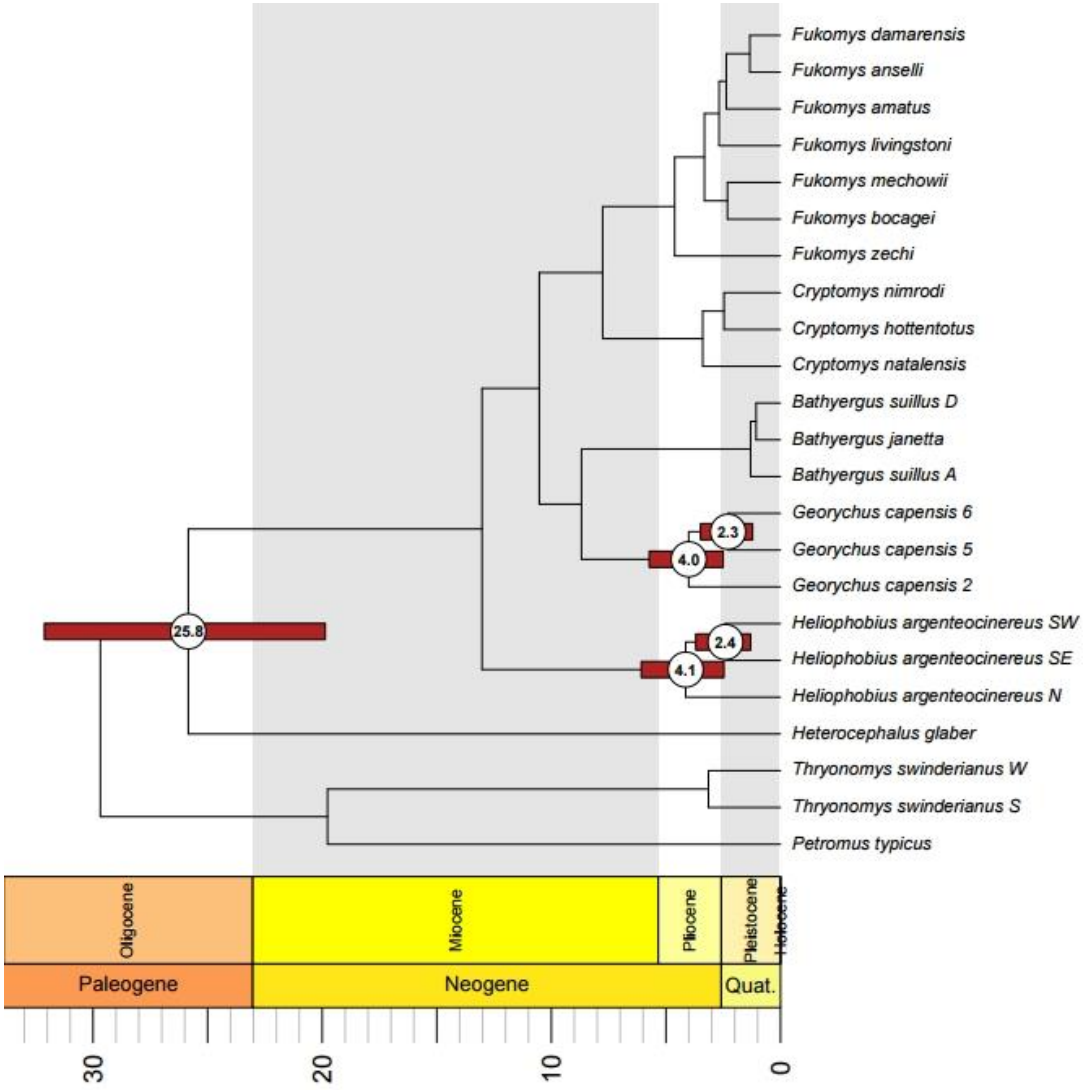

Fig. 16: The divergence dates of the bathyergid family calculated in fossilized birth-death model. The estimated times are highlighted for node representing the separation of the basal *Heterocephalus glaber* from other bathyergids and for the divergences of main clades within *Heliophobius* and *Georychus*. The numbers and letters behind the species names correspond to the names of OTUs.

5 Discussion

5.1 The observed genetic diversity

The Bayesian species delimitation analysis under the multispecies coalescent found nine genetically isolated populations or gene pools, in case of the genus *Heliophobius* and five gene pools in the genus *Georychus* with a high support in both genera. An estimation based on the high number of loci acquired in ddRADseq differs according to a used clustering algorithm as expected. While the fineRADstructure algorithm defined finer structure with 51 and 24 populations within *Heliophobius* and *Georychus* respectively, the Infomap algorithm revealed a significant proportion of the most similar loci even between predefined OTUs. As a result, two distinct gene pools in *Heliophobius* and one gene pool in *Georychus* were estimated.

5.1.1 The genetic diversity of *Heliophobius*

The first extensive study dealing with the molecular phylogenetic reconstruction of the *Heliophobius argenteocinereus* found high genetic structure across its distribution, containing six main clades (Faulkes et al. 2011). However, the result is based only on the cytb marker, and it becomes clear that the evolution of mtDNA does not necessarily correspond to the evolution of the nuclear DNA (e.g. Toews and Brelsford et al. 2012). Moreover, the analysis of cytb marker with extended sampling sites suggested higher structuring with ten mitochondrial clades (Bryja et al. 2018b). The study of Faulkes et al. (2011) also contains additional mistakes. Firstly, two localities (clade 2b) from the northern part of EAM were incorrectly placed in the map, which resulted in a geographic overlap with the clade from the southern part of EAM (clade 3), suggesting an occurring of both clades in these localities (and potential reproductive isolation). Secondly, some sequences from museum samples represent chimeras originated probably from a contamination during PCR amplifications. Published sequences from museum samples comprise only of fragments of cytb connected with unknown nucleotides (N) (unrevealed information). If these fragments were taken as separate sequences, they clustered independently to other parts of an original sequence, in two cases even with another bathyergid, a genus *Cryptomys* (see supplement of Bryja et al. 2018b for further details). Therefore, two clades defined by Faulkes et al. (2011) south-westwards to the EARS (clades 1 and 5), containing only sequences from museum specimens, can not be considered as valid. Nevertheless, it is highly obvious that the population of the silvery mole-rat is genetically very structured.

In order to solve the problems with these lineages of Faulkes et al. (2011) we also assessed phylogenetic placement of newly sequenced museum specimens (Fig. S8), one from Nyika National Park (Zambia) and four from Katanga region (Dem. Rep. Congo). The localities of newly sequenced specimens are identical with the sampled localities in Faulkes et al. (2011). Short cytb sequences were obtained by amplicon sequencing on Illumina platform. More details about samples and the analysis are in the chapter 7.1 of the Supplement. Two Illumina barcodes clustered together with other individuals from nearby localities (one from Nyika NP and one from Katanga region). Three sequences, got from specimens defined by Faulkes et al. as "H. mottoulei", created a monophyletic clade together with the Faulkes et al.'s original sequences. This clade was very divergent and with no clear affinity to any other sampled lineages. Therefore, it was not included in the analysis, as I could not decide whether it is a kind of artefact or a genuine lineage with unresolved phylogenetic position. Yet, it is possible that already published cytb sequences from these specimens are partly correct (as suggested by Bryja at al. 2018 Suppl. 2), and indeed, there is a separate species of *Heliophobius* in the south-eastern part of Dem. Rep. Congo.

The phylogeny based on mtDNA (Faulkes et al. 2011; Bryja et al. 2018b) was also supported by the multilocus analyses of three nuclear markers (NADSYN, TRPV, DHCR) in Bryja et al. (2018b) and by additional three nuclear markers (RAG1, SMO, FGB) used in this thesis. Unfortunately, not all mtDNA lineages from the previously published studies, were used for genotyping of nuclear markers. The lineage SW1 from Rumphi (northern Malawi) is represented only by two published cytb sequences from Faulkes et al. (2011), so no tissue was available for additional nuclear sequencing, either for my thesis or for study of Bryja et al. In addition, Bryja et al. did not manage to get sufficient data about individuals from a lineage SE3 in the Gile National Reserve (eastern Mozambique). Nevertheless, the final number of clustered species depended on the overall assessment. Due to a lower number and variation of chosen nuclear markers, Bryja et al. (2018b) considered collapsing as valid wherever its PP was higher than 0.05. Even with that stance, only a pair of SW2 and SW3 formed a unit. Extended set of markers in my thesis allows to use less conservative approach. As a result, no pair of candidates collapsed. However, if the same conservative criterion (as in Bryja` et al. study) is employed, there will be eight gene pools with merged SE1 and SE2 lineages.

The genomic dataset (ddRADseq, this study) and microsatellites (Bryja et al. 2018b) also revealed a significant genetic structuring of silvery mole-rat populations. At the same time, however, large genetic similarities were found among gene pools delineated with

mitochondrial and nuclear markers. Yet, the form of a phylogenetic structure varies. While the ddRAD dataset revealed more or less identical clades and topology as the phylogeny based on targeted mitochondrial and nuclear markers (Sanger-sequenced mitochondrial and nuclear markers will be called 'targeted' as opposed to randomly detected ddRAD loci), the microsatellite`s populations do not match them exactly. The most important difference is sharing of microsatellite polymorphism between the main clades (northern, southern). Whether it represents retention of ancestral polymorphism or recent gene flow in place of contact zones remains unresolved. The lack of shared polymorphism implies lack of gene flow, but the microsatellite analysis suggests an opposite. More detailed analyses of ddRADseq data may reveal local gene flow between two Infomap clusters, which would provide evidence for incomplete reproductive isolation.

5.1.2 The genetic diversity of *Georychus*

In contrary to *Heliophobius*, all hitherto studies focused on the internal relationships of *Georychus capensis* are mostly in agreement. Although the first study (Visser et al. 2018) revealed six clades based on two mitochondrial markers, the follow-up analyses of cytb (Visser et al. 2019a, b) and three nuclear fragments (Visser et al. 2019a) agreed on the same five genetic clades. Both studies confirmed the high sequence divergences between these clades on a cytb dataset, (6.9-12.2 % in a former and 6-12.1 % in a later study) and noticeable on three nuclear markers (GHR, TTR, Bfibr) ranging from 0.3 to 0.8 %. The multilocus analysis with six nuclear markers in this thesis gave the same result of five distinct clades. From the dataset acquired in ddRADseq, a remarkable genetic structure was revealed as well. However, the similarities among pre-defined clades resulted in collapsing all clades into one gene pool in case of Infomap clustering method, which should define gene pools on a level of phylogenetic lineages or species. It is important to note, that trees / dendrograms / networks obtained in all above mentioned studies together with my findings are of similar topology regardless methods employed (maximum parsimony, maximum likelihood, Bayesian analyses, haplotype networks, and co-ancestry matrix). What does differ between the analyses is the number of clades / gene pools / clusters considered as distinct.

5.1.3 The differences of used approaches in studying genetic diversity

In general, multilocus analyses of Sanger sequences suggested significantly higher genetic diversity than the Infomap clustering based on ddRADseq data, although both methods aim to

target population structure at similar resolution. This observation may be explained either by different approaches used in analyses. Multispecies coalescent (used with the Sanger sequences) assumes no gene flow between discrete populations, while the nearest-neighbour approximation of pair-wise genealogical proximity allows for allele sharing at any phylogenetic scale. In addition, since the sequencing of targeted markers allows us to work with limited number of loci (units or tens of units), the acquired genetic information is restricted only to chosen markers. With the high-throughput sequencing, such as ddRADseq, we can obtain hundreds to hundreds of thousands of loci, which are more or less randomly distributed through the genome (Peterson et al. 2012). Therefore, the final ddRAD dataset can bring us more complex information about genetic variability of sequenced individuals.

Another relevant factor possibly affecting results of both methods are differences in the substitution rates of markers, as it is known to vary across genome and among taxa (Kumar and Subramanian 2002; Alberts et al. 2002). The Sanger sequencing target specific markers, and thus their choice is made to fit the purpose of phylogenetic analysis (Patwardhan et al. 2014), in this case of closely related taxa. The strategy is different to ddRAD sequences, where the goal is to get a realistic picture of differentiation across genomes of high number of individuals. We do not have any *a priori* information about mutation rates of ddRAD loci, which may be highly divergent across the population, but naturally also highly conserved even across wide phylogenetic groups. All these loci, even invariable ones, bear information about divergence times and population sizes and if they really represent a random sample of the genome, they all should be retained in phylogenetic and population genetic analyses. Although some applications may require modelling of mutation rate variation, the nearest-neighbour estimate of co-ancestry does not. This could bias results if the invariable loci were overrepresented in data due to sequencing design and subsequent post-processing. Otherwise, ddRAD datasets are expected to be very useful for phylogenetic analyses of closely related species and genera (DaCosta and Sorenson 2016). And truly, several ddRADseq studies revealed an unexpected cryptic diversity among various taxa (plants: Roy et al. 2017, invertebrates: Kozlov et al. 2017; Amor et al. preprint; Weiss et al. 2018, and vertebrates: Říčan et al. 2016; Garg et al. 2016; Chattopadhyay et al. 2016). Nevertheless, in case of this thesis, it is more the delimiting method than the data itself that revealed very fine (fineRADstructure) or broad (Infomap) genetic diversity.

5.2 The dating of intraspecific divergences in *Heliophobius* and *Georychus*

According to estimates of a fossilised birth-death model based on one mitochondrial and three nuclear markers, the divergence of the recent lineages of both genera started in the mid-Pliocene. This estimate is largely in the contradiction with so far published results (summarized in The causes of intraspecific diversifications of *Heliophobius* and *Georychus*

Credible estimates of diversification times are necessary to formulate any phylogeographic scenario. Because of the wide contradictions in dating of *Heliophobius* and *Georychus* lineages in hitherto studies, different evolutionary scenarios are possible. Nevertheless, relatively recent (Plio- Pleistocene) divergence dates are supported by multiple evidence.). While some studies estimated the beginning of diversification of extant lineages to happen in the Early or Middle Miocene (19 Mya in *Heliophobius* and 16 Mya in *Georychus*; Visser et al. 2019b), much younger estimates shift the same diversifications to the mid-Pliocene (around 4 Mya in both genera; Montgelard et al. 2012; Bryja et al. 2018b; this study).

Estimates by Faulkes et al. (2004; 2011) and Visser et al. (2019a, b), giving significantly older divergences, apply a method of a prior calibration of nodes. Using various fossils and applying them to different nodes resulted in a wide range of possible time scenarios (with difference up to 12 Ma). For instance, two studies of Visser et al. (2019a, b) used the same calibration point 19 Mya, a fossil *Proheliophobius*. However, in the first study, they probably set this point to the split of *Heliophobius* and its sister clade (*Fukomys, Cryptomys, Bathyergus, Georychus*), and in the following study to a node representing the basal divergence of recent *Heliophobius*`s lineages. The approach of a prior calibration is not generally incorrect itself, nevertheless, in case of bathyergids is rather inadequate, because of the uncertainty with classification of fossils to recent taxa (in the Introduction). When a nodes out of Bathyergidae family were used as calibration points (two calibration points within Apodemini and Gerbillurini; Montgelard et al. 2012), significantly younger divergence date (~ 3.4 Mya) of populations in the Western Cape (L1-L4) and lineages in KwaZulu Natal (L5) and Mpumalanga regions (L6) (to simplify the terminology, I will call these two remote populations south-western and north-eastern, respectively) of *Georychus* was obtained.

This thesis and a study of Bryja et al. (2018b) applied a fossilised birth-death model without a prior node calibration provides much recent estimates of diversification in both genera. It is important to note, that both analyses are based on very similar dataset of genetic information from recent taxa and information of fossil taxa. Therefore, the results are more or

less identical. The accuracy of divergence time estimates may be influenced by the fact that recent lineages are represented by restricted molecular data with respect to sequences from nDNA markers (as it is available in Tab S2 in the Supplementary mat.). Since the results are based mainly on sequences of cytb, the estimated divergences can appear older than they truly are. Nevertheless, these final estimations are substantially younger than those presented in the studies mentioned above and, additionally, in concordance with the recent fossil and molecular reconstructions (Sallam et al. 2009; Fang et al. 2014). Plio- Pleistocene origin of recent bathyergid lineages is in agreement with diversification of many (if not all) other rodent taxa in the Eastern Africa (Colangelo et al. 2013; Bryja et al. 2014; McDonough et al. 2015; Mikula et al. 2016; Aghová et al. 2017; Petružela et al. 2018; Mazoch et al. 2018) as well as in the Southern Africa (Rambau et al. 2003; Russo et al. 2006; 2010; Edwards et al. 2011). Thus, very unlikely bathyergid genetic structure have remained unchanged for approx. 15 Ma, while other rodents underwent a massive radiation about 10 Ma later, during climatic oscillations in the Plio- Pleistocene.

Tab. 5: The differences of intrageneric diversification times of two genera *Heliophobius* and *Georychus* in published studies and in this thesis (in million years ago). The confidence intervals are in brackets, if they are available, rounded off to whole numbers. Analyses are based on different markers: [1] mitochondrial, [2] nuclear, [3] a combination of nuclear and mitochondrial markers.

	Faulkes et al. (2004)	Faulkes et al. (2011)	Montgelard et al. (2012)	Bryja et al. (2018b)	Visser et al. (2019a)	Visser et al. (2019b)	this study
Heliophobius diversification:							
north × south	13-10.8[1]	15.1[1]	-	3.7[3] (5.1-2.5)	-	19[1]	4.1[3] (6.1-2.5)
southeast × southwest	7.6-6.3[1]	11.6[1]	-	2.3[3] (3.2-1.4)	-	14[1]	2.4[3] (3.7-1.3)
Georychus diversification:							
south-western × north-eastern	-	-	~ 3.4[1]	-	10.3[1] / 6.4[2] (14-7) / (8-5)	16[1]	4[3] (5.7-2.5)
Wakkerstroom × Nottingham	-	-	-	-	6.1[1] / 4.1[2] (9-3) / (6-3)	10[1]	2.3[3] (3.5-1.2)
Oudshoorn × rest of Cape	-	-	-	-	7.5[1] / 5[2] (11-4) / (6-4)	12[1]	-
Struisbaai × Cape	-	-	-	-	4.8[1] (7-3)	9[1]	-

5.3 The causes of intraspecific diversifications of *Heliophobius* and *Georychus*

Credible estimates of diversification times are necessary to formulate any phylogeographic scenario. Because of the wide contradictions in dating of *Heliophobius* and *Georychus* lineages in hitherto studies, different evolutionary scenarios are possible. Nevertheless, relatively recent (Plio- Pleistocene) divergence dates are supported by multiple evidence.

5.3.1 The biogeographical history of both genera

Similar estimates (about 4 Mya) of the beginning of diversifications of extant lineages in both genera suggest role of one large scale factor. In case of *Heliophobius*, the species occupying the East African Rift System (EARS), some events associated with its formation possibly could have separated the ancestral populations. Although the main tectonic activity, formation of EARS, and an uplift of Eastern Africa finished already in the Late Miocene, there are observations of peak rifting, subsidence and sedimentations in several basins during Plio-Pleistocene (around 1-2 Mya; MacGregor 2015), which could have theoretically affected its ancestral population. In case of *Georychus* living in the South Africa, the EARS could not represent the primary driver for its intrageneric splitting.

More likely, the change or repeated changes in global climate could be responsible for their diversifications. The middle Pliocene represented a warmer period (roughly around 5-3 Mya) with the higher average global temperatures (+3 °C), reduced Antarctic ice cover and with that higher level of sea (+10-20 m) compared to present situation. This period was also characteristic for a more humid climate (Ravelo et al. 2004; deMenocal 2004; Trauth et al 2007). Beginning of initial diversifications could have been also caused by substantial climate variability periods, interrupting the generally warm age of middle Pliocene. These periods of frequent changes from very humid to very arid conditions happened in 4.4-4.2 Mya and afterwards in 2.8-2.5 Mya (Trauth et al. 2007; Potts et al. 2013).

The *Heliophobius* distribution is characterized generally by mesic conditions with > 900 mm annual rainfall, but simultaneously by rain seasonality, which brings them the source of food, geophytes. It inhabits mainly miombo woodlands and avoids humid montane forests where the geophytes are probably absent. I may thus expect that humid forests during the warm middle Pliocene could be responsible for its initial split. In Tanzania, the so called East African “montane circle” may have represented such barrier dividing ancestral

Heliophobius population to the recent northern and southern lineages. This "montane circle" covered the Southern and Western Rifts of EARS and the EAM with forest (thus also called "forest circle") during wet Pleistocene periods (see supplement of Colangelo et al. 2013 for further details). This repeated changes of habitats in diverse mountain ranges was proposed to cause the rich phylogeographic structures in many taxa, such as bats (Fahr et al. 2002; Taylor et al. 2012), shrews (Demos et al. 2014; Stanley et al. 2015), and rodents (Taylor et al. 2009; Colangelo et al. 2013; Bryja et al. 2014; Krásová et al. 2019). Another period of substantial climate variability (2.8-2.5 Mya; Trauth et al. 2007; Potts et al. 2013) could have separated the ancestor populations of south-eastern and south-western lineages around 2.4 Mya. Very similarly to the preceding diversification, the forests along the Southern Rift and Lake Malawi may acted as a dispersal barrier.

As well as *Heliophobius*, the *Georychus* occurrence depends on availability of geophytes. Yet, except for the presence of vleis or rivers, no other habitat preferences are known, as environmental conditions vary remarkably across its distribution (Visser et al. 2017). The geographically widely distributed fossil records of *Georychus* (Fig. S7 in the Supplement; Pickford and Mein 1988 (in Winkler et al. 2010); Avery 1991, 1998, 2001; Klein et al. 2007) in contrast with current restricted and isolated populations suggest, that the suitable environmental conditions are restricted at present compared to past. With respect to repeated changes of climate during Plio- Pleistocene, the *Georychus* distribution probably underwent extensive retractions and expansions. Apparently, some climatic fluctuation, probably a substantial climate variability between 4.4 and 4.2 Mya (Trauth et al. 2007; Potts et al. 2013), could have separated the *Georychus* population during arid and cold periods.

Currently, only the representatives of south-western and south-eastern populations survived. Most probably, the Western Cape served as a stable refugium as it is suggested by multiple evidence. Firstly, the stable climate prevailed in the Cape region throughout Quaternary (Cowling et al. 1997). This climatic stability was also proposed as a hypothetical cause of an extremely high species diversity of plants (Procheş et al. 2006). We may speculate that such suitable conditions were there for a longer period. Secondly, at present, this is the place with the highest abundance of *Georychus* indicating habitat suitability for the species (Visser et al. 2017). Thirdly, local fynbos (according to maps in Cowling et al. 1997) is characteristic for the highest diversity and abundance of geophytes in the world (Cowling et al. 1997; Procheş et al. 2006), ensuring them sufficient amount of food. Nevertheless, the question about disjunctive *Georychus* distribution either today or in the past still remains.

Since many other rodents, such as *Otomys irroratus, Acomys subspinosus, Myomyscus verreauxii, Rhabdomys pumilio, Gerbiliscus afra,* or *Acomys subspinosus,* are currently distributed along the southern and south-eastern coast, up to the grasslands of eastern part of South Africa (Skinner and Chimimba 2005; Monadjem et al. 2015), I assume there is no apparent geomorphological barrier. Thus, *Georychus* distributional pattern is probably driven by not yet revealed habitat requirement or by the competition with another bathyergid, *Cryptomys*, which is more widely distributed across South Africa (Monadjem et al. 2015). Nevertheless, *Georychus* is probably more successful in more humid areas (north-eastern population is supplied by high rainfall and Western Cape by see breezes; Bonnardot et al. 2005) with higher abundance of geophytes. Cooperative food search favour social *Cryptomys* in less humid areas with less geophytes (Spinks and Plaganyi 1999). Comparable disjunct distribution has *Otomys laminatus* (Skinner and Chimimba 2005; Monadjem et al. 2015), but so far, this rodent has been even less studied than *Georychus,* thus the real reasons of this distributional pattern remain unresolved. The additional splitting of lineages, as it is already mentioned in Visser et al. (2018), could have been supported by a presence of the Breede River, separating the population in Oudshoorn (L4), or by the Agulhas Plain, which was periodically flooded during the fluctuation of sea level in Pleistocene and isolated the population in Struisbaai (L3).

5.3.2 The environmental niche modelling

To understand ecological factors which may contribute to the fragmentations of geographic distribution of studied mole-rats, an environmental niche modelling (ENM) based on the presence data, precipitation, maximum and minimum temperatures since the Last Interglacial (120–140 thousand years ago) to the recent was provided by Ondřej Mikula. Despite considerably older origin of recent lineages, this modelling can show the reaction of both bathyergids to equal fluctuations between arid and humid climates in deeper history. More details about the ENM together with all figures are available in the chapter 7.2 in the Supplementary material. According to ENM, *Georychus* (Fig. S11) distribution area was far more affected than that of *Heliophobius* (Fig. S9) by climate changes at least during Last Interglacial and Last Glacial Maximum periods (depicted by green patches in modelled maps). While the overall area with suitable climatic conditions for *Heliophobius* remained almost identical through studied time, the warm and humid Last Interglacial (Dawson 1992) probably caused extensive expansion and the cold and arid Last Glacial Maximum (Dawson 1992)

extensive retraction of *Georychus* distribution. Overall, the ENM suggests that *Heliophobius* population was probably more stable through time, which could have led to higher probability of surviving in new areas after dispersion avents. On the contrary, *Georychus* distributional area could have undergone extreme changes through time, and together with the absence of geomorphological barrier probably resulted in a gene flow events between ancestral populations, as it is also indicated by significant similarities in their genomes (the revealed genetic similarities among ddRAD loci).

5.4 Taxonomic implications

My study confirmed the high genetic structure in both bathyergid genera from previous studies (Faulkes et al. 2011; Bryja et al. 2018b; Visser et al. 2018; 2019a, b).

In case of *Heliophobius*, I suggest two distinct species represented by the northern and southern lineages. Division of these two species is supported by mtDNA markers (Ingram et al. 2004; Faulkes et al. 2004; 2011; Bryja et al. 2018b), by six nuclear markers (this study) and also by Infomap clustering algorithm of ddRAD dataset (this study). The karyotype from Kenyan population is also slightly different from populations in Malawi and Zambia (2n=60 and 62 respectively; Scharff et al. 2001, Šumbera et al. 2007). The split of both potential species is dated to around 4 Mya according to a fossilized-birth death analysis, and nowadays they are separated by Tanganyika Rukwa Malawi segment of EARS and by the EAM. It is important to note, that there is a potential contact zone between northern and southern lineages along the EAM. Without any obvious barrier, the present sampling revealed gene flow only by a microsatellite analysis (Bryja et al. 2018b), but with respect to other evidence, it can represent the ancestral polymorphism. Very similar situation with no real migration barrier but distinct genetic clades was found also in other African rodent, such as *Aethomys* (Mazoch et al. 2018) or *Acomys* (Petružela et al. 2018) which occurs frequently syntopically with *Heliophobius*.

The situation in *Georychus* complex is less clear. Mitochondrial together with nuclear markers, allozymes, and restriction length polymorphisms suggest two distinct species from Western Cape and KwaZulu Natal with Mpumalanga (Janecek et al. 1992; Honeycutt et al. 1987, 1991; Nevo et al. 1987; Faulkes et al. 2004; Ingram et al. 2004; Visser et al. 2018; 2019a, b; this study). The haplotype networks (this study) also show the evident separation of these two populations. Relatively deep historical splits around 4 Mya of these two potential species

would also support their delimitation. On the other hand, the significant genetic similarities among the lineages are visible in a co-ancestry matrix based on ddRAD dataset, and as a result, the Infomap algorithm detected sampled *Georychus* as one gene pool. Moreover, no obvious geomorphological barrier between suggested species implies a possible expansion or retraction during future climatic changes and an instability of current genetic structure. Therefore, I propose keeping the current taxonomy with one *Georychus* species.

Despite molecular methods enabling us to study wide populations and reveal cryptic diversity, the genetic evidence should be understood only as a part of complex information about species. At present, we have highly efficient DNA sequencing technologies, developments in phylogenetic and phylogeographic approaches, access to museum specimens; we have methods for studying population biology or sexual mating behaviour, modern equipment for detecting morphological differences (such as computed tomography), and all this information should be considered in a delimitation of a new species. Applying a combination of different methods is called an integrative taxonomic approach (Dayrat 2005), and nowadays undergo a significant boom in a scientific world (Padial et al. 2010; Riedel et al. 2013). With respect to an integrative taxonomy, the final delimitation of *Heliophobius* and *Georychus* should await other detailed studies comprising more aspects of their biology, for instance, geometric morphometry of skulls.

6 References

Aghová, T. et al. (2017) ‘Multilocus phylogeny of East African gerbils (Rodentia, *Gerbilliscus*) illuminates the history of the Somali-Masai savanna’, Journal of Biogeography, 44(10), pp. 2295–2307.

Ait Belkacem, A. et al. (2016) ‘North African hybrid sparrows (*Passer domesticus* , *P. hispaniolensis*) back from oblivion - ecological segregation and asymmetric mitochondrial introgression between parental species’, Ecology and Evolution. John Wiley and Sons Ltd, 6(15), pp. 5190–5206.

Alberts, B., Johnson, A., Lewis, J., Raff, M., Roberts, K., and Walter, P. (2002) Molecular biology of the cell. 4th edition. Garland Science.

Allard, M. W. and Honeycutt, R. L. (1992) ‘Nucleotide sequence variation in the mitochondrial 12S rRNA gene and the phylogeny of African mole-rats (Rodentia: Bathyergidae).’, Molecular Biology and Evolution, 9(1), pp. 27–40.

Alston, E. R. (1876) ‘2. On the classification of the order Glires.’, Proceedings of the Zoological Society of London, 44(1), pp. 61–98.

Amor, M. D. et al. (no date) ‘Genome-wide sequencing uncovers cryptic diversity and mito-nuclear discordance in the *Octopus vulgaris* species complex’, preprint.

Avery, D. M. (1991) ‘Late Quaternary incidence of some micromammalian species in Natal’, Durban Museum Novitates, 16(1), pp. 1–11.

Avery, D. M. (1998) ‘An assessment of the Lower Pleistocene micromammalian fauna from Swartkrans Members 1-3, Gauteng, South Africa’, Geobios. Elsevier Masson SAS, 31(3), pp. 393–414.

Avery, D. M. (2001) ‘The Plio-Pleistocene vegetation and climate of Sterkfontein and Swartkrans, South Africa, based on micromammals’, Journal of Human Evolution, 41(2), pp. 113–132.

Barbière, F. and Marivaux, L. (2015) ‘Phylogeny and evolutionary history of hystricognathous rodents from the Old World during the Tertiary: new insights into the emergence of modern “phiomorph” families’, in Cox, P. G. and Hautier, L. (eds) Evolution of the Rodents. Cambridge: Cambridge University Press, pp. 87–138.

Begall, S., Burda, H. and Schleich, C. E. (2007) Subterranean rodents: News from underground. Edited by S. Begall, H. Burda, and C. E. Schleich. Berlin, Heidelberg: Springer Berlin Heidelberg.

Bennett, N. C. (2009) 'African mole-rats (family Bathyergidae): Models for studies in animal physiology', African Zoology. Informa UK Limited, 44(2), pp. 263–270.

Bennett, N. C. and Faulkes, C. G. (2000) African mole-rats: Ecology and eusociality. Cambridge University Press.

Bennett, N. C., Maree, S. and Faulkes, C. G. (2006) '*Georychus capensis*', Mammalian Species, 799, pp. 1–4.

Bivand, R. (2019) rgdal: Bindings for the 'geospatial' data abstraction library. Available at: https://cran.r-project.org/web/packages/rgdal/index.html.

Blondel, V. D. et al. (2008) 'Fast unfolding of communities in large networks', Journal of Statistical Mechanics: Theory and Experiment. IOP Publishing, 2008(10), p. P10008.

Bonnardot, V., Planchon, O. and Cautenet, S. (2005) 'Sea breeze development under an offshore synoptic wind in the South-Western Cape and implications for the Stellenbosch wine-producing area', Theoretical and Applied Climatology. Springer Wien, 81(3–4), pp. 203–218.

Bouckaert, R. et al. (2014) 'BEAST 2: A software platform for Bayesian evolutionary analysis', PLoS Computational Biology. Edited by A. Prlic, 10(4), p. e1003537.

Bronner, G. N. (1990) 'New distribution records for four mammal species, with notes on their taxonomy and ecology', Koedoe, 33(2).

Bryja, J. et al. (2014) 'The role of dispersal and vicariance in the Pleistocene history of an East African mountain rodent, *Praomys delectorum*', Journal of Biogeography. Edited by B. Riddle. John Wiley & Sons, Ltd, 41(1), pp. 196–208.

Bryja, J., Kostin, D., et al. (2018a) 'Reticulate Pleistocene evolution of Ethiopian rodent genus along remarkable altitudinal gradient', Molecular Phylogenetics and Evolution. Academic Press Inc., 118, pp. 75–87.

Bryja, J., Konvičková, H., et al. (2018b) 'Differentiation underground: Range-wide multilocus genetic structure of the silvery mole-rat does not support current taxonomy based on mitochondrial sequences', Mammalian Biology, 93, pp. 82–92.

Buffenstein, R. (2000) ‘Ecophysiological responses of subterranean rodents to undergound habitats’, in Lacey, E., Patton, J., and Cameron, G. (eds) Life underground: The biology of subterranean rodents. University of Chicago Press, pp. 62–110.

Buffenstein, R. (2005) ‘The naked mole-rat: A new long-living model for human aging research’, The Journals of Gerontology Series A: Biological Sciences and Medical Sciences, 60(11), pp. 1369–1377.

Buffenstein, R. (2008) ‘Negligible senescence in the longest living rodent, the naked mole-rat: Insights from a successfully aging species’, Journal of Comparative Physiology B. Springer, 178(4), pp. 439–445.

Burda, H. et al. (1990) ‘Magnetic compass orientation in the subterranean rodent *Cryptomys hottentotus* (Bathyergidae)’, Experientia, 46(5), pp. 528–530.

Burda, H. (2001) ‘Determinants of the distribution and radiation of African mole-rats (Bathyergidae, Rodentia): Ecology or geography?’, in African small mammals. Collection colloques et séminaires, Inst de Recherche pour le Developpement Editions, Paris, France, pp. 263–277.

Cannicci, S. et al. (2017) ‘A new species of the genus *Parasesarma* De Man 1895 from East African mangroves and evidence for mitochondrial introgression in sesarmid crabs’, Zoologischer Anzeiger. Elsevier GmbH, 269, pp. 89–99.

Castiglia, R. et al. (2012) ‘Rapid chromosomal evolution in the mesic four-striped grass rat *Rhabdomys dilectus* (Rodentia, Muridae) revealed by mtDNA phylogeographic analysis’, Journal of Zoological Systematics and Evolutionary Research. John Wiley & Sons, Ltd, 50(2), pp. 165–172.

Catchen, J. M. et al. (2011) ‘Stacks: Building and genotyping loci de novo from short-read requences’, G3-Genes Genomes Genetics, 1(3), pp. 171–182.

Chattopadhyay, B. et al. (2016) ‘Genome-wide data reveal cryptic diversity and genetic introgression in an Oriental cynopterine fruit bat radiation’, BMC Evolutionary Biology. BioMed Central Ltd., 16(1), p. 41.

Clement, M. et al. (2002) ‘TCS: Estimating gene genealogies’, in Parallel and Distributed Processing Symposium, International (Vol. 2, pp. 0184-0184).

Colangelo, P. et al. (2013) ‘A mitochondrial phylogeographic scenario for the most widespread African rodent, *Mastomys natalensis*’, Biological Journal of the Linnean Society, 108(4), pp. 901–916.

Cotterill, F. P. D. (2003) ‘Geomorphological influences on vicariant evolution in some Africa mammals in the Zambezi Basin: some lessons for conservation.’, Proceedings of the ecology and conservation of mini-antelope: Proceedings of an International Symposium on Duiker and Dwarf Antelope in Africa., (February), pp. 11–58.

Cotterill, F. P. D., Groves, C. P. and Taylor, P. J. (2017) ‘Taxonomy: Refine rather than stabilize’, Nature. Nature Research, 547(7662), pp. 162–162.

Cowling, R., Richardson, D. and Mustart, P. (1997) ‘Fynbos’, in Cowling, R., Richardson, D., and Pierce, S. (eds) Vegetation of Southern Africa. Cambridge University Press, pp. 99–130.

DaCosta, J. M. and Sorenson, M. D. (2016) ‘ddRAD-seq phylogenetics based on nucleotide, indel, and presence–absence polymorphisms: Analyses of two avian genera with contrasting histories’, Molecular Phylogenetics and Evolution. Academic Press Inc., 94(Pt A), pp. 122–135.

Dammann, P. and Burda, H. (2007) ‘Senescence patterns in African mole-rats (Bathyergidae, Rodentia)’, in Subterranean rodents. Berlin, Heidelberg: Springer Berlin Heidelberg, pp. 251–263.

Davies, K. T. J. et al. (2015) ‘Family wide molecular adaptations to underground life in African mole-rats revealed by phylogenomic analysis’, Molecular Biology and Evolution, 32(12), pp. 3089–3107.

Dawson, A. G. (1992) ‘Ice Age earth: Late Quaternary geology and climate’, Routledge.

Dayrat, B. (2005) ‘Towards integrative taxonomy’, Biological Journal of the Linnean Society, 85(3), pp. 407–415.

De Graaff, G. (1981) The rodents of southern Africa: Notes on their identification, distribution, ecology, and taxonomy. Butterworth-Heinemann.

De Graaff, G. (1968) ‘Rodentia: Bathyergidae’, in Meester, J. and Setzer, H. W. (eds) The mammals of Africa: an identification manual. Smithsonian Institution Press, Washington D.C., USA.

De Graaff, G. (1979) ‘Mole-rats (Bathyergidae, Rodentia) in South African National Parks: Notes on the taxonomic “isolation” and hystricomorph affinities of the family’, Koedoe, 22(1).

deMenocal, P. B. (2004) ‘African climate change and faunal evolution during the Pliocene-Pleistocene’, Earth and Planetary Science Letters, 220(1–2), pp. 3–24.

Demos, T. C. et al. (2014) ‘Uncovering cryptic diversity and refugial persistence among small mammal lineages across the Eastern Afromontane biodiversity hotspot’, Molecular Phylogenetics and Evolution, 71, pp. 41–54.

Deuve, J. L. et al. (2008) ‘Chromosomal phylogeny and evolution of the African mole-rats (Bathyergidae)’, Chromosome Research. Springer, 16(1), pp. 57–74.

Dubach, J. et al. (2005) ‘Molecular genetic variation across the southern and eastern geographic ranges of the African lion, *Panthera leo*’, Conservation Genetics, 6(1), pp. 15–24.

Du Toit, J. T., Jarvis, J. U. M. and Louw, G. N. (1985) ‘Nutrition and burrowing energetics of the Cape mole-rat *Georychus capensis*’, Oecologia, 66(1), pp. 81–87.

Edwards, S. et al. (2011) ‘Evolutionary history of the Karoo bush rat, *Myotomys unisulcatus* (Rodentia: Muridae): disconcordance between morphology and genetics’, Biological Journal of the Linnean Society. Oxford Academic, 102(3), pp. 510–526.

Ellerman, J. R. (1940) The families and genera of living rodents. Vol. I. Rodents other than Muridae. London.

Ellerman, J. R., Morrison- Soott, T. C. S. and Hayman, E. W. (1953) Southern African mammals 1758 to 1951: a reclassification. London: British Museum (Natural History).

Eytan, R. I. and Hellberg, M. E. (2010) ‘Nuclear and mitochondrial sequence data reveal and conceal different demographic histories and population genetic processes in Caribbean reef fishes’, Evolution. John Wiley & Sons, Ltd, 64(12), pp. 3380–3397.

Fahr, J. et al. (2002) ‘A revision of the *Rhinolophus maclaudi* species group with the description of a new species from West Africa (Chiroptera: Rhinolophidae)’, Myotis, 40, pp. 95–126.

Faircloth, B. C. et al. (2012) ‘Ultraconserved elements anchor thousands of genetic markers spanning multiple evolutionary timescales’, Systematic Biology, 61(5), pp. 717–726.

Fang, X. et al. (2014) ‘Adaptations to a subterranean environment and longevity revealed by the analysis of mole mat genomes’, Cell Reports, 8(5), pp. 1354–1364.

Faulkes, C. et al. (2010) ‘Cladogenesis and endemism in Tanzanian mole-rats, genus *Fukomys*: (Rodentia Bathyergidae): A role for tectonics?’, Biological Journal of the Linnean Society, 100(2), pp. 337–352.

Faulkes, C. G. et al. (1997) ‘Ecological constraints drive social evolution in the African mole–rats’, Proceedings of the Royal Society of London. Series B: Biological Sciences, 264(1388), pp. 1619–1627.

Faulkes, C. G. et al. (2004) ‘Phylogeographical patterns of genetic divergence and speciation in African mole-rats (Family: Bathyergidae)’, Molecular Ecology, 13(3), pp. 613–629.

Faulkes, C. G. et al. (2011) ‘Phylogeography and cryptic diversity of the solitary-dwelling silvery mole-rat, genus *Heliophobius* (family: Bathyergidae)’, Journal of Zoology. Edited by A. Kitchener, 285(4), pp. 324–338.

Faulkes, C. G. et al. (2017) ‘Relic populations of *Fukomys* mole-rats in Tanzania: Description of two new species *F. livingstoni sp. nov.* and *F. hanangensis sp. nov.*’, PeerJ, 5, p. e3214.

Faulkes, C. G., Abbott, D. H. and Jarvis, J. U. M. (1990) ‘Social suppression of ovarian cyclicity in captive and wild colonies of naked mole-rats, *Heterocephalus glaber*’, Reproduction, 88(2), pp. 559–568.

Faulkes, C. G. and Bennett, N. C. (2007) ‘African mole-rats: Social and ecological diversity’, in Rodent societies: an ecological and evolutionary perspective, pp. 427–437.

Felsenstein, J. (2006) ‘Accuracy of coalescent likelihood estimates: do we need more dites, more sequences, or more loci?’, Molecular Biology and Evolution, 23(3), pp. 691–700.

Furman, A. et al. (2014) ‘Cytonuclear discordance and the species status of *Myotis myotis* and *Myotis blythii* (Chiroptera)’, Zoologica Scripta. Blackwell Publishing Ltd, 43(6), pp. 549–561.

Galtier, N. et al. (2009) ‘Mitochondrial DNA as a marker of molecular diversity: a reappraisal’, Molecular Ecology. John Wiley & Sons, Ltd, 18(22), pp. 4541–4550.

Garg, K. M. et al. (2016) ‘Genome-wide data help identify an avian species-level lineage that is morphologically and vocally cryptic’, Molecular Phylogenetics and Evolution. Academic Press Inc., 102, pp. 97–103.

Gavryushkina, A. et al. (2014) ‘Bayesian inference of sampled ancestor trees for epidemiology and fossil calibration’, PLoS Computational Biology. Edited by K. Koelle. Public Library of Science, 10(12), p. e1003919.

Gibernau, M. and Montuire, S. (1996) ‘Mammal diversity and environment evolution during the Plio-Pleistocene in East Africa’, Human Evolution, 11(3–4), pp. 193–204.

Gippoliti, S. (2019) ‘Species delimitation in mammals: A comment on Zachos (2018)’, Mammalian Biology. Elsevier GmbH, 94, pp. 127–131.

Gippoliti, S. and Amori, G. (2011) ‘A new species of mole-rat (Rodentia, Bathyergidae) from the Horn of Africa’, Zootaxa, 2918(1), pp. 39–46.

Girman, D. J. et al. (2001) ‘Patterns of population subdivision, gene flow and genetic variability in the African wild dog (*Lycaon pictus*)’, Molecular Ecology. John Wiley & Sons, Ltd, 10(7), pp. 1703–1723.

Gomes Rodrigues, H. et al. (2011) ‘Continuous dental replacement in a hyper-chisel tooth digging rodent’, Proceedings of the National Academy of Sciences, 108(42), pp. 17355–17359.

Good, J. M. et al. (2015) ‘Negligible nuclear introgression despite complete mitochondrial capture between two species of chipmunks’, Evolution. Society for the Study of Evolution, 69(8), pp. 1961-1972.

Happold, D. C. D. (2013) Mammals of Africa - Volume III: Rodents, hares and rabbits.

Hasegawa, M., Kishino, H. and Yano, T. (1985) ‘Dating of the human-ape splitting by a molecular clock of mitochondrial DNA’, Journal of Molecular Evolution, 22(2), pp. 160–174.

Hautier, L. et al. (2011) ‘Hystricognathy vs sciurognathy in the rodent jaw: A new morphometric assessment of hystricognathy applied to the living fossil *Laonastes* (Diatomyidae)’, PLoS ONE. Edited by A. Goswami. Public Library of Science, 6(4), p. e18698.

Heath, T. A., Huelsenbeck, J. P. and Stadler, T. (2014) 'The fossilized birth-death process for coherent calibration of divergence-time estimates', Proceedings of the National Academy of Sciences. National Academy of Sciences, 111(29), pp. e2957–e2966.

Hijmans, R. J. (2019) raster: Geographic data analysis and modeling. R package version 3.0-7. Available at: https://cran.r-project.org/package=raster.

Honeycutt, R. L. et al. (1987) 'Mitochondrial DNA variation and the phylogeny of African mole-rats (Rodentia: Bathyergidae)', Systematic Zoology, 36(3), p. 280.

Honeycutt, R. L. et al. (1991) 'Systematics and evolution of the family Bathyergidae', in Sherman, P. W., Jarvis, J. U. M., and Alexander, R. D. (eds) The biology of the naked mole-rat. Princeton University Press, pp. 45–64.

Huchon, D. and Douzery, E. J. P. (2001) 'From the Old World to the New World: A molecular chronicle of the phylogeny and biogeography of hystricognath rodents', Molecular Phylogenetics and Evolution, 20(2), pp. 238–251.

Ingram, C. M., Burda, H. and Honeycutt, R. L. (2004) 'Molecular phylogenetics and taxonomy of the African mole-rats, genus *Cryptomys* and the new genus *Coetomys* Gray, 1864', Molecular Phylogenetics and Evolution, 31(3), pp. 997–1014.

Janecek, L. L. et al. (1992) 'Allozyme variation and systematics of African mole-rats (Rodentia: Bathyergidae)', Biochemical Systematics and Ecology, 20(5), pp. 401–416.

Jarvis, J. U. M. (2013) 'Bathyergidae', in Happold, D. C. D. (ed.) Mammals of Africa. Volume III: Rodents, hares and rabbits. Bloomsbury Publishing, London, UK, pp. 641–643.

Jarvis, J. U. M., Bennett, N. C. and Spinks, A. C. (1998) 'Food availability and foraging by wild colonies of Damaraland mole-rats (*Cryptomys damarensis*): Implications for sociality', Oecologia, 113(2), pp. 290–298.

Jarvis, J. U. M. and Sale, J. B. (1971) 'Burrowing and burrow patterns of East African mole-rats *Tachyoryctes, Heliophobius* and *Heterocephalus'*, Journal of Zoology. John Wiley & Sons, Ltd, 163(4), pp. 451–479.

Jones, G. (2017) 'Algorithmic improvements to species delimitation and phylogeny estimation under the multispecies coalescent', Journal of Mathematical Biology, 74(1–2), pp. 447–467.

Jones, G., Aydin, Z. and Oxelman, B. (2015) ‘DISSECT: An assignment-free Bayesian discovery method for species delimitation under the multispecies coalescent’, Bioinformatics. Oxford Academic, 31(7), pp. 991–998.

Jukes, T. and Cantor, C. (1969) ‘Evolution of protein molecules’, Mammalian protein metabolism, 3(21), p. 132.

Junker, K., Lutermann, H. and Mutafchiev, Y. (2017) ‘A new ascaridid nematode, *Mammalakis zambiensis n. sp.* (Heterakoidea: Kiwinematidae), from the mole rat *Fukomys anselli* (Burda, Zima, Scharff, Macholán & Kawalika) (Rodentia: Bathyergidae) in Zambia’, Systematic Parasitology. Springer Netherlands, 94(5), pp. 557–566.

Kelley, J. B. et al. (2019) ‘Mechanism for establishing and maintaining the reproductive hierarchy in a eusocial mammal, the Damaraland mole-rat’, Animal Behaviour. Academic Press, 158, pp. 193–200.

Klein, R. G. et al. (2007) ‘The mammalian fauna associated with an archaic hominin skullcap and later Acheulean artifacts at Elandsfontein, Western Cape Province, South Africa’, Journal of Human Evolution, 52(2), pp. 164–186.

Kock, D. et al. (2006) ‘On the nomenclature of Bathyergidae and *Fukomys* n. gen. (Mammalia: Rodentia)’, Zootaxa, 1142(1), pp. 51–55.

Kott, O. et al. (2016) ‘Behavioural tests reveal severe visual deficits in the strictly subterranean African mole-rats (Bathyergidae) but efficient vision in the fossorial rodent Coruro (*Spalacopus cyanus*, Octodontidae)’, Ethology. Edited by L. Fusani. Blackwell Publishing Ltd, 122(8), pp. 682–694.

Kozlov, M. V. et al. (2017) ‘Cryptic diversity in the long-horn moth *Nemophora degeerella* (Lepidoptera: Adelidae) revealed by morphology, DNA barcodes and genome-wide ddRAD-seq data’, Systematic Entomology. Blackwell Publishing Ltd, 42(2), pp. 329–346.

Krásová, J. et al. (2019) ‘Evolution of the Grey-bellied pygmy mouse group: Highly structured molecular diversity with predictable geographic ranges but morphological crypsis’, Molecular Phylogenetics and Evolution, 130, pp. 143–155.

Kumar, S. and Subramanian, S. (2002) ‘Mutation rates in mammalian genomes’, Proceedings of the National Academy of Sciences. National Academy of Sciences, 99(2), pp. 803–808.

Lacey, E., Patton, J. and Cameron, G. (2000) Life underground: The biology of subterranean rodents. University of Chicago Press.

Langmead, B. and Salzberg, S. L. (2012) ‘Fast gapped-read alignment with Bowtie 2’, Nature Methods, 9(4), pp. 357–359.

Lavrenchenko, L. A., Voyta, L. L. And Hutterer, R. (2016) ‘Diversity of shrews in Ethiopia, with the description of two new species of *Crocidura* (Mammalia: Lipotyphla: Soricidae)’, Zootaxa, 4196(1), p. 38.

Lawson, D. J. et al. (2012) ‘Inference of population structure using dense haplotype data’, PLoS Genetics. Edited by G. P. Copenhaver, 8(1), p. e1002453.

Leigh, J. W. and Bryant, D. (2015) ‘Popart: full-feature software for haplotype network construction’, Methods in Ecology and Evolution. Edited by S. Nakagawa. British Ecological Society, 6(9), pp. 1110–1116.

Lessa, E. (1990) ‘Morphological evolution of subterranean mammals: integrating structural, functional, and ecological perspectives’, Progress in Clinical and Biological Research, 335, pp. 211–230.

López-Antoñanzas, R. (2016) ‘Family Ctenodactylidae (Gundis)’, in Wilson, D. E., Lacher, T. E. J., and Mittermeier, R. A. (eds) Handbook of the mammals of the World - Volume 6 lagomorphs and rodents I. Lynx Edicions.

Macgregor, D. (2015) ‘History of the development of the East African Rift System: A series of interpreted maps through time’, Journal of African Earth Sciences. Elsevier Ltd, 101, pp. 232–252.

Malinsky, M. et al. (2018) ‘RADpainter and fineRADstructure: Population Inference from RADseq Data’, Molecular Biology and Evolution. Edited by N. Takezaki, 35(5), pp. 1284–1290.

Mayaux, P. et al. (2004) ‘A new land-cover map of Africa for the year 2000’, Journal of Biogeography. John Wiley & Sons, Ltd, 31(6), pp. 861–877.

Mazoch, V. et al. (2018) ‘Phylogeography of a widespread sub-Saharan murid rodent *Aethomys chrysophilus*: the role of geographic barriers and paleoclimate in the Zambezian bioregion’, Mammalia. Walter de Gruyter GmbH, 82(4), pp. 373–387.

McDonough, M. M. et al. (2015) ‘Multilocus phylogeography of a widespread savanna-woodland-adapted rodent reveals the influence of Pleistocene geomorphology and climate change in Africa’s Zambezi region’, Molecular Ecology. Blackwell Publishing Ltd, 24(20), pp. 5248–5266.

Mein, P. and Pickford, M. (2008) ‘Early miocene rodentia from the northern Sperrgebiet, Namibia’, Memoir of the Geological Survey of Namibia.

Mikula, O. et al. (2016) ‘Evolutionary history and species diversity of African pouched mice (Rodentia: Nesomyidae: *Saccostomus*)’, Zoologica Scripta. Blackwell Publishing Ltd, 45(6), pp. 595–617.

Miller, G. S. and Gidley, J. W. (1918) ‘Synopsis of the supergeneric groups of rodents’, Journal of the Washington Academy of Sciences, 8(13), pp. 431–448.

Monadjem, A. et al. (2015) Rodents of sub-Saharan Africa: A biogeographic and taxonomic synthesis. Walter de Gruyter GmbH.

Montgelard, C. and Matthee, C. A. (2012) ‘Tempo of genetic diversification in southern African rodents: The role of Plio-Pleistocene climatic oscillations as drivers for speciation’, Acta Oecologica. Elsevier Masson, 42, pp. 50–57.

Moodley, Y. and Bruford, M. W. (2007) ‘Molecular biogeography: Towards an integrated framework for conserving pan-African biodiversity’, PLoS ONE. Edited by B. Brembs, 2(5), p. e454.

Moritz, R. E. et al. (2007) ‘Magnetic compass: A useful tool underground’, in Subterrenean rodents: News from underground, pp. 161–174.

Nedbal, M. A., Allard, M. W. and Honeycutt, R. L. (1994) ‘Molecular systematics of hystricognath rodents: Evidence from the mitochondrial 12S rRNA Gene’, Molecular Phylogenetics and Evolution, 3(3), pp. 206–220.

Nevo, E. (1979) ‘Adaptive convergence and divergence of subterranean mammals.’, Annual review of ecology and systematics. Springer, Berlin, Heidelberg, 10(1), pp. 269–308.

Nevo, E. et al. (1987) ‘Allozyme differentiation and systematics of the endemic subterranean mole rats of South Africa’, Biochemical Systematics and Ecology, 15(4), pp. 489–502.

Nevo, E. (1995) ‘Mammalian evolution underground. The ecological-genetic-phenetic interfaces’, Acta Theriologica., 3, pp. 9–31.

Nevo, E. (1999) Mosaic evolution of subterranean mammals: Regression, progression, and global convergence. Oxford University Press.

Nevo, E. (2007) ‘Mosaic evolution of subterranean mammals: Tinkering, regression, progression, and global convergence’, in Subterranean Rodents: News from underground. Springer Berlin Heidelberg, pp. 375–388.

Ogilvie, H. A., Bouckaert, R. R. and Drummond, A. J. (2017) ‘StarBEAST2 brings faster species tree inference and accurate estimates of substitution rates’, Molecular Biology and Evolution, 34(8), pp. 2101–2114.

Padial, J. M. et al. (2010) ‘The integrative future of taxonomy’, Frontiers in Zoology. BioMed Central, 7(1), p. 16.

Paradis E. & Schliep K. (2018). ‘ape 5.0: an environment for modern phylogenetics and evolutionary analyses in R‘. Bioinformatics 35(3): 526-528.

Parker, G. A. et al. (1997) ‘Sperm competition games: a prospective analysis of risk assessment’, Proceedings of the Royal Society of London. Series B: Biological Sciences. Royal Society, 264(1389), pp. 1793–1802.

Patterson (2016) ‘Family Heterocephalidae (naked mole-rat)’, in Wilson, D. E., Lacher, T. E. J., and Mittermeier, R. A. (eds) Hanbook of the Mammals of the World - Volume 6 Lagomorphs and Rodents I. Lynx Edicions.

Patterson, B. D. and Upham, N. S. (2014) ‘A newly recognized family from the Horn of Africa, the Heterocephalidae (Rodentia: Ctenohystrica)’, Zoological Journal of the Linnean Society, 172(4), pp. 942–963.

Patwardhan, A., Ray, S. and Roy, A. (2014) ‘Molecular Markers in Phylogenetic Studies-A Review’, Journal of Phylogenetics & Evolutionary Biology, 2(2), p. 131.

Patzenhauerová, H., Bryja, J. and Šumbera, R. (2010) ‘Kinship structure and mating system in a solitary subterranean rodent, the silvery mole-rat’, Behavioral Ecology and Sociobiology. Springer, 64(5), pp. 757–767.

Peterson, B. K. et al. (2012) ‘Double digest RADseq: An inexpensive method for de novo SNP discovery and genotyping in model and non-model species’, PLoS ONE. Edited by L. Orlando, 7(5), p. e37135.

Petružela, J. et al. (2018) ‘Spiny mice of the Zambezian bioregion – phylogeny, biogeography and ecological differentiation within the *Acomys spinosissimus* complex’, Mammalian Biology. Elsevier GmbH, 91(1), pp. 79–90.

Pickford, M. and Mein, P. (1988) ‘The discovery of fossiliferous Plio-Pleistocene cave fillings in Ngamiland, Botswana’, Comptes rendus de l’Académie des sciences. Série 2, Mécanique, Physique, Chimie, Sciences de l’univers, Sciences de la Terre, 307(14), pp. 1681–1686.

Pitra, C. et al. (2002) ‘An exceptional case of historical outbreeding in African sable antelope populations’, Molecular Ecology. John Wiley & Sons, Ltd, 11(7), pp. 1197–1208.

Potts, R. (1998) ‘Environmental hypotheses of hominin evolution’, American Journal of Physical Anthropology. John Wiley & Sons, Ltd, 107(S27), pp. 93–136.

Potts, R. (2013) ‘Hominin evolution in settings of strong environmental variability’, Quaternary Science Reviews. Elsevier Ltd, 73, pp. 1–13.

Procheş, Ş. et al. (2006) ‘An overview of the Cape geophytes’, Biological Journal of the Linnean Society. Oxford Academic, 87(1), pp. 27–43.

Rambau, R. V., Robinson, T. J. and Stanyon, R. (2003) ‘Molecular genetics of *Rhabdomys pumilio* subspecies boundaries: mtDNA phylogeography and karyotypic analysis by fluorescence in situ hybridization’, Molecular Phylogenetics and Evolution. Academic Press Inc., 28(3), pp. 564–575.

Rambaut, A. et al. (2018) ‘Posterior summarization in Bayesian phylogenetics using Tracer 1.7.’, Systemic biology, 67(5), pp. 901–904.

Rannala, B. and Yang, Z. (2003) ‘Bayes estimation of species divergence times and ancestral population sizes using DNA sequences from multiple loci’, Genetics, 164(4), pp. 1645–1656.

Ratnam, J. et al. (2011) ‘When is a “forest” a savanna, and why does it matter?’, Global Ecology and Biogeography. John Wiley & Sons, Ltd, 20(5), pp. 653–660.

Ravelo, A. C. et al. (2004) ‘Regional climate shifts caused by gradual global cooling in the Pliocene epoch’, Nature, 429(6989), pp. 263–267.

Říčan, O. et al. (2016) ‘Diversity and evolution of the Middle American cichlid fishes (Teleostei: Cichlidae) with revised classification’, Vertebrate Zoology, 66(1), pp. 1–102.

Riedel, A. et al. (2013) ‘Integrative taxonomy on the fast track - towards more sustainability in biodiversity research’, Frontiers in Zoology. BioMed Central, 10(1), p. 15.

Rodríguez-Prieto, A., Igea, J. and Castresana, J. (2014) ‘Development of rapidly evolving intron markers to estimate multilocus species trees of rodents’, PLoS ONE. Edited by J. Brosius, 9(5), p. e96032.

Romer, A. S. (1958) Vertebrate paleontology. 2th edn. Chicago: The University of Chicago Press.

Roper, T. J. et al. (2001) ‘Environmental conditions in burrows of two species of African mole-rat, *Georhychus capensis* and *Cryptomys damarensis*’, Journal of Zoology, 254(1), p. 101–107.

Rosvall, M., Axelsson, D. and Bergstrom, C. T. (2009) ‘The map equation’, The European Physical Journal Special Topics. Springer, 178(1), pp. 13–23.

Rosvall, M. and Bergstrom, C. (2008) ‘Maps of random walks on complex networks reveal community structure’, PNAS. National Academy of Sciences, 105(4), pp. 1118–1123.

Rowan, J. et al. (2016) ‘Strong influence of palaeoclimate on the structure of modern African mammal communities’, Proceedings of the Royal Society B: Biological Sciences, 283(1840), p. 20161207.

Roy, S. C., Moitra, K. and De Sarker, D. (2017) ‘Assessment of genetic diversity among four orchids based on ddRAD sequencing data for conservation purposes’, Physiology and Molecular Biology of Plants. Springer India, 23(1), pp. 169–183.

Runck, A. M., Matocq, M. D. and Cook, J. A. (2009) ‘Historic hybridization and persistence of a novel mito-nuclear combination in red-backed voles (genus *Myodes*)’, BMC Evolutionary Biology, 9(1), p. 114.

Russo, I.-R. M., Chimimba, C. T. and Bloomer, P. (2006) 'Mitochondrial DNA differentiation between two species of *Aethomys* (Rodentia: Muridae) from Southern Africa', Journal of Mammalogy. Oxford University Press (OUP), 87(3), pp. 545–553.

Sahm, A. et al. (2018) 'Higher gene expression stability during aging in long-lived giant mole-rats than in short-lived rats', Aging. Impact Journals LLC, 10(12), pp. 3938–3956.

Sallam, H. M. et al. (2009) 'Fossil and molecular evidence constrain scenarios for the early evolutionary and biogeographic history of hystricognathous rodents', Proceedings of the National Academy of Sciences, 106(39), pp. 16722–16727.

Sankaran, M. et al. (2005) 'Determinants of woody cover in African savannas', Nature, 438(7069), pp. 846–849.

Scharff, A. et al. (2001) 'A new karyotype of *Heliophobius argenteocinereus* (Bathyergidae, Rodentia) from Zambia with field notes on the species', Mammalian Biology-Zeitschrift fur Saugetierkunde, 66(6), pp. 376–378.

Schmidt, R. C., Bart, H. L. and Nyingi, W. D. (2017) 'Multi-locus phylogeny reveals instances of mitochondrial introgression and unrecognized diversity in Kenyan barbs (Cyprininae: Smiliogastrini)', Molecular Phylogenetics and Evolution. Academic Press Inc., 111, pp. 35–43.

Seluanov, A. et al. (2009) 'Hypersensitivity to contact inhibition provides a clue to cancer resistance of naked mole-rat', PNAS, 106(46), pp. 19352–19357.

Skinner, J. D. and Chimimba, C. T. (2005) The mammals of the Southern African sub-region. Cambridge University Press.

Šklíba, J., Jirků, M. and Šumbera, R. (2016) 'Burrow systems of mole-rats as refuges for frogs in the Miombo woodlands of south-east Africa', Journal of Tropical Ecology. Cambridge University Press, 32(2), pp. 158–161.

Spinks, A. C. and Plaganyi, E. E. (1999) 'Reduced starvation risks and habitat constraints promote cooperation in the common mole-rat, Cryptomys hottentotus hottentotus: A computer-simulated foraging model', Oikos. JSTOR, 85(3), pp. 435–444.

Stanley, W. T. et al. (2015) 'Phylogeny, phylogeography and geographical variation in the *Crocidura monax* (Soricidae) species complex from the montane islands of Tanzania, with

descriptions of three new species', Zoological Journal of the Linnean Society. Blackwell Publishing Ltd, 174(1), pp. 185–215.

Stephens, M. and Sheet, P. (2005) 'Accounting for decay of linkage disequilibrium in haplotype inference and missing-data imputation.', The American Journal of Human Genetics, 76(3).

Stephens, M., Smith, J. and Donnelly, P. (2001) 'A new statistical method for haplotype reconstruction from population data.', The American Journal of Human Genetics, 68(4), pp. 978–989.

Steppan, S. J. et al. (2005) 'Multigene phylogeny of the Old World mice, Murinae, reveals distinct geographic lineages and the declining utility of mitochondrial genes compared to nuclear genes', Molecular Phylogenetics and Evolution, 37(2), pp. 370–388.

Šumbera, R. et al. (2004) 'Microclimatic stability in burrows of an Afrotropical solitary bathyergid rodent, the silvery mole-rat (*Heliophobius argenteocinereus*)', Journal of Zoology, 263(4), pp. 409–416.

Šumbera, R., Burda, H. and Chitaukali, W. N. (2003) 'Reproductive biology of a solitary subterranean bathyergid rodent, the silvery mole-rat (*Heliophobius argenteocinereus*)', Journal of Mammalogy, 84(1), pp. 278–287.

Šumbera, R., Chitaukali, W. N. and Burda, H. (2007) 'Biology of the silvery mole-rat (*Heliophobius argenteocinereus*). Why study a neglected subterranean rodent species?', in Subterranean Rodents News from Underground, pp. 221–236.

Taylor, P. J. et al. (2009) 'Speciation mirrors geomorphology and palaeoclimatic history in African laminate-toothed rats (Muridae: Otomyini) of the *Otomys denti* and *Otomys lacustris* species-complexes in the "Montane Circle" of East Africa', Biological Journal of the Linnean Society. Oxford Academic, 96(4), pp. 913–941.

Taylor, P. J. et al. (2012) 'Four new bat species (*Rhinolophus hildebrandtii* complex) reflect Plio-Pleistocene divergence of dwarfs and giants across an Afromontane Archipelago', PLoS ONE. Edited by A. Janke. Public Library of Science, 7(9), p. e41744.

Taylor, P. J., Denys, C. and Cotterill, F. P. D. (Woody) (2019) 'Taxonomic anarchy or an inconvenient truth for conservation? Accelerated species discovery reveals evolutionary

patterns and heightened extinction threat in Afro-Malagasy small mammals', Mammalia, 83(4), pp. 313–329.

Teeling, E. C. et al. (2000) 'Molecular evidence regarding the origin of echolocation and flight in bats', Nature, 403(6766), pp. 188–192.

Thomas, O. (1896) '6. On the genera of rodents: An attempt to bring up to date the current arrangement of the order', Proceedings of the Zoological Society of London, 64(4), pp. 1012–1028.

Toews, D. P. L. and Brelsvord, A. (2012) 'The biogeography of mitochondrial and nuclear discordance in animals', Molecular Ecology. John Wiley & Sons, Ltd, 21(16), pp. 3907–3930.

Trauth, M. H. et al. (2007) 'High- and low-latitude forcing of Plio-Pleistocene East African climate and human evolution', Journal of Human Evolution. Academic Press, 53(5), pp. 475–486.

Trouessart, E. L. (1899) Catalogus Mammalium tam viventium quam fossilium a doctore E.-L. Trouessart. R. Friedländer and Sohn.

Tullberg, T. (1899) Ueber das system der Nagethiere: eine phylogenetische studie. Akademische Buchdruckerei.

Van Daele, P. A. A. G. et al. (2004) 'Chromosomal diversity in mole-rats of the genus *Cryptomys* (Rodentia: Bathyergidae) from the Zambezian region: with descriptions of new karyotypes', Journal of Zoology, 264(3), pp. 317–326.

Van Daele, P. A. A. G., Faulkes, C. G., et al. (2007a) 'African mole-rats (Bathyergidae): A complex radiation in tropical soils', in Subterranean rodents: News from underground, pp. 357–373.

Van Daele, P. A. A. G., Verheyen, E., et al. (2007b) 'Cytochrome b sequence analysis reveals differential molecular evolution in African mole-rats of the chromosomally hyperdiverse genus *Fukomys* (Bathyergidae, Rodentia) from the Zambezian region', Molecular Phylogenetics and Evolution, 45(1), pp. 142–157.

Van Daele, P. A. A. G. et al. (2013) 'A new species of African Mole-rat (*Fukomys*, Bathyergidae, Rodentia) from the Zaire-Zambezi watershed', Zootaxa, 3636(1), pp. 171–189.

Verheyen, W. et al. (2011) ‘Contribution to the systematics and zoogeography of the East-African Acomys spinosissimus Peters 1852 species complex and the description of two new species (Rodentia: Muridae)’, Zootaxa, 3059(1), p. 1.

Visser, J. H., Bennett, N. C. and Jansen van Vuuren, B. (2014) ‘Local and regional scale genetic variation in the Cape dune mole-rat, *Bathyergus suillus*’, PLoS ONE, 9(9), p. e107226.

Visser, J. H., Bennett, N. C. and Jansen van Vuuren, B. (2018) ‘Spatial genetic diversity in the Cape mole-rat, *Georychus capensis*: Extreme isolation of populations in a subterranean environment’, PLoS ONE. Edited by T.-Y. Chiang, 13(3), p. e0194165.

Visser, J. H., Bennett, N. C. and Jansen van Vuuren, B. (2019a) ‘Evolutionary and ecological patterns within the South African Bathyergidae: Implications for taxonomy’, Molecular Phylogenetics and Evolution. Elsevier, 130(October 2018), pp. 181–197.

Visser, J. H., Bennett, N. C. and Jansen van Vuuren, B. (2019b) ‘Phylogeny and biogeography of the African Bathyergidae: a review of patterns and processes’, PeerJ, 7(10), p. e7730.

Visser, J. H., Bennett, N. C. and Jansen Van Vuuren, B. (2017) ‘Distributional range, ecology and mating system of the Cape mole-rat, *Georychus capensis* family Bathyergidae’, Canadian journal of zoology, 95(10), pp. 713–726.

Walton, A. H., Nedbal, M. A. and Honeycutt, R. L. (2000) ‘Evidence from intron 1 of the nuclear transthyretin (prealbumin) gene for the phylogeny of African mole-rats (Bathyergidae)’, Molecular Phylogenetics and Evolution, 16(3), pp. 467–474.

Waterhouse, G. R. (1841) ‘IX.- Observations on the Rodentia’, The Annals and magazine of Natural History, 8(49), pp. 81–84.

Weber, M. (1928) Die Säugetiere. 2nd edn. Verlag von Gustav Fischer.

Weibel, A. C. and Moore, W. S. (2002) ‘A test of a mitochondrial gene-based phylogeny of woodpeckers (genus *Picoides*) using an independent nuclear gene, β-fibrinogen intron 7’, Molecular Phylogenetics and Evolution. Elsevier, 22(2), pp. 247–257.

Weiss, M. et al. (2018) ‘Genome-wide single-nucleotide polymorphism data reveal cryptic species within cryptic freshwater snail species-The case of the *Ancylus fluviatilis* species complex’, Ecology and Evolution. John Wiley and Sons Ltd, 8(2), pp. 1063–1072.

Wickliffe, K. J. et al. (2003) ‘Intron 7 (Fgb/I7) of the fibrinogen, B beta polypeptide (FGB): a nuclear DNA phylogenetic marker for mammals’, Museum of Texas Tech University, 219.

Wilson, D. E., Lacher, T. E. J. and Mittermeier, R. A. (2016) Handbook of the mammals of the World - Volume 6 lagomorphs and rodents I.

Winge, H. (1924) ‘PattedyrSlaegter. II. Rodentia, Carnivora’, Primates, 1, p. 321.

Winkler, A., Denis, C. and Avery, D. (2010) ‘Fossil rodents of Africa’, in Werdelin, L. and Sanders, W. J. (eds) Cenozoic mammals of Africa. Unniversity of California Press, Berkeley, pp. 263–304.

Wood, A. E. (1955) ‘A revised classification of the rodents’, Journal of Mammalogy, 36(2), p. 165.

Wood, A. E. (1985) ‘The relationships, origin and dispersal of the hystricognathous rodents’, in Evolutionary Relationships among Rodents. vol. 92. Boston, MA: Springer US, pp. 475–513.

Zachos, F. E. et al. (2013) ‘Species inflation and taxonomic artefacts—A critical comment on recent trends in mammalian classification’, Mammalian Biology. Springer, 78(1), pp. 1–6.

Zachos, F. E., Christidis, L. and Garnett, S. T. (2019) ‘Mammalian species and the twofold nature of taxonomy: a comment on Taylor et al. 2019’, Mammalia. De Gruyter, 84(1), pp. 1–5.

Zhao, J. et al. (no date) ‘Dampened PI3K/AKT signaling contributes to cancer resistance of the naked mole rat’, preprint.

Zinner, D. et al. (2009) ‘Mitochondrial phylogeography of baboons (*Papio* spp.) – Indication for introgressive hybridization?’, BMC Evolutionary Biology. BioMed Central Ltd., 9(1), p. 83.

7 Supplement

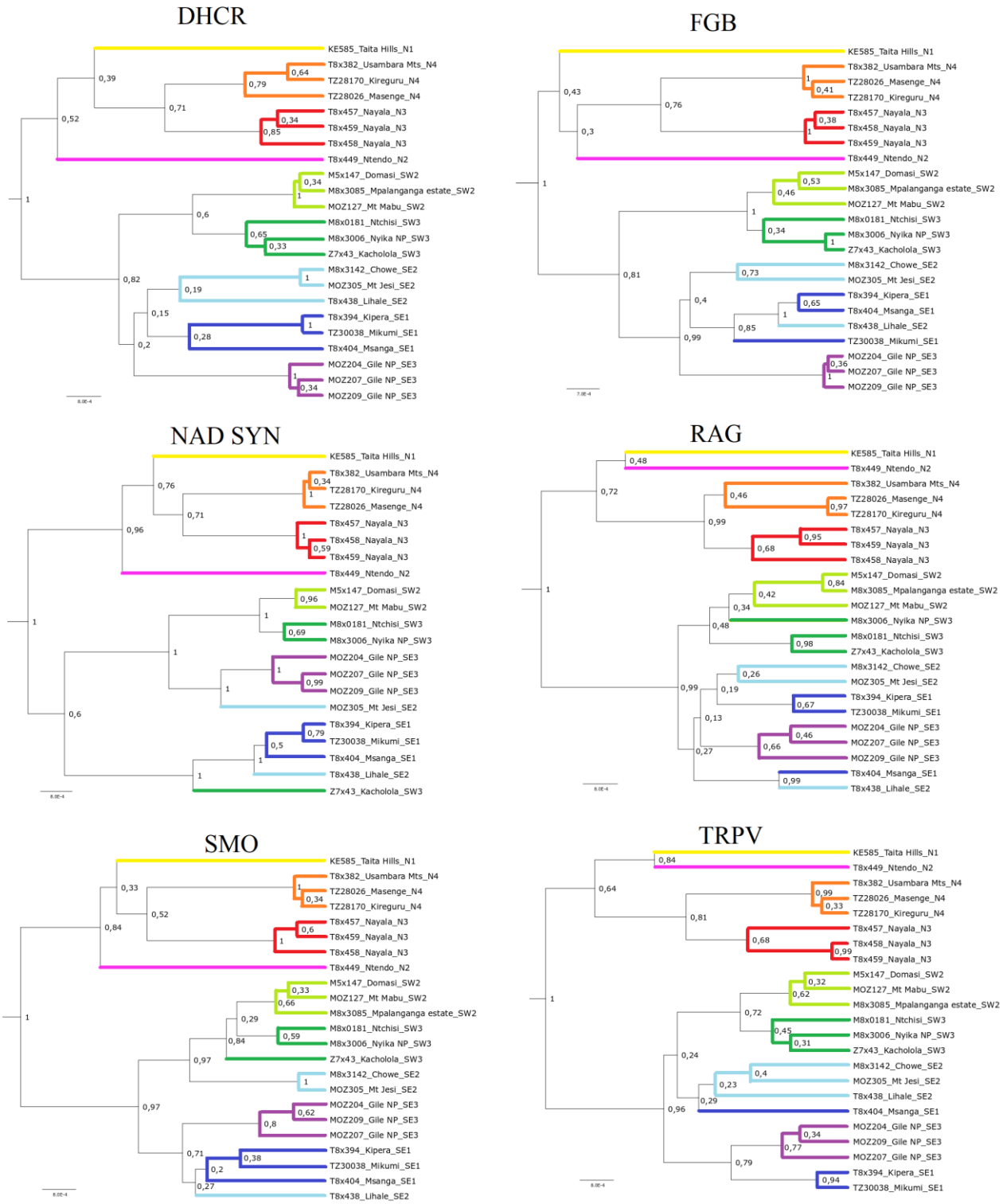

Fig. S1: The maximum clade credibility trees for separate genes from StarBEAST analysis for the genus *Heliophobius*. The numbers next to nodes show the posterior probabilities and terminal nodes are named according to samples (ID of sample_locality_OTU). Branches are coloured according to OTUs.

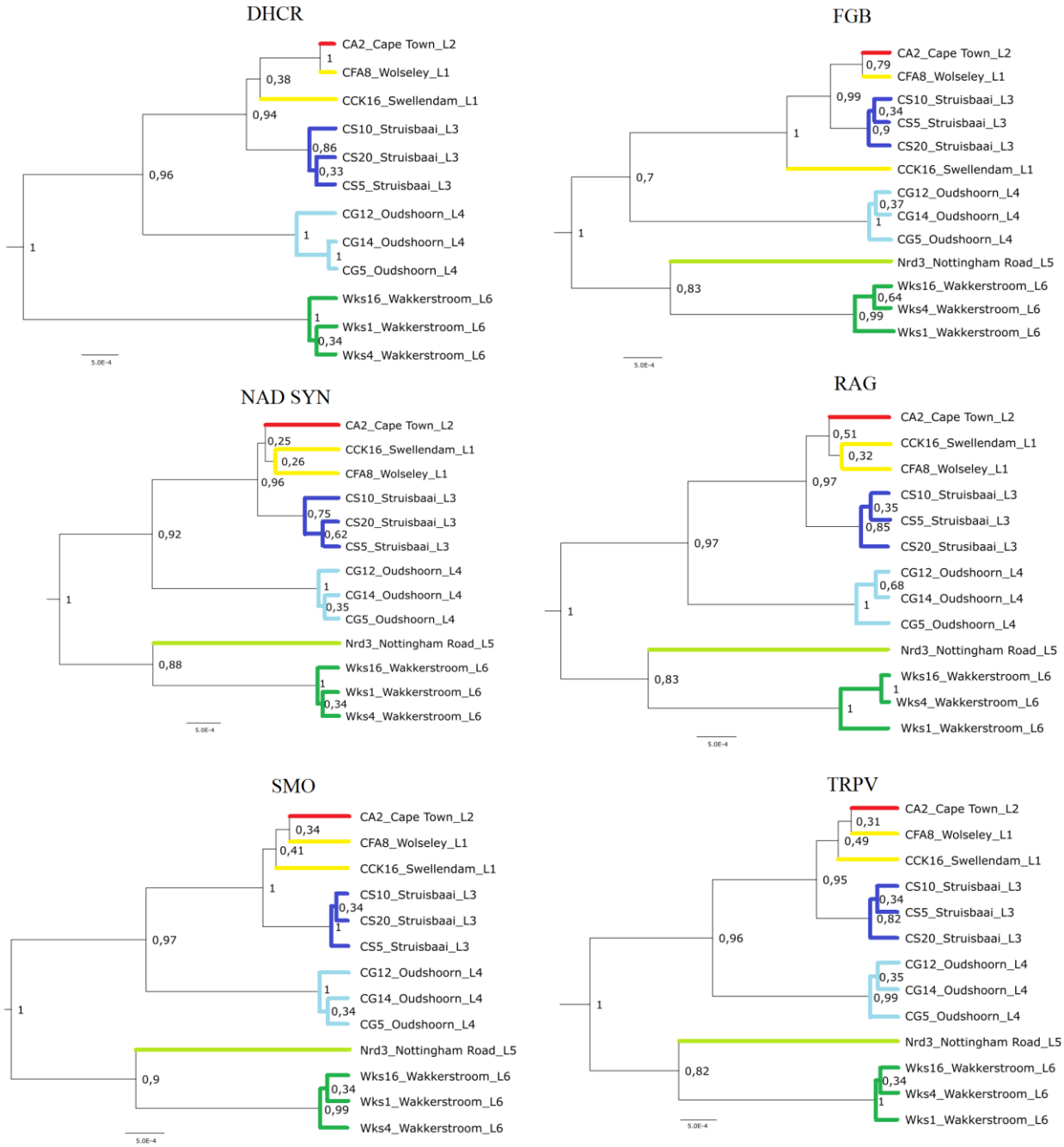

Fig. S2: The maximum clade credibility trees for separate genes from StarBEAST analysis for the genus *Georychus*. The numbers next to nodes show the posterior probabilities and terminal nodes are named according to samples (ID of sample_locality_OTU). Branches are coloured according to OTUs.

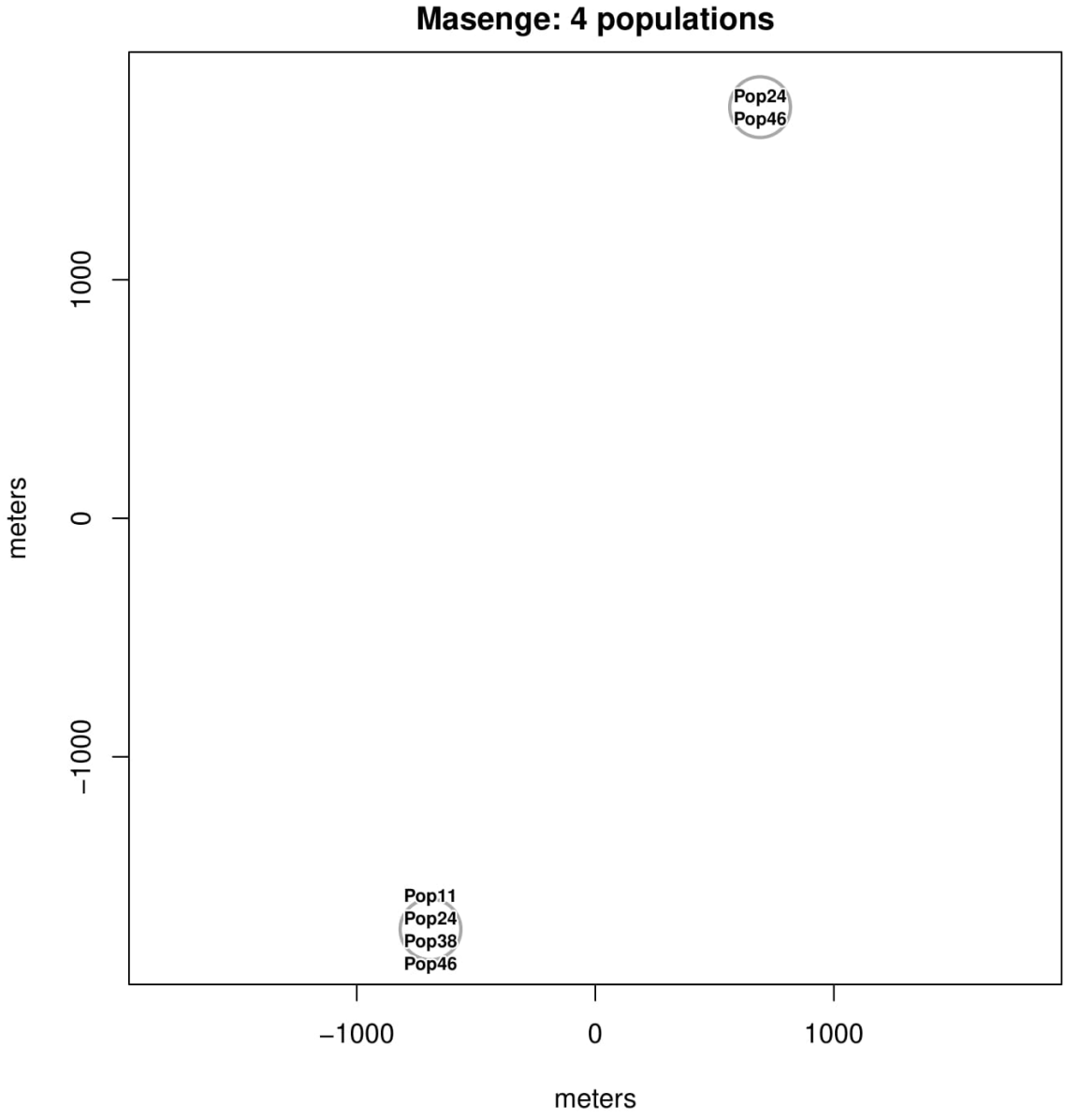

Fig. S3: Spatial distribution of fineRADstructure populations of *Heliophobius*, locality Masenge (6.38˚S, 36.92˚E). Sampling sites are shown as grey circles, population labels are placed wherever the populations were found.

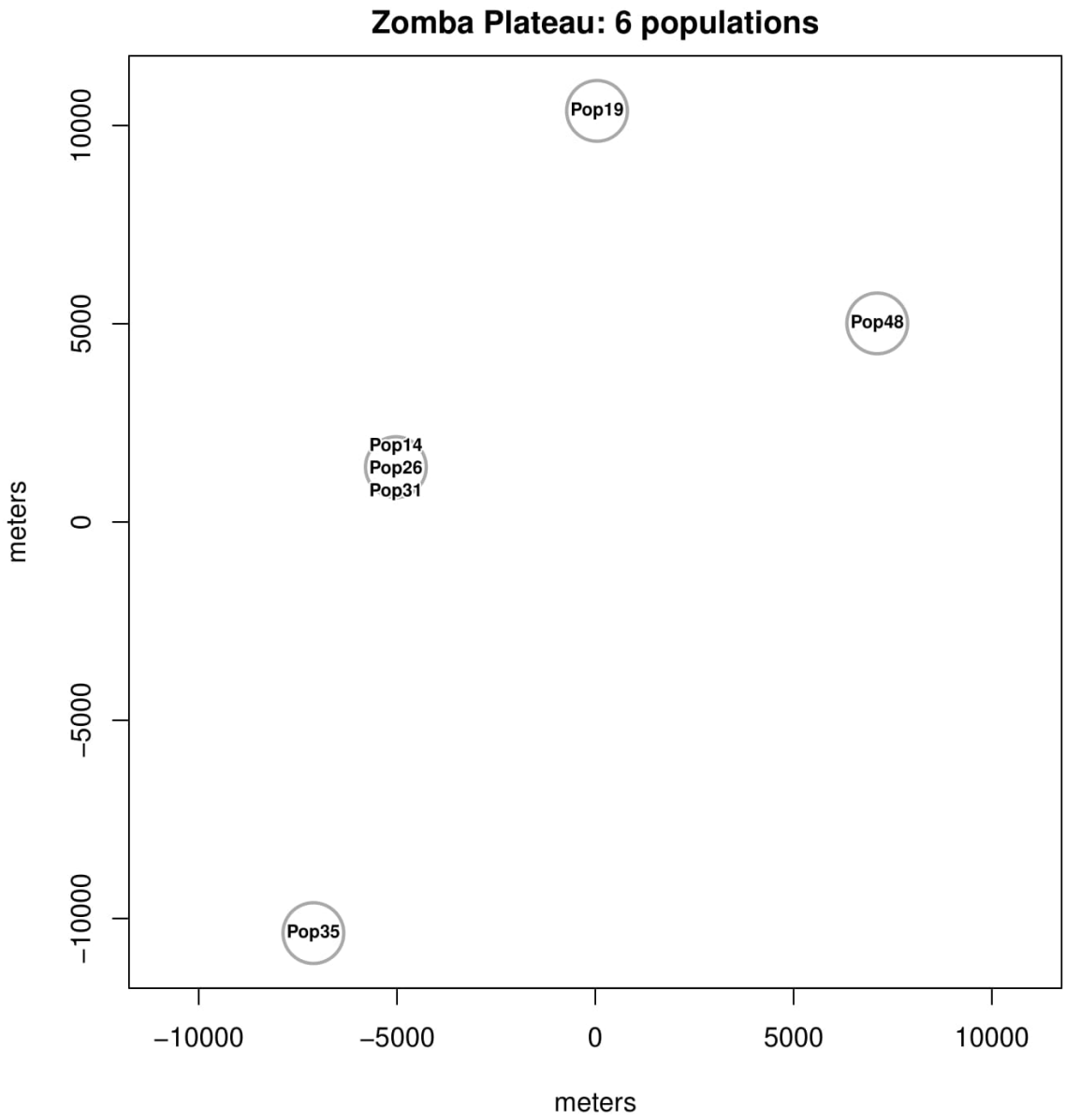

Fig. S4: Spatial distribution of fineRADstructure populations of *Heliophobius*, locality Zomba Plateau (15.34˚S, 35.31˚E).

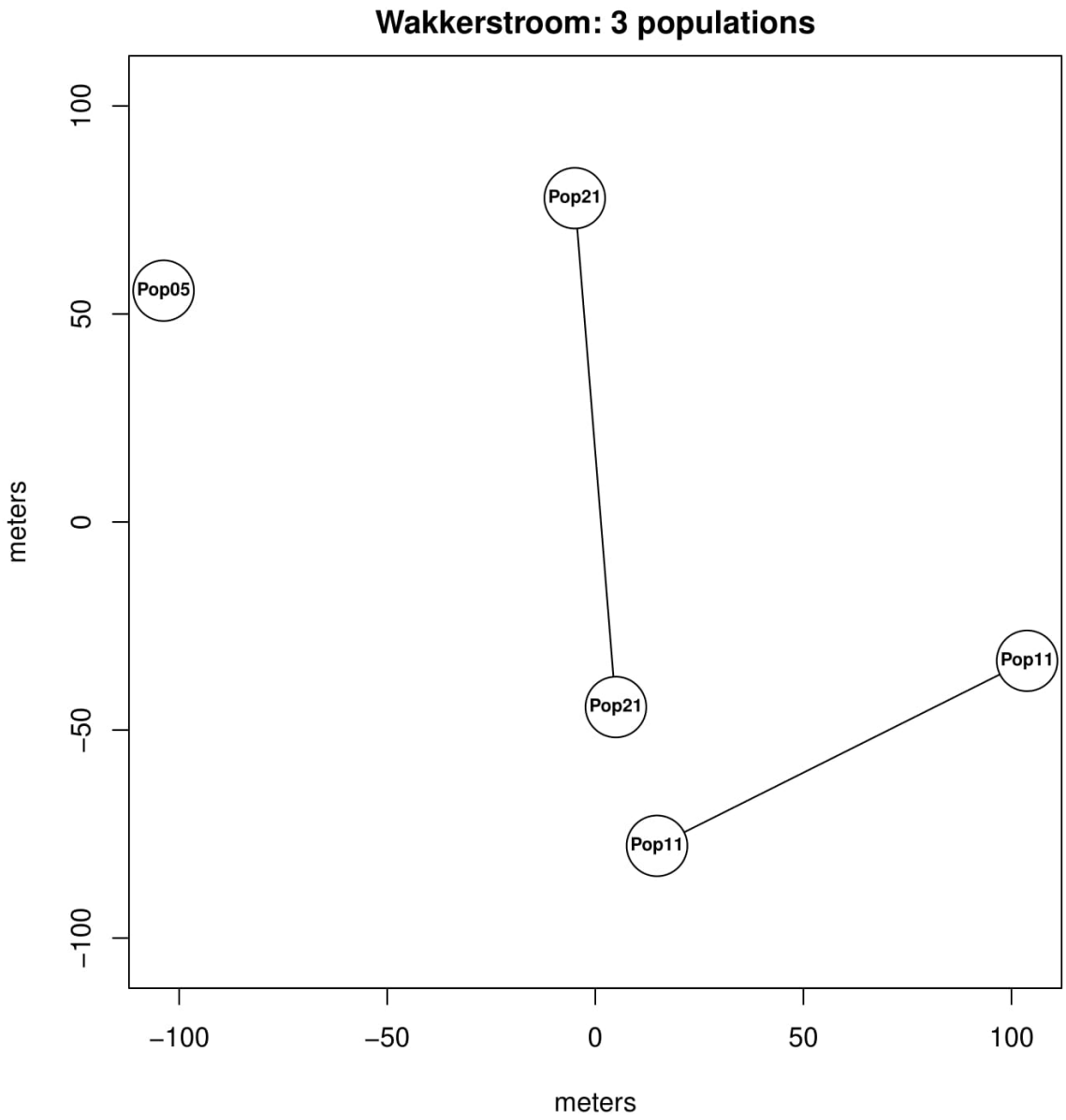

Fig. S5: Spatial distribution of fineRADstructure populations of *Georychus*, locality Wakkerstroom (27.30˚S, 30.36˚E).

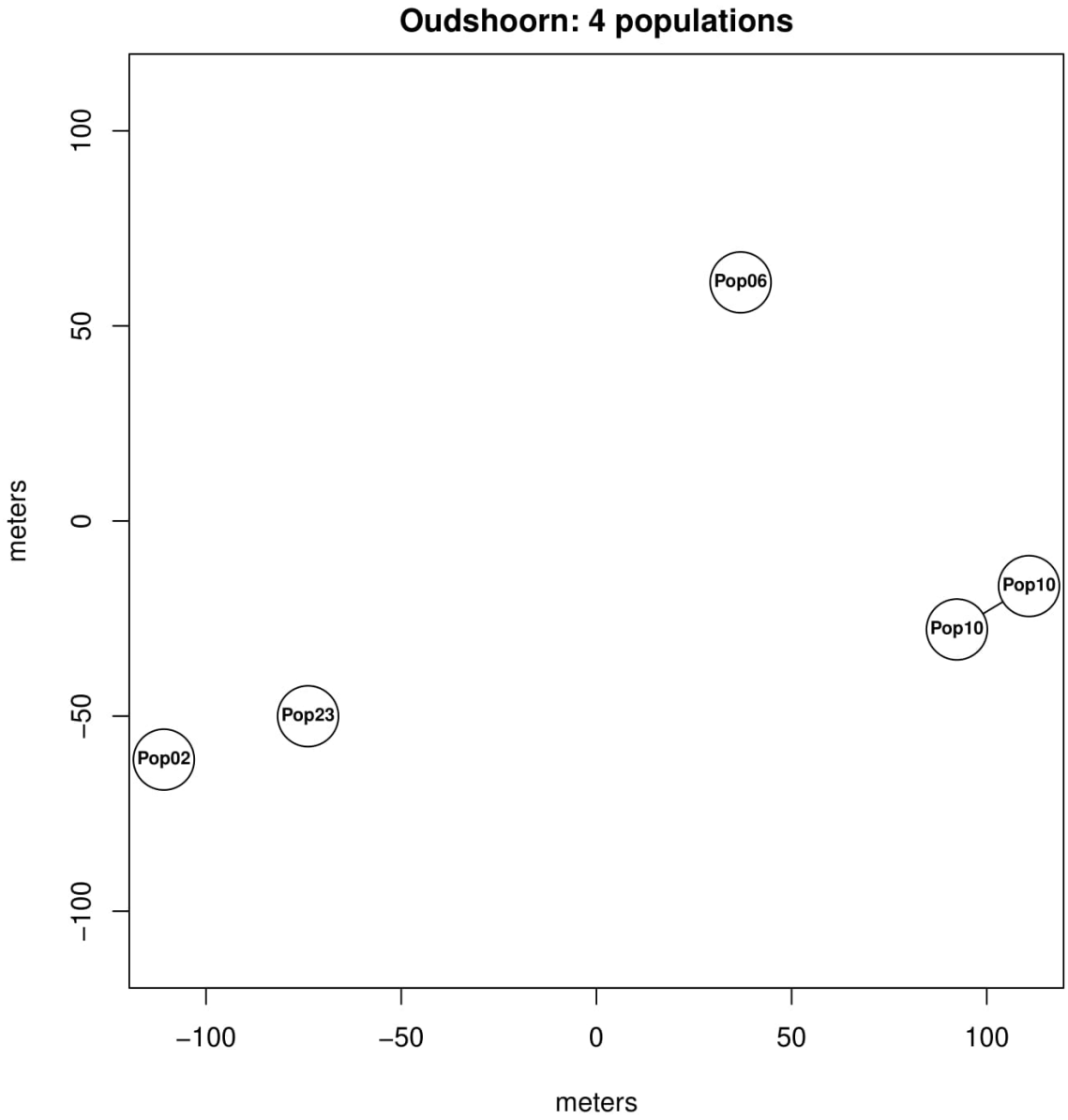

Fig. S6: Spatial distribution of fineRADstructure populations of *Georychus*, locality Oudshoorn (33.85˚S, 22.04˚E).

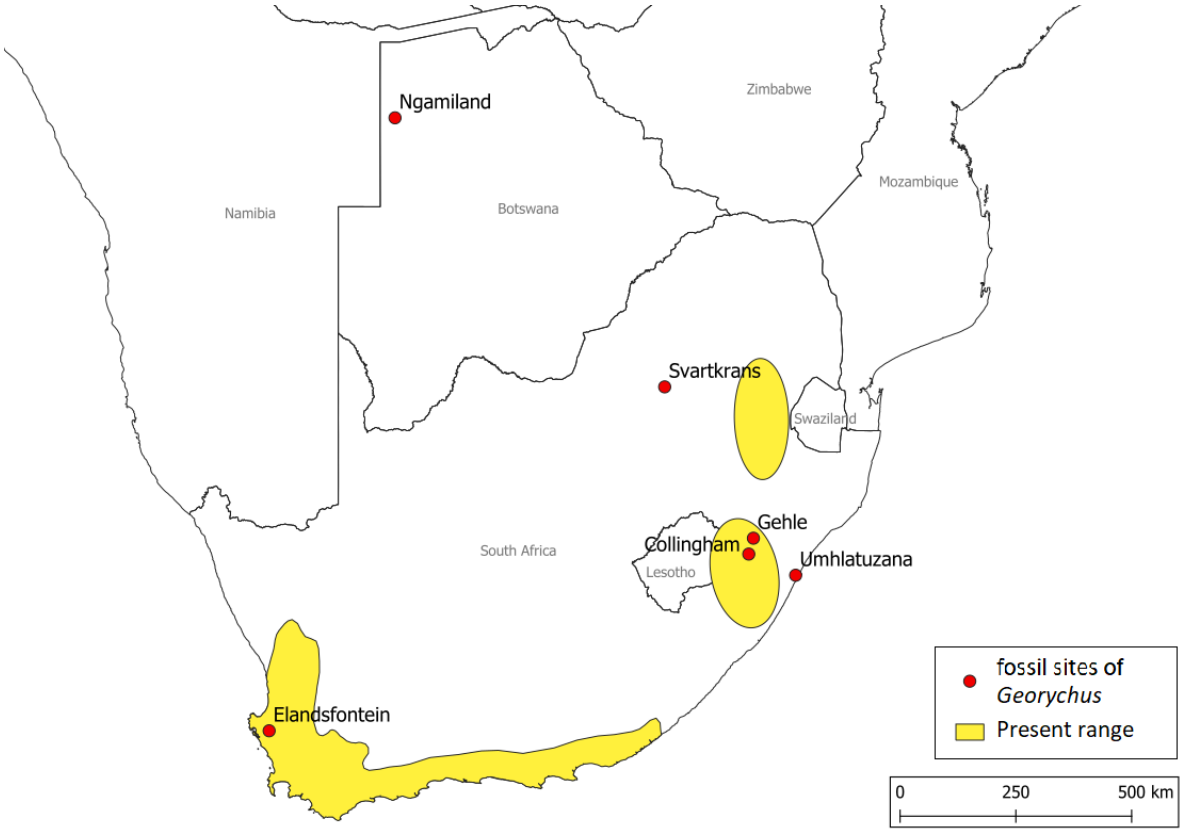

Fig. S7: The geographic distribution of fossil sites of *Georychus*. Yellow areas stand for a present distribution of *Georychus capensis* (IUCN 2020).

7.1 The assesment of cytb fragments

Short cytb sequences (molecular barcodes designed by Galan et al. 2012) were obtained by amplicon sequencing on Illumina platform from five museum specimens. One of the specimens is from Nyika National Park (10.583S, 33.700E; Zambia) and four from three localities in Katanga region at southeast of Dem. Rep. Congo; Dubie (8.330S, 28.320E), Kiambi (7.140S, 27.520E), Kisandji Mitwala (8.420S, 27.220E). Their skin clips were obtained from museums; specimens from Nyika National Park from Livingstone Museum (Livingstone, Zambia) and specimens from Dem. Rep. Congo from Royal Museum for Central Africa (Tervuren, Belgium).

Cytochrome b tree was inferred in the Bayesian framework using software MrBayes 3.2.6 (Ronquist et al. 2012). The alignment was partitioned according to codon positions (1+2 vs. 3), for which separate HKY+G nucleotide substitution models were used. Branch lengths were unconstrained and the tree was rooted using two *Fukomys* sequences as outgroups (pruned off

the tree for the visualization). Four independent runs were conducted to check for convergence and their outputs merged (after discarding of burn-ins). Figure S8 shows the maximum clade credibility tree representing the combined posterior sample. Only unique haplotypes longer than 700bp were included, phylogenetic placement of all other available sequences including two Illumina barcodes was estimated using the evolutionary placement algorithm (Berger et al. 2011) as implemented in RAxML 8 (Stamatakis 2014).

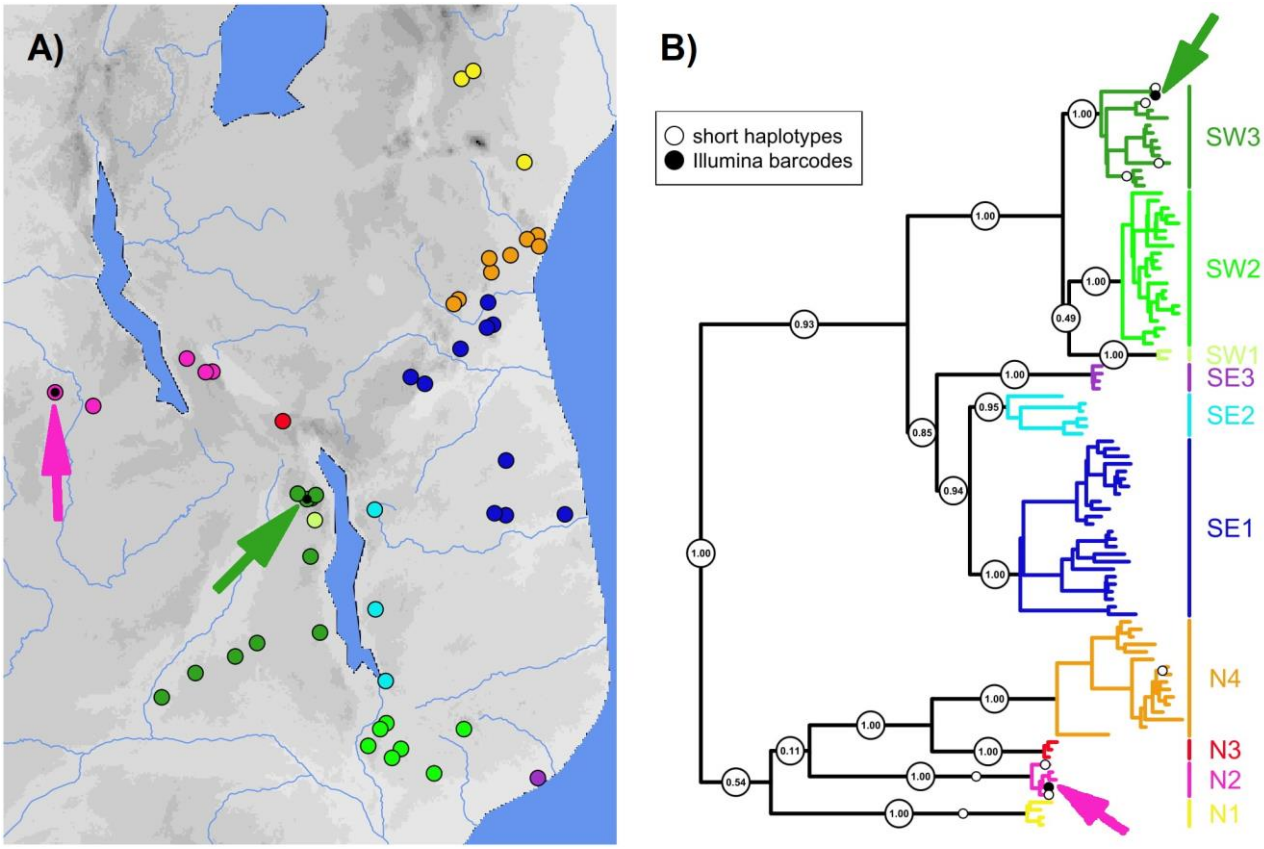

Fig. S8: A) A geographical distribution of sampled localities for cytb analysis. B) The maximum clade credibility tree from Bayesian analysis based on cytb dataset for the genus *Heliophobius*. Branch labels show posterior probabilities. The filled and open circles indicate phylogenetic positions of Illumina barcodes and additional unique but short haplotypes, respectively. Colours of branches match the OTUs and are identical to sites in the map. Arrows highlight positions of Illumina barcodes in the map and the tree.

7.2 MaxEnt:

Species distribution modeling was performed by MaxEnt method (Phillips et al. 2006) as implemented in R package 'maxnet' (Phillips et al. 2017). This method is based on the maximum entropy principle, i.e. on maximization of uncertainty in predictions, limited only by constraints imposed by data (Harte & Newman 2014). This foundation makes it suitable for predicting potential species distributions based on presence-only data. In this case, the data were georeferenced presence records from this work, published studies and museum collections. The predictors were average monthly precipitations and maximum and minimum temperatures as provided at WorldClim website (Hijmans et al. 2005). Both predictor variables and presence records were sampled at $1/3$ degree resolution and refer, therefore, to quadrates of this size. In its basic form, MaxEnt predicts relative occurrence rates (RORs), which can be thought as fractions of a hypothetical population of the species living in particular quadrates. The prediction spreads RORs as evenly as possible over some specified set of background quadrates, while satisfying constraints imposed presence data. Satisfying the constraints means keeping similar two density distributions of predictor variables: one at the presence quadrates and another weighted RORs. The background quadrates covered area with suitable biomes in the countries where presence of the genus in question was proven or can be assumed. Biome maps were taken from Olson et al. (2001) and these biomes were considered suitable: for *Georychus* "Deserts and xeric shrublands", "Mediterranean Forests, woodlands and scrubs" and "Montane grasslands and shrublands" and for *Heliophobius* "Montane grasslands and shrublands" and "Tropical and subtropical grasslands, savannas and shrublands".

To balance flexibility and robustness of the fit, two statistical tools are applied. One is transformation of predictor variables, while the other is regularization of the fit by application of LASSO penalty (Tibshirani 1996). Here, the transformation of predictors took advantage of them being in the form of ordered series, which can be though as climatic curves. Each of the three curves was spline-transformed by projecting a set of ordered monthly values onto a natural cubic spline basis built on interval $\langle 1,12 \rangle$ with five evenly placed knots (Hastie et al. 2009, pp. 148–151). Thus, each climatic curve was decomposed into five components replacing original twelve values.

No attempt was made to transform RORs into presence probabilities, but instead, RORs were divided by their uniform prior value equal to $1/N$, where N is the number of background points. Thus, values > 1 indicate quadrates where available evidence was strong enough to provide stronger support for presence of the species than would be possible without any data.

To get an idea about changes in climatic suitability in time, the fitted model was used to predict RORs also for paleoclimatic layers, namely for monthly temperature and precipitation values estimated for Mid-Holocene (6 thousand years ago, ka, Gent et al. 2011), Last Glacial Maximum (22 ka; Gent et al., 2011) and Last Interglacial (120–140 ka; Otto-Bliesner et al., 2006), all available at the WorldClim website (https://www.worldclim.org).

7.2.1 Results of MaxEnt

Maps (Fig. S9) showing the relative occurrence rates in space during different times suggest that *Heliophobius* probably does not prefer climate that was rare through the analysed time and across its distribution (the wide areas of green patches depicting a probable occurrence). This trend is also apparent in climatic curves (Fig. S10), as the actual presence points (green curves) overlap the mean climatic value over the studied area (grey circles of violin plots). Only from the maximum temperature curve (Fig. S10) is evident, that this bathyergid occur in areas with lower temperatures than is the mean month value, probably mainly in higher elevations.

The causes of fragmentation of *Georychus*`s population is probably different to *Heliophobius*. As shows the map (Fig. S11), this bathyergid more likely lives in areas with relatively rare conditions throughout the studied time (restricted green areas). The curves of climatic conditions (precipitation and maximum temperature in Fig. S12) support the fact, that *Georychus* occupies rare areas, as the actual presence points (green curves) do not coincide with the mean values of the studied area (grey circles of violin plots). Observed considerable changes of probable distribution areas during the studied time suggest, that this bathyergid have probably undergone several distributional retractions and expansions with the repeated changes of climate.

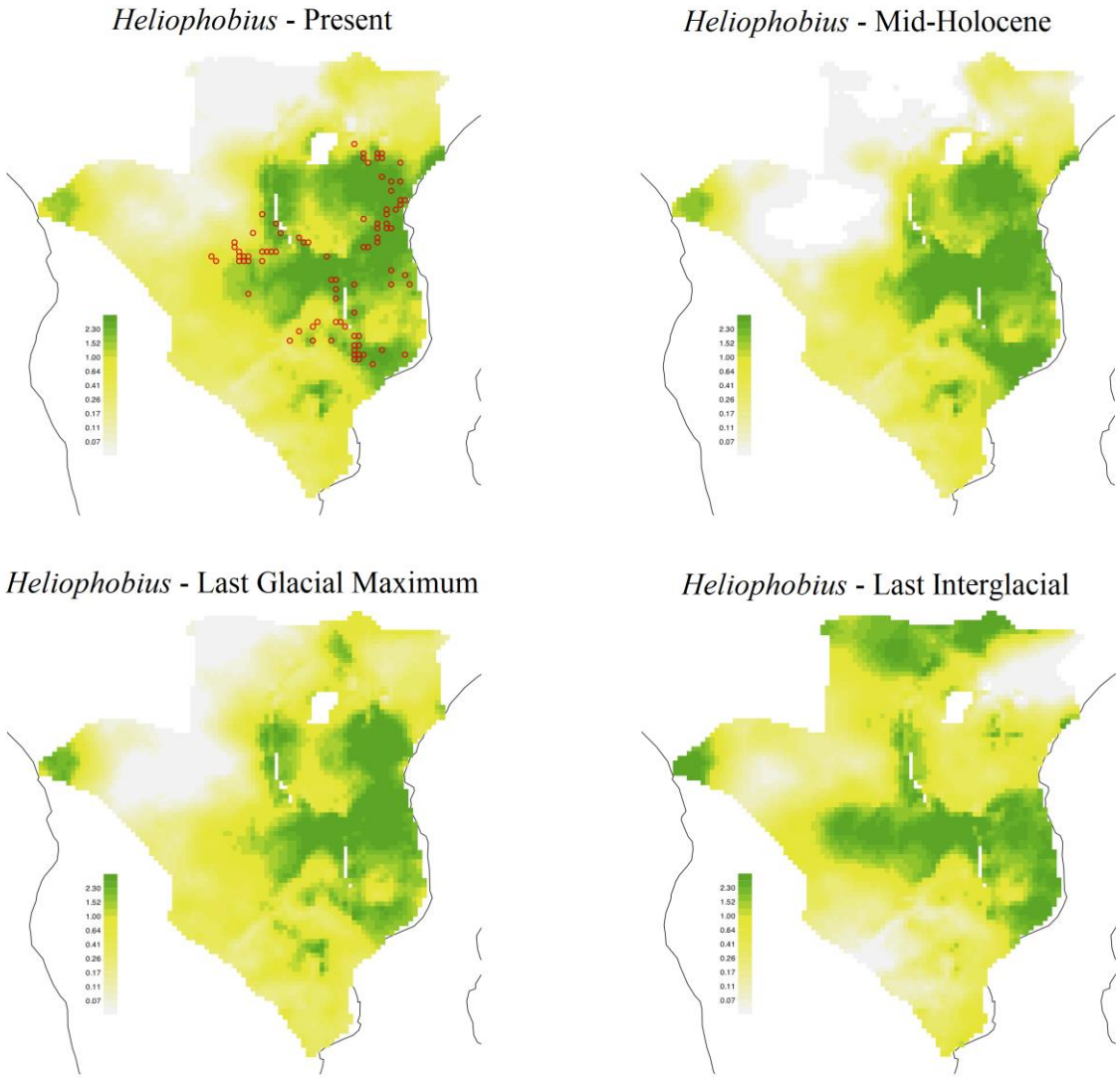

Fig. S9: The predictions of relative occurrence rates of *Heliophobius* from presence and three historical times: Mid-Holocene (6 thousand years ago, ka), Last Glacial Maximum (22 ka) and Last Interglacial (120–140 ka). The colour scale shows the resulting quocient of RORs with the number of background points (values > 1 are depicted with green shades, < 1 with yellow shades).

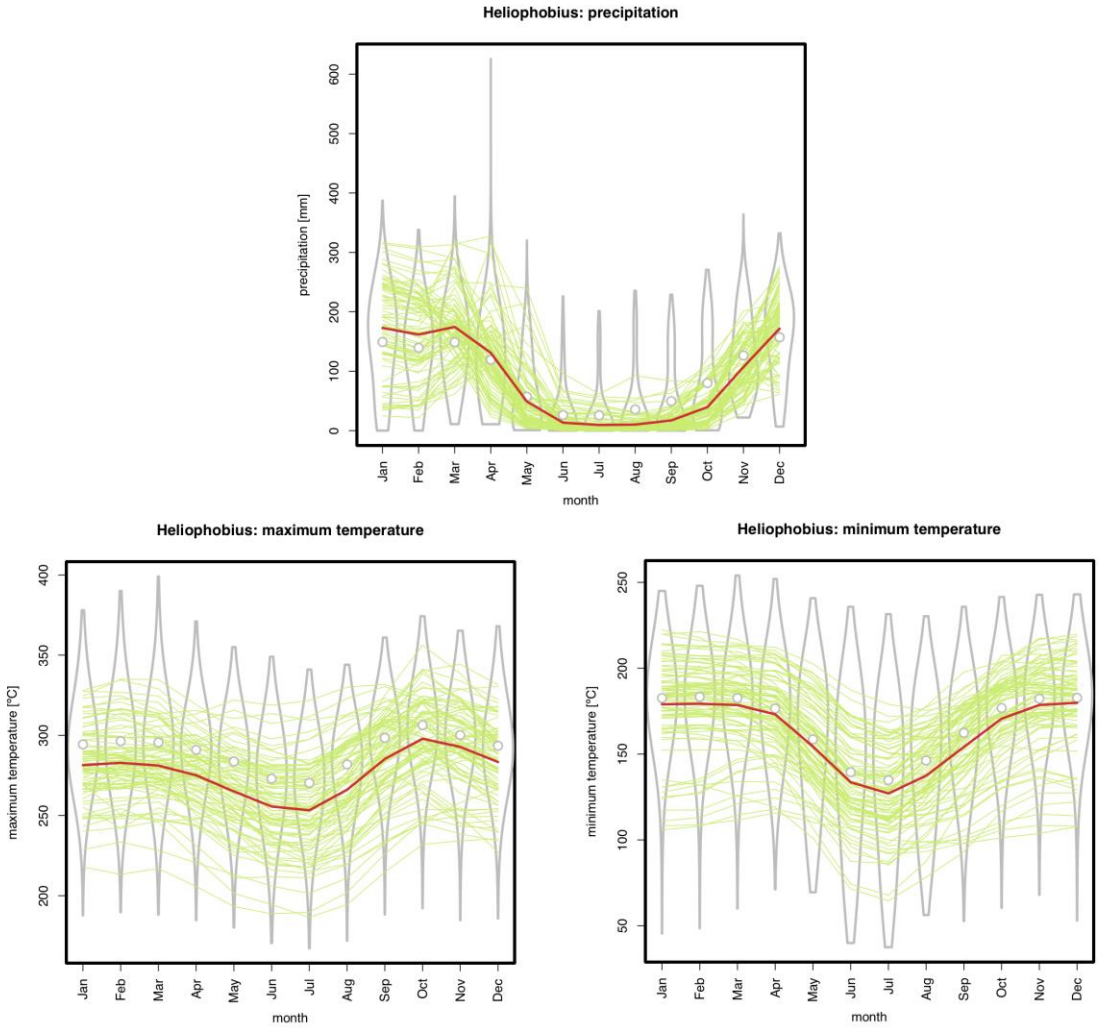

Fig. S10: The curves depicting the precipitation, maximum and minimum temperatures during the year. The temperatures (y-axis) are tenfold the real value (300 means 30°C). Violin plots show distribution of values over all background points, the open circles are background-wide means, green curves are the actual climatic curves observed at the presence points, and red curves join background-wide means weighted by the predicted suitability.

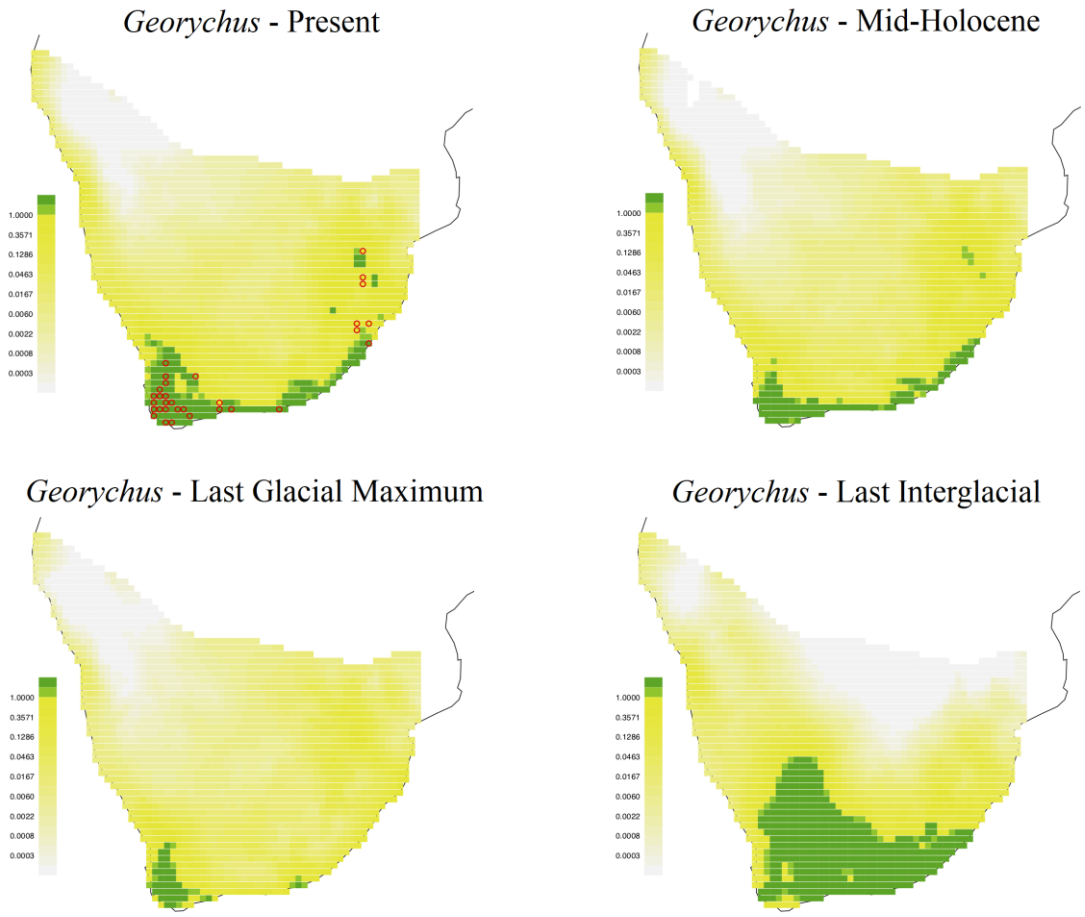

Fig. S11: The predictions of relative occurrence rates of *Georychus* from presence and three historical times: Mid-Holocene (6 thousand years ago, ka), Last Glacial Maximum (22 ka) and Last Interglacial (120–140 ka). The colour scale shows the resulting quocient of RORs with the number of background points (values > 1 are depicted with green shades, < 1 with yellow shades).

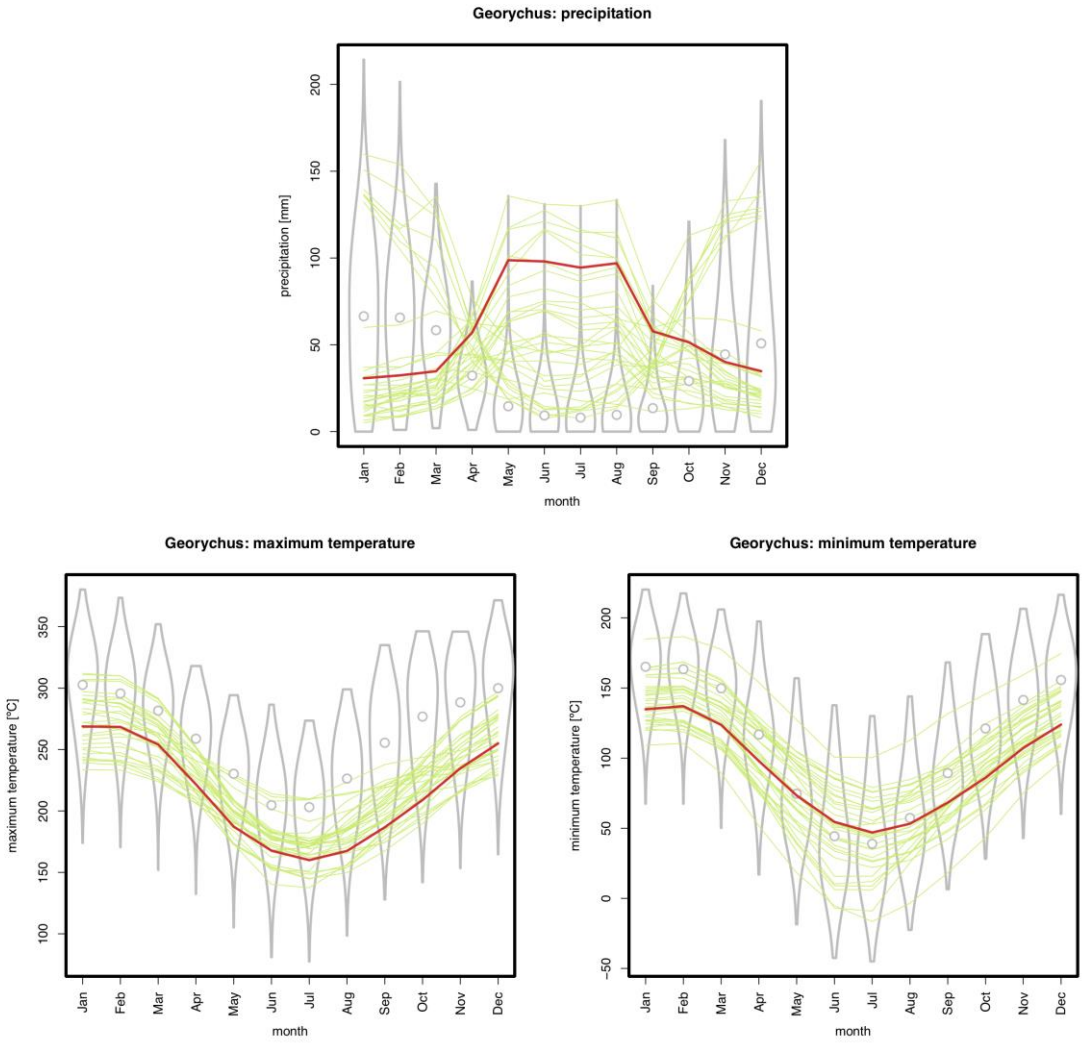

Fig. S12: The curves depicting the precipitation, maximum and minimum temperatures during the year. The temperatures (y-axis) are tenfold the real value (300 means 30°C). Violin plots show distribution of values over all background points, the open circles are background-wide means, green curves are the actual climatic curves observed at the presence points, and red curves join background-wide means weighted by the predicted suitability.

7.3 References from Supplement

Berger, S. A., Krompass, D. and Stamatakis, A. (2011) ‘Performance, accuracy, and Web server for evolutionary placement of short sequence reads under maximum likelihood’, Systematic Biology, 60, pp. 291–302.

Galan, M., Pagès, M., Cosson, J. F. (2012) ‘Next-generation sequencing for rodent barcoding: Species identification from fresh, degraded and environmental samples’ PLoS ONE, 7, p. e48374.

Gent, P. R., Danabasoglu, G., Donner, L. J., Holland, M. M., Hunke, E. C., ..., Zhang, M. (2011) ‘The community climate system model version 4’, Journal of Climate, 24, pp. 4973–4991.

Harte, J., Newman, E. A. (2014) ‘Maximum information entropy: ‘A foundation for ecological theory’, Trends in Ecology & Evolution, 29, pp. 384-389.

Hastie, T., Tibshirani, R., Friedman, J. (2009) ‘The elements of statistical learning: Data mining, inference, and prediction’, 2nd edition. Springer-Verlag.

Hijmans, R. J., Cameron, S. E., Parra, J. L., Jones, P. G. , Jarvis, A. (2005) ‘Very high resolution interpolated climate surfaces for global land areas’, International Journal of Climatology, 25, pp. 1965–1978.

Merow, C., Smith, M. J., Silander J. A. Jr. (2013) ‘A practical guide to MaxEnt for modeling species' distributions: What it does, and why inputs and settings matter’, Ecography, 36, pp. 1058-1069.

Olson, D. M., Dinerstein, E., Wikramanayake, E. D., Burgess, N. D., Powell, G. V. N., ..., Kassem, K. R. (2001) ‘Terrestrial ecoregions of the world: a new map of life on earth’, Bioscience, 51, pp. 933-938.

Otto-Bliesner, B. L., Marshall, S. J., Overpeck, J. T., Miller, G. H., Hu, A. (2006) ‘Simulating Arctic climate warmth and icefield retreat in the last interglaciation’, Science 311, pp. 1751–1753.

Phillips, S. J., Anderson, R. P., Schapire, R. E. (2006) ‘Maximum entropy modeling of species geographic distributions’, Ecological Modelling, 190, pp. 231-259.

Phillips, S. J., Anderson, R. P., Dudik, M., Schapire, R. E., Blair, M. E. (2017) ‘Opening the black box: An open-source release of Maxent’, Ecography, 40, pp. 887-893.

Ronquist, F., Teslenko, M., van der Mark, P., Ayres, D. L., Darling, A., Höhna, S., Larget, B., Liu, L., Suchard, M. A., Huelsenbeck, J. P. (2012) ‘MrBayes 3.2: Efficient Bayesian phylogenetic inference and model choice across a large model space’, Systematic Biology 61, pp. 539–542.

Stamatakis, A. (2014) ‘RAxML version 8: A tool for phylogenetic analysis and post-analysis of large phylogenies’. Bioinformatics, 30, pp. 1312–1313.

Tibshirani, R. (1996) ‘Regression shrinkage and selection via the lasso’, Journal of the Royal Statistical Society. Series B, 58, pp. 267–288.

Tab. S1: List of all specimens used for this study.

ID	ddRAD seq.	Sanger seq.	conc. of DNA (ng/µl)	cytb lineage	Country	Locality	Latitude	Longitude	Alt (m)	Habitat
Heliophobius argenteocinereus:										
11-02-2002	Y		5.08	SW3	Zambia	Chipata	-13,6445	32,6447	1138	NA
JS114	Y		7.35	SW3	Zambia	Kacholola	-14,7618	30,5965	900	cultivated area
KE585	Y	Y	133	N1	Kenya	Taita Hills WS	-3,4767	38,3423	1592	cultivated area
M0x137	Y		4.6	SW2	Malawi	Blantyre	-15,7861	35,0058	1051	grassland
M5x086	Y		33.5	SW2	Malawi	Zomba Plateau	-15,3411	35,2801	1540	NA
M5x102	Y		20.8	SW2	Malawi	Zomba Plateau	-15,3411	35,2801	1540	NA
M5x105	Y		42.1	SW2	Malawi	Mulanje	-16,0402	35,5153	640	cultivated area
M5x117	Y		7.97	SW2	Malawi	Mulanje	-16,0402	35,5153	640	cultivated area
M5x143	Y		36.7	SW2	Malawi	Mulanje	-16,0402	35,5153	640	cultivated area
M5x147	Y	Y	9.25	SW2	Malawi	Domasi	-15,3085	35,3933	780	cultivated area
M5x149	Y		42.1	SW2	Malawi	Domasi	-15,3085	35,3933	780	cultivated area
M5x172	Y		22.3	SW2	Malawi	Malosa	-15,2603	35,3274	1660	NA
M5x173	Y		14.9	SW2	Malawi	Malosa	-15,2603	35,3274	1660	NA
M5x184	Y		4.93	SW2	Malawi	Zomba Plateau	-15,3411	35,2801	1540	NA
M5x196	Y		24.8	SW2	Malawi	Mpalanganga estate	-15,4468	35,2607	960	miombo woodland
M8x0008	Y		26.7	SW2	Malawi	Mulanje Mts FR	-15,8681	35,7028	1666	miombo woodland
M8x0015	Y		148	SW2	Malawi	Mulanje Mts FR	-15,8681	35,7028	1753	miombo woodland
M8x0041	Y		26	SW2	Malawi	Mulanje Mts FR	-15,8489	35,7049	1016	cultivated area
M8x0049	Y		139	SW2	Malawi	Mulanje Mts FR	-15,8489	35,7049	1016	cultivated area
M8x0051	Y		10.2	SW2	Malawi	Mulanje Mts FR	-15,8489	35,7049	1016	cultivated area
M8x0052	Y		157	SW2	Malawi	Mulanje Mts FR	-15,8489	35,7049	1016	cultivated area
M8x0057	Y		13.4	SW2	Malawi	Mulanje Mts FR	-15,8489	35,7049	1016	cultivated area

M8x0181	Y	Y	18.9	SW3	Malawi	Ntchisi	-13,3814	34,0031	1440	cultivated area
M8x0183	Y		228	SW3	Malawi	Ntchisi	-13,3814	34,0031	1440	cultivated area
M8x0185	Y		6.47	SW3	Malawi	Ntchisi	-13,3814	34,0031	1440	cultivated area
M8x0235	Y		392	SW3	Malawi	Ntchisi	-13,4267	33,9239	1625	cultivated area
M8x0236	Y		28.6	SW3	Malawi	Ntchisi	-13,4267	33,9239	1625	cultivated area
M8x3002	Y		96.9	SW3	Malawi	Nyika NP	-10,5662	33,7901	2350	grassland
M8x3003	Y		175	SW3	Malawi	Nyika NP	-10,5662	33,7901	2350	grassland
M8x3004	Y		69.5	SW3	Malawi	Nyika NP	-10,5662	33,7901	2350	grassland
M8x3006	Y	Y	132	SW3	Malawi	Nyika NP	-10,4964	33,8878	2088	dambo
M8x3037	Y		291	SW3	Malawi	Nyika NP	-10,4959	33,8862	2099	grassland
M8x3085	Y	Y	12.4	SW2	Malawi	Mpalanganga estate	-15,4468	35,2607	960	miombo woodland
M8x3140	Y		14.3	SE2	Malawi	Mandimba Estate	-14,4216	35,6047	811	cultivated area
M8x3141	Y		113	SE2	Malawi	Chowe	-14,4180	35,3791	920	miombo woodland
M8x3142	Y	Y	8.07	SE2	Malawi	Chowe	-14,4180	35,3791	920	miombo woodland
MOZ127	Y	Y	22.5	SW2	Mozambique	Mt Mabu	-16,3670	36,4134	383	cultivated area?
MOZ128	Y		44.2	SW2	Mozambique	Mt Mabu	-16,3670	36,4134	383	cultivated area?
MOZ129	Y		8.68	SW2	Mozambique	Mt Mabu	-16,3670	36,4134	383	cultivated area?
MOZ130	Y		8.72	SW2	Mozambique	Mt Mabu	-16,3670	36,4134	383	cultivated area?
MOZ159	Y		9.52	SW2	Mozambique	Mt Mabu	-16,3670	36,4134	383	cultivated area?
MOZ204	Y	Y	18.6	SE3	Mozambique	Gile NR	-16,7396	38,8266	32	cultivated area
MOZ206	Y		46.3	SE3	Mozambique	Gile NR	-16,7396	38,8266	32	cultivated area
MOZ207	Y	Y	16	SE3	Mozambique	Gile NR	-16,7396	38,8266	32	cultivated area
MOZ208	Y		5.37	SE3	Mozambique	Gile NR	-16,7396	38,8266	32	cultivated area
MOZ209	Y	Y	6.83	SE3	Mozambique	Gile NR	-16,7396	38,8266	32	cultivated area
MOZ305	Y	Y	11.1	SE2	Mozambique	Mt Jesi	-12,9064	35,1619	1366	cultivated area
MOZ306	Y		6.1	SE2	Mozambique	Mt Jesi	-12,9064	35,1619	1366	cultivated area
T8x358	Y		62.9	N4	Tanzania	Usambara Mts	-5,0295	38,6033	1187	village
T8x359	Y		35.3	N4	Tanzania	Usambara Mts	-5,0295	38,6033	1187	grassland

T8x381	Y		105	N4	Tanzania	Usambara Mts	-5,0437	38,6142	968	cultivated area
T8x382	Y	Y	363	N4	Tanzania	Usambara Mts	-5,0437	38,6142	968	cultivated area
T8x384	Y		348	N4	Tanzania	Usambara Mts	-5,0437	38,6142	968	cultivated area
T8x392	Y		10.4	N4	Tanzania	Usambara Mts	-5,2499	38,6555	299	cultivated area
T8x393	Y		6.37	SE1	Tanzania	Kipera	-6,9801	37,5516	618	cultivated area
T8x394	Y	Y	217	SE1	Tanzania	Kipera	-6,9397	37,5350	561	cultivated area
T8x395	Y		133	SE1	Tanzania	Kipera	-6,9801	37,5516	618	cultivated area
T8x404	Y	Y	10.1	SE1	Tanzania	Msanga	-10,9025	39,2073	439	miombo mixed with cultivated area
T8x405	Y		160	SE1	Tanzania	Mkowela	-10,9218	37,9453	362	cultivated area
T8x406	Y		170	SE1	Tanzania	Mkowela	-10,9218	37,9453	362	cultivated area
T8x407	Y		77.4	SE1	Tanzania	Mtonya	-10,8798	37,7054	399	cultivated area
T8x408	Y		103	SE1	Tanzania	Mtonya	-10,8798	37,7054	399	cultivated area
T8x409	Y		11.3	SE1	Tanzania	Mtonya	-10,8798	37,7054	399	cultivated area
T8x438	Y	Y	8.85	SE2	Tanzania	Lihale	-10,7975	35,1674	913	miombo
T8x439	Y		138	SE2	Tanzania	Lihale	-10,8073	35,1353	995	miombo
T8x440	Y		29.1	SE2	Tanzania	Lihale	-10,8073	35,1353	995	miombo
T8x449	Y	Y	116	N2	Tanzania	Ntendo	-7,9047	31,5364	1846	cultivated area
T8x457	Y	Y	11.8	N3	Tanzania	Nayala	-8,9384	33,1825	1307	NA
T8x458	Y	Y	148	N3	Tanzania	Nayala	-8,9384	33,1825	1307	NA
T8x459	Y	Y	8.99	N3	Tanzania	Nayala	-8,9384	33,1825	1307	NA
T8x460	Y		52.4	N3	Tanzania	Nayala	-8,9384	33,1825	1307	NA
T8x461	Y		20.8	N3	Tanzania	Nayala	-8,9384	33,1825	1307	NA
T8x462	Y		46.1	N3	Tanzania	Nayala	-8,9384	33,1825	1307	NA
T8x546	Y		32.6	SE1	Tanzania	Ulangambi FR, Lulanzi	-8,0066	35,9144	2053	grassland
T8x547	Y		32.9	SE1	Tanzania	Ulangambi FR, Lulanzi	-8,0066	35,9144	2053	grassland
T8x548	Y		26.5	SE1	Tanzania	Morogoro	-6,9363	37,5256	560	NA
TZ27501	Y		54.1	N4	Tanzania	Handeni	-5,4373	38,0459	750	miombo with cultivated area
TZ27800	Y		33.8	N4	Tanzania	Kireguru	-5,4660	37,6142	848	cultivated area

TZ27975	Y		27.5	N4	Tanzania	Masenge (Ukaguru Mts)	-6,3950	36,9166	1879	NA
TZ27976	Y		21.8	N4	Tanzania	Masenge (Ukaguru Mts)	-6,3640	36,9291	1780	NA
TZ28024	Y		30.2	N4	Tanzania	Masenge (Ukaguru Mts)	-6,3640	36,9291	1780	NA
TZ28025	Y		188	N4	Tanzania	Masenge (Ukaguru Mts)	-6,3640	36,9291	1780	NA
TZ28026	Y	Y	8.6	N4	Tanzania	Masenge (Ukaguru Mts)	-6,3640	36,9291	1780	NA
TZ28027	Y		26.3	N4	Tanzania	Masenge (Ukaguru Mts)	-6,3950	36,9166	1879	NA
TZ28028	Y		19.3	N4	Tanzania	Masenge (Ukaguru Mts)	-6,3950	36,9166	1879	NA
TZ28029	Y		5.5	N4	Tanzania	Masenge (Ukaguru Mts)	-6,3950	36,9166	1879	NA
TZ28032	Y		24.2	N4	Tanzania	Masenge (Ukaguru Mts)	-6,3950	36,9166	1879	NA
TZ28034	Y		22.6	N4	Tanzania	Masenge (Ukaguru Mts)	-6,3950	36,9166	1879	NA
TZ28035	Y		30.7	N4	Tanzania	Masenge (Ukaguru Mts)	-6,3950	36,9166	1879	NA
TZ28036	Y		20.9	N4	Tanzania	Masenge (Ukaguru Mts)	-6,3950	36,9166	1879	NA
TZ28170	Y	Y	68.8	N4	Tanzania	Kireguru	-5,4660	37,6142	848	cultivated area
TZ29665	Y		8.23	N4	Tanzania	Kimbe	-5,7974	37,6361	698	edge of cultivated area
TZ29669	Y		33.2	N4	Tanzania	Kimbe	-5,7974	37,6361	698	edge of cultivated area
TZ29683	Y		28.1	N4	Tanzania	Kimbe	-5,7974	37,6361	698	edge of cultivated area
TZ29696	Y		23.5	N4	Tanzania	Kimbe	-5,7974	37,6361	698	edge of cultivated area
TZ30036	Y		20.5	SE1	Tanzania	Mikumi	-7,4125	36,9767	521	grassy edges of cultivated area
TZ30037	Y		10.1	SE1	Tanzania	Mikumi	-7,4125	36,9767	521	grassy edges of cultivated area
TZ30038	Y	Y	61.4	SE1	Tanzania	Mikumi	-7,4125	36,9767	521	grassy edges of cultivated area
TZ30039	Y		36.4	SE1	Tanzania	Mikumi	-7,4125	36,9767	521	grassy edges of cultivated area
Z7x43	Y	Y	429	SW3	Zambia	Kacholola	-14,7618	30,5965	900	NA
Z7x48	Y		159	SW3	Zambia	Kacholola	-14,7618	30,5965	900	NA

Georychus capensis:

A06	Y		10.7	2+1	South Africa	Moorreesburg	-33,28123333	18,58218	820	grazed area near vlei
A40	Y		42.8	2+1	South Africa	Moorreesburg	-33,29038333	18,57278	817	grazed area near vlei
A43	Y		17.4	2+1	South Africa	Moorreesburg	-33,30281667	18,5632	817	grazed area near vlei

CA2	Y	Y	21.2	2	South Africa	Cape Town	-34,00191667	18,48348	735	lawn near vlei
CA3	Y		13.4	2	South Africa	Cape Town	-34,00221667	18,48328	735	lawn near vlei
CA5	Y		10.7	2	South Africa	Cape Town	-34,00228333	18,48298	735	lawn near vlei
CCK14	Y		13.0	1	South Africa	Swellendam	-34,04338333	20,41707	591	grazed area near river
CCK16	Y	Y	7.58	1	South Africa	Swellendam	-34,04421667	20,41755	592	grazed area near river
CCK19	Y		37.1	1	South Africa	Swellendam	-34,04278333	20,4183	592	grazed area near river
CD12	Y		10.9	1	South Africa	Citrusdal	-32,59451667	19,00978	735	grazed area near vlei and river
CD15	Y		6.3	1	South Africa	Citrusdal	-32,59515	19,01125	736	grazed area near vlei and river
CD5	Y		15.2	1	South Africa	Citrusdal	-32,5941	19,01053	735	grazed area near vlei and river
CFA21	Y		7.61	1	South Africa	Wolseley	-33,40758333	19,20092	590	grazed area near vlei
CFA4	Y		19.9	1	South Africa	Wolseley	-33,4067	19,20182	799	grazed area near vlei
CFA8	Y	Y	23.8	1	South Africa	Wolseley	-33,40566667	19,20338	799	grazed area near vlei
CG11	Y		22.1	4	South Africa	Oudshoorn	-33,84903333	22,04002	584	grazed area near vlei and river
CG12	Y	Y	13.3	4	South Africa	Oudshoorn	-33,8494	22,03762	584	grazed area near vlei and river
CG14	Y	Y	37.7	4	South Africa	Oudshoorn	-33,84931667	22,03795	584	grazed area near vlei and river
CG5	Y	Y	24.1	4	South Africa	Oudshoorn	-33,84828333	22,03915	581	grazed area near vlei and river
CG7	Y		22.9	4	South Africa	Oudshoorn	-33,84906667	22,03982	580	grazed area near vlei and river
CJ13	Y		7.21	2	South Africa	Paarl	-33,73813333	18,97367	591	rugby field near river
CJ16	Y		5.17	2	South Africa	Paarl	-33,73795	18,97387	591	rugby field near river
CJ4	Y		10.7	2	South Africa	Paarl	-33,73873333	18,97423	799	rugby field near river

CS10	Y	Y	18.4	3	South Africa	Struisbaai	-34,68768333	20,00038	736	grazed area near vlei
CS15	Y		26.6	3	South Africa	Struisbaai	-34,68765	20,00077	736	grazed area near vlei
CS20	Y	Y	27.7	3	South Africa	Struisbaai	-34,6866	20,00087	735	grazed area near vlei
CS3	Y		8.6	3	South Africa	Struisbaai	-34,68681667	19,99973	736	grazed area near vlei
CS5	Y	Y	26.4	3	South Africa	Struisbaai	-34,68615	19,99897	736	grazed area near vlei
CT09	Y		11.4	1	South Africa	Ceres	-33,19256667	19,24487	891	grazed area near vlei and river
CT13	Y		6	1	South Africa	Ceres	-33,1951	19,24743	904	grazed area near vlei and river
CT18	Y		19.5	1	South Africa	Ceres	-33,1949	19,24968	900	grazed area near vlei and river
CW10	Y		22.5	2	South Africa	Worcester	-33,65978333	19,51808	591	grazed area near vlei
CW11	Y		34.3	2	South Africa	Worcester	-33,65975	19,51795	590	grazed area near vlei
CW6	Y		31	2	South Africa	Worcester	-33,66035	19,51858	590	grazed area near vlei
Da1	Y		13.5	2	South Africa	Darling	-33,40063333	18,40133	800	grazed area near vlei
Nrd3	Y	Y	11.9	5	South Africa	Nottingham Road	-29,47971667	29,86325	1807	grazed area near vlei
Wks1	Y	Y	27.9	6	South Africa	Wakkerstroom	-27,29806667	30,26262	1948	grazed area near vlei
Wks15	Y		18.9	6	South Africa	Wakkerstroom	-27,29933333	30,26378	2003	grazed area near vlei
Wks16	Y	Y	14.4	6	South Africa	Wakkerstroom	-27,29901667	30,26373	2002	grazed area near vlei
Wks4	Y	Y	17.3	6	South Africa	Wakkerstroom	-27,29788333	30,26363	1990	grazed area near vlei
Wks9	Y		22.4	6	South Africa	Wakkerstroom	-27,29891667	30,26465	2005	grazed area near vlei
Z12	Y		21.8	2	South Africa	Darling	-33,40358	18,42966	151	grazed area near vlei
Z6	Y		12.1	2	South Africa	Darling	-33,40303	18,42951	153	grazed area near vlei

Tab. S2: Fossils and molecular data used in the fossilized birth-death dating (GenBank accession numbers of the sequences). Fossil data are based on Table S4 of Bryja et al. (2018). Molecular data were downloaded from GenBank; accession numbers of the sequences are in the table.

Species	**Mya (before present)**	**Phylogenetic placement**	**Reference**	***CYTB***	***GHR***	***IRBP***	***VWF***
Fossil data:							
Paraphiomys	24	monophyletic with *Thryonomys* and *Petromus*	Winkler et al., 2010	-	-	-	-
Paraulacodus	14	sister to *Thryonomys*	Winkler et al., 2010	-	-	-	-
Thryonomys	6	sister to extant *Thryonomys*	Manthi, 2007	-	-	-	-
Petromus	6	sister to extant *Petromus*	Mein and Pickford, 2006	-	-	-	-
Bathyergoides	23	Bathyergidae	Mein and Pickford, 2003	-	-	-	-
Efeldomys	20	Bathyergidae	Mein and Pickford 2008	-	-	-	-
Geofossor	20	Bathyergidae	Mein and Pickford, 2003	-	-	-	-
Microfossor	20	Bathyergidae	Mein and Pickford 2008	-	-	-	-
Proheliophobius	20	Bathyergidae	Mein and Pickford, 2003	-	-	-	-
Richardus	15	Bathyergidae	Lavocat, 1988	-	-	-	-
Gypsorhychus	5	Bathyergidae	Broom, 1948	-	-	-	-
Bathyergus hendei	5	sister to extant *Bathyergus*	Denys, 1998	-	-	-	-
Cryptomys broomi	5	monophyletic with *Cryptomys* and *Fukomys*	Denys, 1998	-	-	-	-
Heterocephalus	4,3	sister to extant *Heterocephalus*	Denys, 2011	-	-	-	-
Molecular data:							
Bathyergus janetta	-	-	-	MH186532	MH186276	-	-
Bathyergus suillus A	-	-	-	AF012242	FM162080	AJ427251	AJ238384

Bathyergus suillus D	-	-	-	KJ866575	MH186316	-	-
Cryptomys hottentotus	-	-	-	AF012240	FJ855202	-	AJ251132
Cryptomys natalensis	-	-	-	MH186544	MH186346	-	-
Cryptomys nimrodi	-	-	-	AF012237	-	-	-
Fukomys amatus	-	-	-	EF043468	-	-	-
Fukomys anselli	-	-	-	AF012233	-	-	-
Fukomys bocagei	-	-	-	AF012229	-	-	-
Fukomys damarensis	-	-	-	AY425857	FN984748	FN984749	FN984751
Fukomys livingstoni	-	-	-	KX905192	-	-	-
Fukomys mechowii	-	-	-	EF043452	-	-	-
Fukomys zechi	-	-	-	KX905198	-	-	-
Georychus capensis 2	-	-	-	MG496777	MH186377	-	-
Georychus capensis 5	-	-	-	MG496905	MH186368	-	-
Georychus capensis 6	-	-	-	MG496908	MH186366	-	
Heliophobius argenteocinereus N	-	-	-	MG911074	FJ855204	-	AJ251133
Heliophobius argenteocinereus SE	-	-	-	MG911071	-	-	-
Heliophobius argenteocinereus SW	-	-	-	MG911051	-	-	-
Heterocephalus glaber	-	-	-	AF155870	AF332034	AM407925	AJ251134
Petromus typicus	-	-	-	MH186591	FM162079	AJ427244	AJ251144
Thryonomys swinderianus S	-	-	-	KJ742647	-	-	-
Thryonomys swinderianus W	-	-	-	KJ193480	AF332035	AJ427243	AJ224674